Tiny Ordovician brachiopods from the eastern United States: An assessment of their systematics, phylogenetic, and biogeographic trends

A Thesis Presented for the
Master of Science
Degree
The University of Tennessee, Knoxville

Mariana Andrade
August 2024

ACKNOWLEDGEMENTS

I would like to first thank my advisor, Dr. Alycia Stigall, for her inestimable support and the trust she put in me during these two years. I can't say it was easy to move to another country and pursue a graduate degree in a different language, but having a mentor who respects you and your ideas, makes you laugh in every weekly meeting, and shares a bottle of good wine when talking about science makes things easier. I could not be prouder to say I worked with such an amazing scientist, and more than that, I belong to the Stigall family, thank you very much, Professor Alycia.

I would like to thank my collaborators who made this work possible. My committee members, Dr. Bradley Thomson, and Dr. Colin Sumrall for their thoughtful revisions and suggestions. Dr. Colin Sproat, who as a co-author provided specimen measurements data to this work and feedback on the systematic and phylogenetic portion of this study. Dr. Davey Wright who helped me through the coding phase, but also provided insightful thoughts and questions on my work.

I would like to thank my family, these amazing five people who did their best to be present and support me even from another continent. I love science, but they are the ones that keep me motivated to keep studying and working every single day. I live to make them proud and happy.

I would like to thank my cats, as a standard practice in my academic acknowledgments, my cats are my daily emotional support, and although they drive me crazy at night, feeling their love when purring or licking me is the best part of my day.

I would like to thank the friends I have made in the U.S., the Brazilian and non-Brazilian ones, my lab mates, and my EEPS colleagues, thank you very much. These amazing people helped me so much, sometimes even by explaining to me things I didn't understand (from lacrosse to U.S. politics), but mainly by accepting me for who I am.

Finally, I would like to thank the Cincinnati Dry Dredgers, the University of Tennessee, Knoxville, the IGCP 735, and the Paleontological Society for their financial support.

These opportunities made it possible for me to progress in my scientific career and build new connections in science. I would also like to thank the institutions and the researchers at the Smithsonian National Museum of Natural History, and the Cincinnati Museum Center who kindly received and helped me in their institutions during my data collection phase.

ABSTRACT

The evolution and biogeography of three genera of Late Ordovician anazygid brachiopods were investigated using a time-calibrated species-level Bayesian phylogeny and probabilistic biogeographic models. Specifically, the species-level phylogenetic relationships were inferred for the three genera within the family Anazygidae: *Anazyga* Davidson, 1882; *Zygospira* Hall, 1862, and *Catazyga* Hall and Clarke, 1894. Recovered evolutionary relationships indicate that the genera's common ancestor origination was at 453 Mya. The phylogeny resolved into the two subfamilies: Anazyginae (*Anazyga* + *Zygospira)* and Catazyginae (*Catazyga)*. *Anazyga* and *Zygospira* do not correspond to two distinct clades as previously interpreted, but are instead combined herein into a single genus, *Zygospira*. Additionally, two new *Zygospira* species were described, *Zygospira multicostata* n. sp. from the Montoya Group, TX; and *Zygospira idahoensis* n. sp. from the Saturday Mountain Formation, ID. The recovered evolutionary relationships were used to develop an evolutionary biogeographic framework for the clade using the R package BioGeoBEARS. The reconstructed timing of cladogenetic events, geographic patterns, and the timing of dispersal and vicariance speciation events were used to correlate biotic changes with tectonic shifts and eustasy. Results indicate that dispersal was the main speciation mode in this clade. The geographic patterns observed within species' dispersal pathways are supported by pulses of sea level rise which promoted connections between Laurentian midwestern, and southern basins influenced by the Sebree Trough. Estimated speciation and extinction rates indicate that the three genera experienced the highest diversification in the early Late Ordovician (Katian 3), explained by higher dispersal events, and became extinct during the mid Late Ordovician (Katian 4).

TABLE OF CONTENTS

LIST OF TABLES

LIST OF FIGURES

LIST OF ATTACHMENTS

CHAPTER 1: INTRODUCTION

Speciation events are the main drivers of diversification; thus, generating well-constrained phylogenetic hypotheses to investigate speciation processes and facilitators can provide key data on links between biogeography, speciation, and diversification. In this thesis, the evolutionary and biogeographic history of three atrypid brachiopod genera (*Anazyga*, *Catazyga*, and *Zygospira*) is reconstructed as a case study to explore the relationship between biotic evolution and Earth system changes during the Late Ordovician. The Ordovician epicontinental seas in eastern Laurentia provided an excellent environment to examine speciation, with sea-level fluctuations, shifting climatic conditions, and active tectonic settings.

The Ordovician strata of the eastern United States are characterized by an abundant and diverse fossil record of marine life that inhabited a range of tropical to subtropical shallow marine environments (Jin et al., 2013) that covered extensive regions of the Laurentian paleocontinent (McLaughlin and Stigall, 2023; **Figure 1**). The east Laurentian tropical, highly oxygenated, and shallow ocean provided an ideal environment for marine life to disperse and thrive (Kröger, 2018; Servais and Harper, 2018; Rasmussen et al., 2019; Stigall et al., 2019). In the Eastern United States, the period is recorded mainly from the Late Ordovician, an interval also characterized by tectonic and oceanographic changes.

The Taconic Orogeny resulted in the shifting from a passive margin to a convergent boundary between the collision of eastern Laurentia and island arcs (Quinlan and Beaumont, 1984; Ettensohn, 2010; McLaughlin and Stigall, 2023). Tectopulses are recorded by mixed carbonate-siliciclastic sediment accommodation, and the presence of

soft-sediment deformation (Quinlan and Beaumont, 1984; Holland, 1997; Holland and Patzkowsky, 1998). The intense tectonic loading resulted in the formation of a retro-arc foreland basin, which caused the subsequent arching in adjacent areas, including the Nashville Dome, and the Cincinnati Arch (Quinlan and Beaumont, 1984). Cycles of tectonic loading and unloading facilitated the rise and fall of intracratonic arches, which created barriers to and connections for dispersal, respectively.

Moreover, these intervals include a series of biotic shifts and adaptations coordinated with environmental changes, such as the rapid diversification event during the Middle Ordovician, referred to as the Great Ordovician Biodiversification Event (GOBE) (Sepkoski, 1981; Stigall et al., 2017; Servais and Harper, 2018) and a subsequent high diversity interval in the Late Ordovician characterized by distinct pulses of dispersal, colonization, and biotic invasions, which are well documented in the scientific literature (Wright and Stigall, 2013; Stigall et al., 2019; Purcell and Stigall, 2021; Forsythe and Stigall, 2023). By the end of the Ordovician, the Late Ordovician Mass Extinction records deep changes in temperature, sea level, and dominant fauna due to the 2-million years long glaciation (Finnegan et al., 2016). Hence, the Ordovician system provides an ideal environment for investigating evolutionary changes, biodiversity accumulation, and speciation modes in the fossil record.

The high abundance and diversity of articulate brachiopods in Ordovician sequences make them an excellent group within which to assess phylogenetic and biogeographical questions (e.g., Wright and Stigall, 2013; Stigall et al., 2017; Lam et al., 2018).

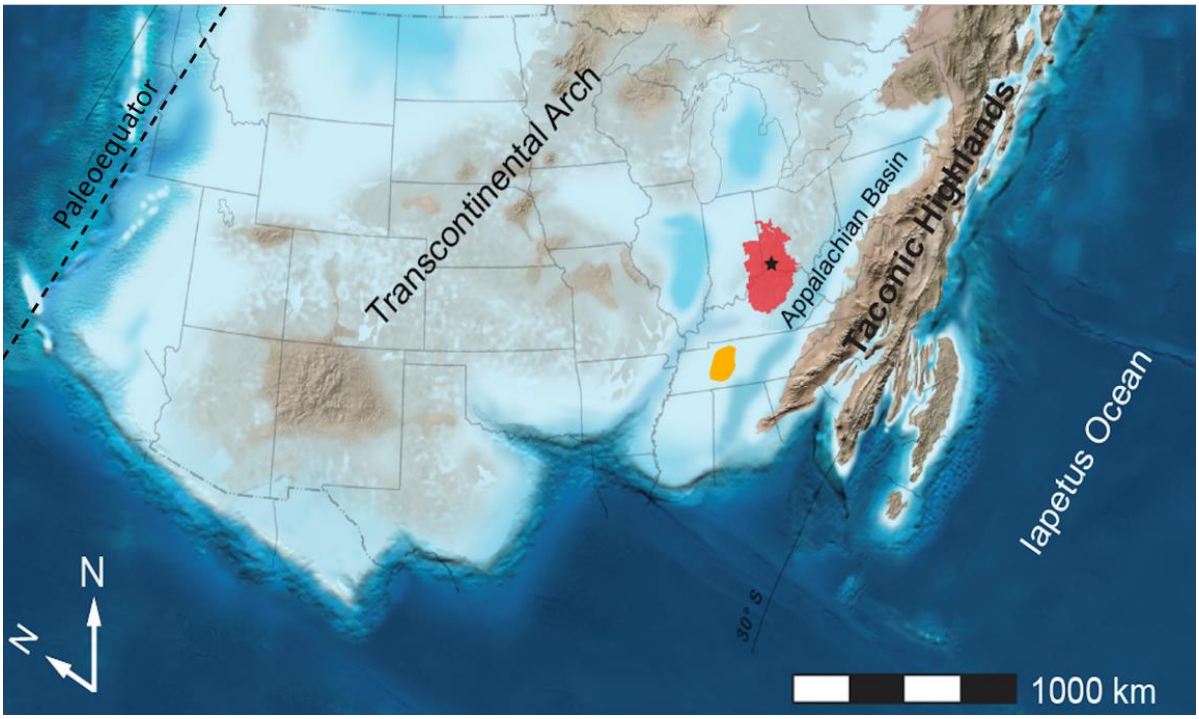

Figure 1. Paleocontinental reconstruction with modern Cincinnati Arch exposures in red and Nashville Dome exposure in orange. Dashed line represents the paleoequator. Base map from Blakey (2013).

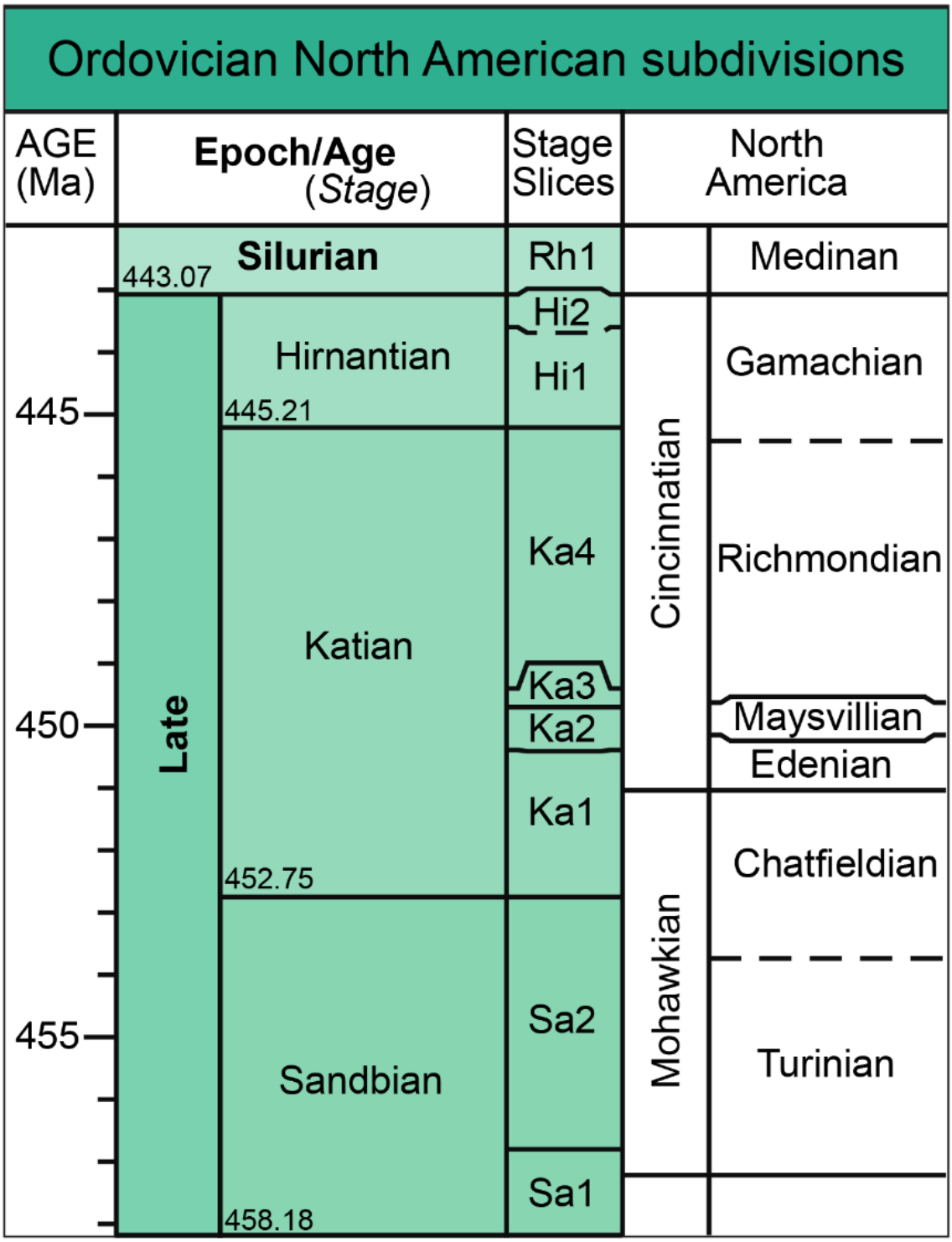

Figure 2. Late Ordovician North American subdivisions, on the left, Global Stages are shown in green, and regional subdivisions are shown on the right. Modified from Goldman et al. (2020).

Within the Order Atrypida, widely spread and abundant brachiopods such as *Catazyga*, *Anazyga*, and *Zygospira* within the subfamilies, Catazyginae Copper, 1977 and Anazyginae Davidson, 1883, respectively, are excellent model taxa for investigating speciation processes across basins. Although monophyly is shared among these taxa (Baarli et al., 2022; **Figure 3**), little was previously known about the speciation patterns and biogeography of the atrypids. Atrypids' evolutionary and geographical responses to contemporaneous environmental shifts can provide insights into how and what to expect from current species reactions to global climate change, such as dispersal patterns, niche stability, and speciation. Recently, the phylogenetic relationships within the entire Order Atrypida (**Figure 3**) were revised by Baarli et al. (2022). In addition, morphological and historical traits of the genus *Zygospira* were examined by Sproat and McLeod (2023). Still, the lack of systematic studies within the subfamily level necessitates carefully reviewing *Anazyga* and *Catazyga* species descriptions, distribution, and morphological distinction before assessing phylogenetic questions.

Historically, species within the family Anazygidae have been diagnosed by their external and internal morphology (Hall, 1847, 1862; Hall and Clarke, 1894; Copper, 1977, 1986; Sproat and McLeod, 2023). However, very few anazygid species have fully documented internal morphology, with *Zygospira modesta*, *Anazyga recurvirostra*, and *Catazyga headi* as notable exceptions. Still, based on these three original descriptions, species have been assigned to one of the three genera relying on internal morphological assumptions (Hall, 1847; Winchell and Schuchert, 1892; Hall and Clarke, 1894; Foerste, 1910; Williams, 1962). Recently, more detailed internal data were provided by Sproat and Mcleod (2023) for *Zygospira cincinnatiensis* and *Zygospira kentuckiensis*. Still, these

data are not enough to clarify all the hypothesized species-level relationships within the subfamilies. Therefore, a full systematic revision of Anazygidae is required to better understand the evolutionary relationships among the three genera.

Chapter 2 uses phylogenetic analyses to inform a systematic revision of Late Ordovician species assigned to Anazygidae. The species-level phylogeny was estimated using a time-calibrated Bayesian framework to reconstruct the evolutionary relationships within the group and to assess the clade's diversification and evolutionary relationships. This study is the first to address an evolutionary framework which the systematic status of species relationships within Anazygidae. **Chapter 3** applies a probabilistic evolutionary biogeographic analysis to the phylogenetic framework developed in **Chapter 2**. From this biogeographic analysis, assessment of speciation tempo and mode and dispersal pathways are reconstructed and then compared with Earth system events. The combination of these analyses facilitates a holistic evaluation of the co-evolution of *Anazyga*, *Catazyga*, and *Zygospira*, and the Earth system during the Late Ordovician.

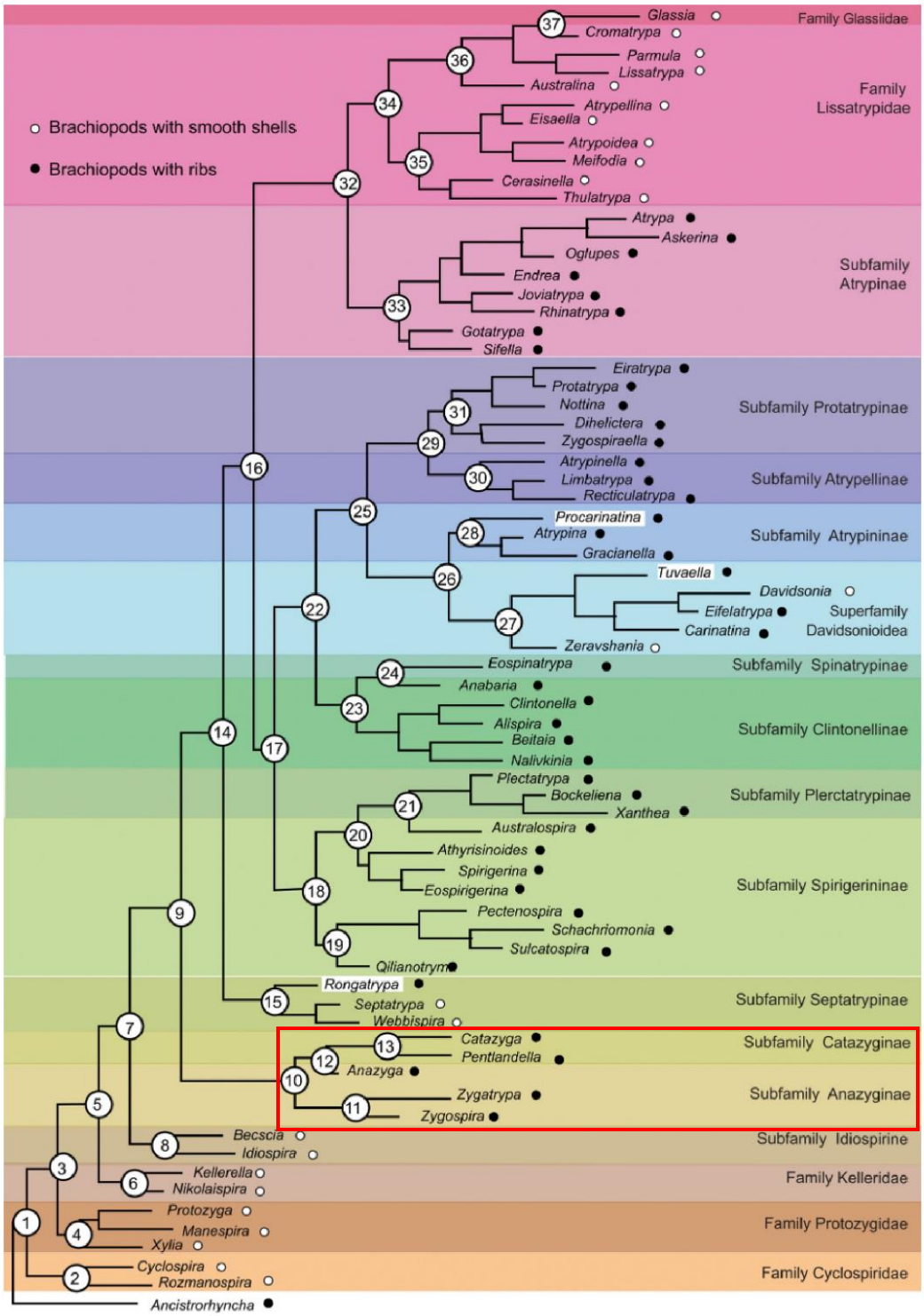

Figure 3. Phylogenetic relationships in the Order Atrypida. The three focal genera are highlighted in red, and the clade origination is marked by the number 10. Modified from Baarli et al. (2023).

CHAPTER 2: A SPECIES-LEVEL BAYESIAN PHYLOGENETIC FRAMEWORK FOR THREE LATE ORDOVICIAN GENERA (ATRYPIDA: ANAZYGIDAE)

Abstract

During the Ordovician, the brachiopod order Atrypida originated and diversified extensively, evolving novelties such as helical and skeletal-supported lophophores. However, speciation patterns and evolutionary drivers within three widely distributed atrypid genera, *Anazyga*, *Catazyga*, and *Zygospira* remain poorly known. Herein, we develop a robust Bayesian phylogenetic framework for these clades. Morphological character data, including 34 internal and external characters, were collected from literature and museum collections for a focal group of 20 species, including seven recently reviewed species of *Zygospira*, six species previously assigned to *Anazyga*, and seven species previously assigned to *Catazyga*. These data were analyzed in BEAST2.5, via the morphological model (Mk Model) of character evolution, subsequently implemented in a three-interval skyline fossilized-birth-death model (FBDSK), where rates of extinction, origination, and differential sampling are considered independently for each branch in three different Late Ordovician (Katian) time intervals. Primary results include: (1) polyphyly of the three genera; (2) re-evaluation of *Anazyga* and *Catazyga* species' positioning and systematic nomenclature within Anazygidae, resulting in the transfer of all *Anazyga* and two *Catazyga* species to *Zygospira*; (3) recognition of two new *Zygospira* species; and (4) updated timing for origination, and speciation of the clade, presenting an early origination and diversification for the clade. The origination date for the common ancestor of these genera calibrated to be 453 Ma (Sandbian 2 Stage). Recovered biodiversification rates indicate that the highest speciation and extinction rates occurred in the Katian 3 Stage, when the diversification of the genera reached its peak. Subsequently, an abrupt decline in biodiversification rates lead to an extinction episode in the Katian 4 Stage for all clades. *Catazyga*, and *Zygospira* are interpreted as early Late Ordovician atrypids that experienced both rapid radiation and extinction during Katian Stage.

2.1 Introduction

The Order Atrypida originated and diversified in the Middle Ordovician (Darriwilian), flourished during the Late Ordovician, and persisted through the Early Silurian until its extinction in the Late Devonian (Harper et al., 2017). Anazygidae Davidson, 1882 is a geographically widespread brachiopod family within the Order Atrypida that ranges from the Middle to Late Ordovician. Anazygidae species are stratigraphically important and substantially impact community structures and ecosystems (Copper, 1977; Patzkowsky and Holland, 1999; Sproat and McLeod, 2023). Typical species within the Anazygidae are small (5-15 mm), oval-shaped, with fine-

ribbed shells characterized by brachidia with "*the apex of their vertical spiral cones directed towards the bottom of the dorsal valve*" (Davidson, 1882). The interior morphology consists of a calcified, whorled lophophore, which plays an important role in atrypid taxonomy and preservation (Sproat and McLeod, 2023).

Members of the family include the widespread genera *Anazyga*, *Catazyga*, and *Zygospira*, which are palaeoecologically significant taxa (Copper, 1977; Patzkowsky and Holland, 1999). These genera were included in a genus-level phylogeny of the Order Atrypida (Baarli et al., 2022), and some *Zygospira* species were recently systematically revised (Sproat and McLeod, 2023); however, no prior studies have explored species-level evolutionary relationships of anazygid species. The goal of this study is to infer species-level relationships within this clade. Additionally, this analysis investigates the relative importance of incorporating internal and external characters vs. only external characters into Bayesian phylogenetics in a fossilized birth-death model for this group. The recovered phylogenetic framework will also be used to investigate speciation and extinction rates and biogeographic evolution within the clade during the Late Ordovician in **Chapter 3**.

This study focuses on species of *Zygospira* Hall 1862, *Anazyga* Davidson 1882, and *Catazyga* Hall and Clarke 1894. *Zygospira* was first described by Hall (1862) and was defined as being externally distinct from other atrypids due to its size and number of ribs as well as discrete combination of internal structures, specifically five to eight lophophore whorls that coil outwards. A closely related genus, *Anazyga,* was described 20 years later by Davidson (1882) and was characterized as being longitudinally oval and having a one to three lophophore whorls. Later, Copper (1977) characterized *Anazyga* as

the earliest known wholly ribbed atrypid and described it as being coarsely ribbed. The earliest species attributed to *Anazyga* are Sandbian 2 in age, whereas species previously attributed to *Zygospira* are Katian in age. They are commonly found in North America, but *Anazyga* species have also been reported from Laurentian terranes in the UK and Baltoscandia (Copper, 1977). Similarities in the internal structure of *Zygospira* and *Anazyga* suggest very close evolutionary affinities. Species have been transferred between *Anazyga* and *Zygospira* by various authors over the past 140 years. For example, a total of ten *Zygospira* species were transferred to *Anazyga* (Copper, 1977) based on stratigraphic ranges, the presence of teeth cavities, and a fused jugum. Baarli et al. (2022) inferred *Zygospira* + *Anazyga* as a monophyletic group, but it is possible each genus may be paraphyletic as historically defined.

The third anazygid genus, *Catazyga*, was proposed by Hall and Clarke (1894) and is currently assigned to the monotypic the subfamily Catazyginae. *Catazyga* is diagnosed as an oval-shaped rotund brachiopod with fine striated ribs. *Catazyga*'s origination is assumed to have occurred during the early Katian and is therefore younger than both *Anazyga* and *Zygospira. Catazyga* species are recorded from eastern North America and Europe. From the literature, there is no apparent doubt on the division between *Catazyga* and its related genera, given its uniqueness in terms of its rotundity and the high abundance of fine ribs. There are, however, uncertainties in *Anazyga*'s phylogenetic position in the clade, since externally, the genus appears to be related to *Zygospira*, but internally, shares multiple morphological features with both *Catazyga* and *Zygospira*, such as the dorsal spiralia with fewer whorls (Copper, 1977).

Internal characters have been given substantial taxonomic importance in differentiating *Anazyga* and *Zygospira*; however, the internal morphology of most species within the clade is not well understood. In total, only two species have well-documented brachidia, *Anazyga recurvirostra* and *Zygospira modesta* (Hall, 1862; Davidson, 1882). Due to variable internal taphonomic conditions and time constraints required to obtain the lophophore morphology in anazygids, little is known about species-specific internal anatomy. Generalizations from these two well-constrained species are frequently made when describing species and genera (Ross and Dutro, 1966) or no internal morphology is discussed at all (Cowper Reed, 1905; Fenton and Fenton, 1922; Cooper, 1956). These biases in species' descriptions make it difficult to fully account for the importance of internal morphology in evolutionary history of anazygid taxa. In this analysis, both internal and external characters were used to better comprehend internal relationships of the three genera, i.e., *Anazyga*, *Catazyga*, and *Zygospira*. I aim to show the importance of utilizing internal characters to describe the broadly distributed family, and to clarify the taxonomy within the family based on a holistic framework combining both internal and external morphology.

This chapter represents the first species-level phylogeny for the atrypid clades *Anazyga*, *Catazyga*, and *Zygospira*. The relative importance of internal vs. external characteristics to phylogeny estimation is examined, and the monophyly of each named genus is assessed and systematically revised as needed. By incorporating the fossilized birth-death and character evolution models, this analysis provides a framework for evaluating how evolution and origination patterns were impacted in these lineages during the globally recorded rise in Late Ordovician brachiopod diversity.

2.2 Materials and Methods

2.2.1 Focal Taxa

All available Late Ordovician Laurentian species of *Zygospira*, *Anazyga*, and *Catazyga* were analyzed and morphologically examined. In total, 147 specimens (**Table A1**) representing 20 anazygid species (**Table 1**) were included within the dataset. *Zygospira* species diagnoses follow recent revisions of Sproat and McLeod (2023). *Anazyga* and *Catazyga* species were identified following the original descriptions and revisions by Copper (1977). *Protozyga exigua* Hall, 1847 was included as the outgroup for comparison. This species was chosen because earlier phylogenetic analyses by Baarli et al. (2022) recovered *Protozyga* as a sister-group to Anazygidae.

The subspecies *Zygospira resupinata multicostata* Howe, 1965 from the Montoya Group in Texas is poorly understood, and its placement within *Zygospira resupinata* was suggested by Sproat and McLeod (2023) to possibly indicate an early lineage split between *Anazyga* and *Zygospira*. Because of that, *Z. resupinata multicostata* was added to the dataset as a separate operational taxonomic unit (OTU) in order to elucidate its phylogenetic relationships within the clade. Two *Catazyga* species from Scoto-Avalonia, *Catazyga arcana* Williams, 1962, and *Catazyga hicksi* (Cowper Reed, 1905), were also included in the analysis as this region has close paleoenvironmental and tectonic affinities with Laurentia (Harper et al., 2023). Similarly, *Catazyga homeospiroides* Ross and Dutro, 1966 from Alaska, was included within the dataset given its geographical proximity with Laurentia and tectonic displacement from Laurentian subterranes (Servais et al., 2023).

2.2.2 Characters and Coding

A total of 34 characters including external and internal traits were coded for the measured specimens (**Table 2**, and shown in **Figure 4**). The traits were selected based on the assessment of the published literature on the group (Copper, 1977; Baarli et al., 2022; Sproat and McLeod, 2023). Atrypida was the first brachiopod order to evolve the lophophore as a helical structure with ribbons of calcite (Brunton et al., 2001). Within Anazygidae, the number and directionality of lophophore whorls is considered a diagnostic trait, which is significant for systematics and classification. *Zygospira* spp. comprise species ranging from 4 to 10 mm in length, and the lophophore has 5 to 8 whorls bearing an outward orientation (Hall, 1862; Copper, 1977). *Anazyga* spp. are similar in size, ranging from 4 to 6 mm, and are described as typically possessing 1 to 3 whorls in their lophophore (Davidson, 1882; Copper, 1977). *Catazyga* spp. typically have larger valves than the other genera, with lengths ranging from 10 to 19 mm and bear 3 to 10 lophophore whorls (Hall and Clarke, 1894; Copper, 1977). The number of shell ribs, maximum length, and maximum width are also expected to have a strong phylogenetic signal. Therefore, these traits were included in the character set. Moreover, an empirical assessment of every sampled specimen allowed the identification of additional traits. Many of these traits are continuous characters. However, the incorporation of continuous traits in morphological phylogenetics has long been challenging (Rae, 1998; Goloboff et al., 2006; Parins-Fukuchi, 2018) due to the mathematical limitations of incorporating continuous values into analyses. Consequently, the ten characters within this dataset that represent continuous traits (i.e., maximum shell length, maximum shell width, and maximum shell height) were converted into categorical character states for analysis. The

categorization was initially graphically executed, by looking for natural breaks in the slopes in a plot as is typical for phylogenetic analyses of similar clades (Stigall Rode, 2005; Wright and Stigall, 2013, 2014; Bauer and Stigall, 2016).

After manual identification of character state ranges, an analysis of variance (ANOVA) was conducted in R to identify whether the character states were statistically distinct. Therefore, for each continuous character, observed measurements were binned into proposed character states. The data within bins were assessed to determine statistical significance. If the bins were statistically distinct, they were accepted as valid states. If not, the process was repeated until statistically distinct character states were identified. In general, for each continuous trait, the data were divided into multistate characters. Conversely, categorical traits (such as presence or absence) were mainly binary characters. Polymorphism was commonly observed in anazygids, and therefore, incorporated into the final character matrix as well.

2.2.3 Phylogenetic Analysis

Phylogenetic analysis was conducted using a Bayesian phylogenetic approach in BEAST 2.5 v2.7.6 (Bouckaert et al., 2019). The fossilized-birth-death skyline model (or FBDSKY) was incorporated into the Bayesian framework to reconstruct evolutionary

Table 1. Species included in the phylogenetic analysis. Names on the first and second columns indicate original and current taxonomic nomenclature, respectively. Anazyga species are transferred to Zygospira herein, therefore, names on the third column indicate the updated nomenclature (this study). * Indicates outgroup species.

Original nomenclature	Current nomenclature	This study
*Protozyga exigua** Hall, 1897	*Protozyga exigua** Hall, 1897	*Protozyga exigua** Hall, 1897
Anazyga calhouensis Fenton and Fenton, 1922	*Anazyga calhouensis* Fenton and Fenton, 1922	*Zygospira calhouensis* (Fenton and Fenton, 1922)
Zygospira circularis Cooper, 1956	*Anazyga circularis* (Cooper, 1956)	*Zygospira circularis* Cooper, 1956
Zygospira lebanonensis Cooper, 1956	*Anazyga lebanonensis* (Cooper, 1956)	*Zygospira lebanonensis* Cooper, 1956
Zygospira aff. Z. putilla Ross, 1959	*Zygospira aff. putilla* Ross, 1959	*Zygospira idahoensis* new sp.
Atrypa recurvirostra Hall, 1847	*Anazyga recurvirostra* (Hall, 1847)	*Zygospira recurvirostra* (Hall, 1847)
Zygospira variabilis Fenton and Fenton, 1922	*Anazyga variabilis* (Fenton and Fenton, 1922)	*Zygospira variabilis* Fenton and Fenton, 1922
Zygospira anticostiensis Billings, 1862	*Catazyga anticostiensis* (Billings, 1862)	*Catazyga anticostiensis* (Billings, 1862)
Catazyga arcana Williams, 1962	*Catazyga arcana* Williams, 1962	*Catazyga arcana* Williams, 1962
Catazyga cartieri Cooper and Kindle, 1936	*Catazyga cartieri* Cooper and Kindle, 1936	*Catazyga cartieri* Cooper and Kindle, 1936
Athyris headi Billings, 1862	*Catazyga headi* (Billings, 1862)	*Catazyga headi* (Billings, 1862)
Zygospira hicksi Cowper Reed, 1905	*Catazyga hicksi* (Cowper Reed, 1905)	*Zygospira* hicksi Cowper Reed, 1905
Catazyga homeospiroides Ross and Dutro, 1966	*Catazyga homeospiroides* Ross and Dutro, 1966	*Catazyga homeospiroides* Ross and Dutro, 1966
Zygospira uphami Winchell and Schuchert, 1893	*Catazyga uphami* (Winchell and Schuchert, 1893)	*Zygospira uphami* Winchell and Schuchert, 1893
Zygospira cincinnatiensis James in Meek, 1873	*Zygospira cincinnatiensis* James in Meek, 1873	*Zygospira cincinnatiensis* James in Meek, 1873
Zygospira concentrica Ulrich, 1879	*Zygospira concentrica* Ulrich, 1879	*Zygospira concentrica* Ulrich, 1879

Table 1 Continued

Zygospira kentuckiensis Nettelroth, 1889	*Zygospira kentuckiensis* Nettelroth, 1889	*Zygospira kentuckiensis* Nettelroth, 1889
Zygospira modesta Say in Hall, 1847	*Zygospira modesta* Say in Hall, 1847	*Zygospira modesta* Say in Hall, 1847
Zygospira resupinata Wang, 1949	*Zygospira resupinata* Wang, 1949	*Zygospira resupinata* Wang, 1949
Zygospira resupinata multicostata Howe, 1965	*Zygospira resupinata multicostata* Howe, 1965	*Zygospira multicostata* new sp.
Zygospira sulcata Howe, 1965	*Zygospira sulcata* Howe, 1965	*Zygospira sulcata* Howe, 1965

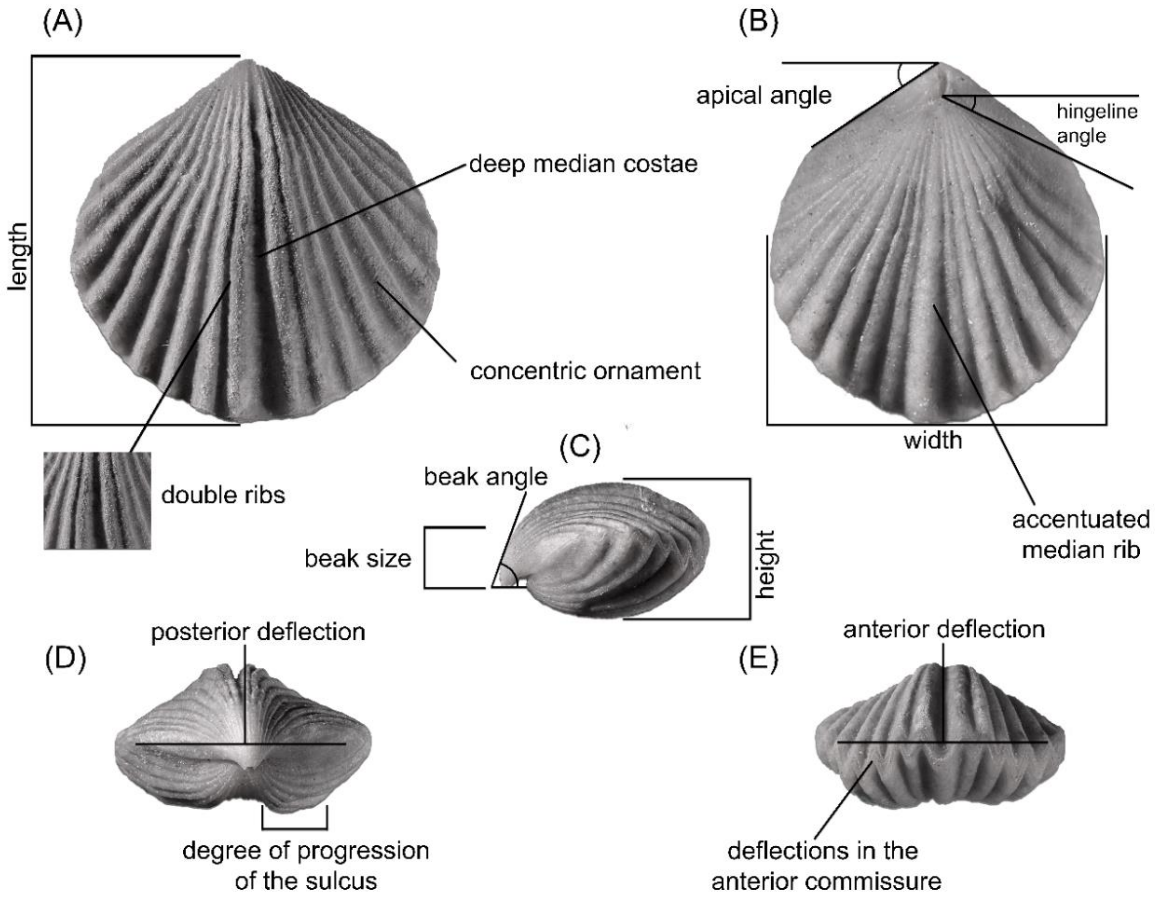

Figure 4. External characters used in the analysis for all the species Table 1. Zygospira modesta Say in Hall, 1847 from the Arnheim Formation of Brookville, Indiana. (A) Dorsal view; (B) Ventral view; (C) Lateral view; (D) Posterior view (hinge line); and (E) Anterior view (commissure opening).

Table 2. Characters used in the phylogeny. * Indicates internal characters.

Character	Character states
1. Maximum length (mm)	(0) 0-5, (1) 5-10, (2) 10-15, (3) +15
2. Maximum width (mm)	(0) 0-5, (1) 5-10, (2) 10-15, (3) +15
3. Maximum height (mm)	(0) 0-5, (1) 5-10, (2) 10-15, (3) +15
4. L/W ratio	(0) 0-1, (1) 1-2
5. Outline	(0) Quadrate, (1) Rectangular, (2) Transverse, (3) Elliptical, (4) Elongate, (5) Pentagonal
6. Number of ribs ventral valve	(0) 0-10, (1) 10-20, (2) 20-30, (3) +30
7. Number of ribs dorsal valve	(0) 0-10, (1) 10-20, (2) 20-30, (3) +30
8. Concentric ornament	(0) Absent, (1) Growth lines
9. Ribs appearance	(0) Weak, (1) Strong, (2) Very fine
10. Profile	(0) Biconvex, (1) Dorsibiconvex, and (2) Ventribiconvex
11. Beak angle (°)	(0) 0-20, (1) 20-40, (2) 40-60, (3) +60
12. Beak size (mm)	(0) 0-5, (1) +5
13. Position fold/sulcus	(0) Not developed, (1) Originating near the umbo and extending to the anterior margin, (2) Originating anterior to the umbo
14. Apical angle (°)	(0) 0-40, (1) 40-60, (2) +60
15. Hinge line angle (°)	(0) 0-40, (1) 40-60, (2) +60
16. Accentuated median costa	(0) Absent, (1) Present

Table 2 Continued

17. Sinuosity of the anterior commissure	(0) Rectimarginate, (1) Parasulcate, (2) Paraplicate, (3) Unisulcate, (4) Sulciplicate, (5) Bisulcate
18. Anterior deflection (mm)	(0) 0-3, (1) 3-5, (2) +6
19. Posterior deflection (mm)	(0) 0-2, (1) 2-6, (2) +6
20. Deep median costa	(0) Absent, (1) Present
21. Deflections in the anterior commissure	(0) Absent, (1) Zig-zag
22. Double ribs	(0) Absent, (1) Present
23. Degree of progression of the sulcus (mm)	(0) 0-2, (1) 2-4, (2) 4-6, (3) +6
24. Accentuated median rib (ventral)	(0) Absent, (1) Present
25. Sulcus and fold appearance	(0) Weak, (1) Strong
26. Ribs spacing (number of ribs dorsal valve / maximum width)	(0) 0-2, (1) 2-4, (2) 4-6, (3) +6
27. Deflection rate (anterior)	(0) 0-2, (1) 2-4, (2) +4
28. Deflection rate (posterior)	(0) 0-2, (1) 2-4, (2) +4
29. Number of whorls*	(0) 0-5, (1) 5-10, (2) +10
30. Jugum position*	(0) Absent, (1) Short, (2) Posteroventral, (3) Mediodorsal
31. Cardinal processes*	(0) Absent, (1) Present

Table 2 Continued

32. Teeth*	(0) Absent, (1) Weak, (2) Strong
33. Jugum shape*	(0) D-shaped, (1) V-shaped, (2) W-shaped
34. Hinge plates*	(0) Absent, (1) Present

Table 3. Coded character matrix for the phylogeny. Names indicate prior taxonomic assignments. All *Anazyga* species are transferred to *Zygospira* herein. Character numbers (C) correlate with **Table 2**. Parenthesis indicate multistate characters.

C	*Z. modesta*	*Z. sulcata*	*Z. kentuckiensis*	*Z. resupinata*	*Z. cincinnatiensis*	*Z. concentrica*	*Z. multicostata*	*A. circularis*	*A. lebanonensis*	*A. pupilla*	*A. recurvirostra*	*A. variabilis*	*A. calhounensis*	*C. headi*	*C. cartieri*	*C. homeospiroides*	*C. anticostiensis*	*C. arcana*	*C. hicksi*	*C. uphami*	*P. exigua*
1	0	0	1	0	1	0	0	0	0	0	0	0	0	(12)	1	1	1	1	0	0	0
2	0	0	1	0	1	1	0	0	0	0	0	0	0	(12)	1	1	1	1	0	0	0
3	0	0	1	0	1	0	0	0	0	0	0	0	0	(12)	1	1	1	0	?	0	0
4	(12)	1	1	(12)	1	(12)	(12)	1	1	2	(12)	1	2	2	2	2	2	2	2	2	(12)
5	1	(13)	(12)	(23)	1	(23)	3	1	1	3	(124)	1	3	(235)	3	3	(35)	4	3	5	(24)
6	(12)	2	(12)	(12)	1	2	(23)	2	1	1	(12)	1	1	(23)	3	1	3	3	0	(23)	0
7	1	2	(12)	(12)	1	1	(23)	2	1	1	(12)	(12)	1	(23)	3	(12)	(23)	3	0	(12)	0
8	0	0	1	0	1	1	0	0	0	0	0	0	0	1	0	1	1	1	1	1	0
9	1	1	1	1	1	0	1	1	1	1	1	1	2	2	2	1	1	2	1	1	2
10	2	0	1	2	(12)	0	0	1	1	0	1	0	(12)	1	0	0	1	1	0	1	(12)
11	(123)	2	(23)	(23)	(12)	2	(23)	?	(12)	2	(12)	2	(23)	(23)	2	2	(23)	?	?	(23)	2
12	0	0	1	0	1	0	1	?	0	0	0	0	0	(12	12	1	1	?	?	1	0
13	(12)	(12)	(12)	(12)	(12)	(12)	2	2	1	2	(12)	2	1	(12)	2	2	(12)	1	1	2	1
14	(12)	1	1	2	1	2	1	1	1	(12)	1	1	(12)	(12)	1	1	1	?	?	2	1
15	(12)	(23)	2	2	2	2	1	2	2	3	2	(12)	(23)	(23)	2	2	2	?	?	2	2
16	0	1	0	0	0	0	1	0	0	0	0	0	0	0	0	0	0	0	0	0	0
17	(125)	(13)	(15)	2	(145)	4	(13)	1	1	2	1	1	3	(23)	0	0	0	3	?	1	1
18	1	1	(12)	1	1	1	1	0	1	1	1	1	1	(12)	1	1	(12)	?	?	1	0
19	1	1	(123)	1	1	2	1	1	1	1	1	1	1	(123)	(23)	2	(12)	?	?	1	1
20	1	1	1	1	1	1	1	0	0	0	0	0	0	1	0	0	0	0	1	0	0
21	1	1	1	1	1	0	?	1	1	1	1	1	1	1	1	1	1	?	?	0	0
22	1	1	0	0	1	0	1	0	0	1	0	0	0	0	0	0	0	0	0	1	0
23	1	0	1	0	1	0	0	0	0	0	1	0	?	1	1	?	0	?	?	0	0
24	1	1	0	0	1	1	1	0	0	1	0	0	0	0	0	0	0	0	0	0	0
25	1	1	1	0	1	1	?	1	1	1	1	1	0	1	0	0	1	1	0	0	0
26	1	1	1	1	1	1	(12)	2	1	1	1	1	1	1	1	1	1	1	1	(12)	1
27	0	0	1	0	1	0	0	0	0	0	0	0	0	1	1	1	1	?	?	0	0
28	0	1	1	0	1	0	0	0	0	0	0	0	0	1	1	2	0	?	?	0	0
29	0	?	?	?	?	?	?	?	?	?	0	?	?	?	?	?	?	?	?	?	0
30	2	?	?	?	?	?	?	?	?	?	3	?	?	?	?	?	?	?	?	?	3
31	0	?	?	?	?	?	?	?	?	?	0	?	?	1	?	0	?	?	?	?	?
32	2	?	?	?	?	?	?	?	?	?	2	?	?	2	?	?	?	?	1	?	1
33	1	?	?	?	?	?	?	?	?	?	2	?	?	?	?	?	?	?	?	?	2
34	?	?	?	?	?	?	?	?	?	?	?	?	?	1	?	?	?	?	?	?	?

rates during the Late Ordovician. The birth-death model is a divergence time estimation model (Wright, 2019). As proposed by Stadler (2010), the birth-death model is a stochastic model which simulate rates of birth (λ) and death (μ) for individuals sampled in the past at a rate (ψ). When applied to a fossilized birth-death model, λ is considered as species' origination (speciation events), μ is the extinction rate of a branch, and ψ as fossils' taphonomic biases (Stadler et al., 2018). The fossilized birth-death model can also be viewed as a hierarchical Bayesian model, composed of three parts: (1) non-negative constant rates (i.e., extinction, and speciation); (2) chronostratigraphic data for fossil dating; and (3) the morphological character matrix (Wright et al., 2021). FBD's principal strength is that the model returns absolute time-dated phylogenetic trees, allowing inference of divergence times (Wright, 2019). When applied to FBD models, skyline models allow the independent estimation of evolutionary rates for each different time bin (Stadler et al., 2013; Wright, 2019).

Extinction and origination rates were obtained from the Paleobiology Database or PBDB (paleobiodb.org) platform based on generalized rates for the Rhynchonelliformea clade (=all articulated brachiopods). 21,242 occurrences of Ordovician rhynchonelliform taxa were extracted from the PBDB and the mean origination rate was calculated for each of the seven Ordovician Ages (i.e., Tremadocian, Floian, Dapingian, Darriwilian, Sandbian, Katian, and Hirnantian). The origination formula was based on the per-capita rate of origination proposed by Foote (2000), which considers the time interval duration and the number of boundary crossers. Mean per-capita origination rate and the total number of occurrences was then used to calculate mean extinction and turnover rates in R using a lognormal likelihood model (see **Attachments**).

Chronostratigraphic ranges were created for each individual species based on data obtained from oldest and earliest-known occurrences from museum specimens augmented with data from the PBDB (**Table 4**). To avoid regional synonyms and outdated nomenclature, all geologic formations and units' names were revised and adapted to the recently revised Cincinnatian Series' sequence stratigraphy (Brett et al., 2020). Absolute ages follow the Ordovician timescale of Goldman et al. (2020). FBD dating was applied through the log-normal relaxed clock in BEAST2.5 (Bouckaert et al., 2019), with a mean substitution rate of 0.1 per millions of year in a gamma distribution model. The log-normal clock model predicts that the evolutionary rate in branches is generally low and allows a better implementation in fossil-only phylogenies (Ho and Phillips, 2009; Wright et al., 2021).

The FBD model was applied using a Monte Carlo Markov-Chain (MCMC) to infer the highest marginal likelihood for each model; this process employs random values for the assumed parameters in each of 2,000,000 runs. The burn-in value was set to 10,000 initial generations. The substitution model for categorical characters was constrained by the Mk Model (Lewis, 2001). The Mk Model assumes that the changes between states have equal probability of occurring. For this model, we predicted a gamma distribution in the rates dynamics (extinction, origination, and turnover).

Table 4. Chronostratigraphic data for the 21 analyzed species in millions of years (MYA). Age range is from Middle Ordovician (453.5 Ma) to the Ordovician-Silurian boundary (443.07) follow dates within Goldman et al. (2020). Names indicate prior taxonomic assignments. First appearance (FA), and last appearance (LA) are given for all analyzed species. All *Anazyga* species are transferred to *Zygospira* herein. * Indicates outgroup species.

Taxon	**FA**	**LA**
*Protozyga exigua**	453.5	450
Zygospira modesta	450.5	446.04
Zygospira sulcata	451	450.5
Zygospira resupinata	450	450
Zygospira cincinnatiensis	451	450
Zygospira kentuckiensis	451	448
Zygospira concentrica	451	450.5
Zygospira resupinata multicostata	451	450.5
Anazyga circularis	453.5	451
Anazyga lebanonensis	453.5	451
Anazyga aff. *Putilla*	453.5	451
Anazyga recurvirostra	453.5	450
Anazyga variabilis	453.5	451
Anazyga calhounensis	451	450
Catazyga headi	448	443.07
Catazyga cartieri	451	450
Catazyga homeospiroides	451	450
Catazyga anticostiensis	450	445.5
Catazyga arcana	453.5	451
Catazyga hicksi	450.5	450
Catazyga uphami	451	450

Both the total-evidence phylogenetic models (Ronquist et al., 2012) and clade constraints relevant to a fossil-only phylogeny based singularly in morphological data (Barido-Sottani et al., 2020) were incorporated into the model design. The use of these constraints works to stabilize the topology (as suggested by Barido-Sottani et al., 2023), and was employed after considering the outputs of the first two total-evidence scenarios. To assess the effects of the internal traits dataset on anazygid phylogeny, I analyzed four potential scenarios: (1) A tree composed of external + internal traits with no phylogenetic constraints; (2) A tree composed of external traits only with no phylogenetic constraints; (3) A tree composed of external traits only and implementing a Catazyginae constraint, which requires *Catazyga* species (exclusive of *Catazyga hicksi* and *C. uphami*) to resolve as a clade; and (4) A tree composed of external traits only which applied three monophyletic constraints (one for each genera).

To assess the highest posterior probability of each scenario, the software TRACER (Rambaut et al., 2018) was used to evaluate each individual run as suggested by Nascimento et al. (2017). The most probable run was chosen based on its posterior probability mean, its ESS values, and its tracer mixing. Additionally, the selected MCMC run was summarized through the Maximum Clade Credibility (MCC) method considering the median heights in TreeAnnotator (distributed with BEAST2). MCC operates by searching for the MCMC sample with the largest sum of posterior probabilities (Heled and Bouckaert, 2013).

Subsequently, a skyline model was applied to the optimal resulting MCC tree (Scenario 3). Four time intervals were considered for the skyline model, based on the North-American Ordovician stages: Interval 1: Chatfieldian (Sandbian 2 and Katian 1

stage slices), Interval 2: Edenian (Katian 2), Interval 3: Maysvillian (Katian 3), and Interval 4: Richmondian (Katian 4) and Gamachian (Hirnantian) Stage. Exponential priors were considered for each estimated rate i.e., birth (speciation), death (extinction), and sampling probability. To assess different birth, death, and sampling probability rates for each individual time interval, a 5,000,000 Monte Carlo Markov-Chain (MCMC) was performed, with a set burn-in of 500,000 runs.

2.2.4 Repositories and institutional abbreviations

Specimens from the type series for each species were analyzed when available. Additionally, or when types were not available, non-type and illustrated specimens from the literature were coded to incorporate the wide range of morphological and geographical variation for each species. For all specimens, both the dorsal and ventral valves were analyzed. The measures of internal characters was limited; therefore, internal characters were coded mainly from literature sources (Davidson, 1882; Cowper Reed, 1905; Foerste, 1910; Williams, 1962; Copper, 1977, 1986).

Types, figures, and other specimens examined in this study are deposited in the following institutions: Smithsonian National Museum of Natural History (NMNH), Washington D.C, USA; Cincinnati Museum Center (CMC), Cincinnati, USA; Field Museum of Natural History (FMNH), Chicago, USA; Minnesota Geological Survey (MGS); University of Iowa Museum of Natural History (UIMNH), Iowa City, USA; Sedgwick Museum at Cambridge University (SMCU), UK; and Walker Museum (WM).

2.3 Systematic Paleontology

The original description and later revisions were sufficient to characterize some anazygids species; species that do not require additional revision or description are listed on **Table 5**. The original and subsequent descriptions of these species may be combined with the data in **Table 3** to provide enhanced diagnosis.

Revised generic descriptions and species descriptions for seven species are presented below. The genera *Anazyga* and *Zygospira* are synonymized as *Zygospira. Zygospira aff. putilla* Ross, 1959 is recognized as a new species, *Zygospira idahoensis* n. sp. The subspecies *Zygospira resupinata multicostata* Howe, 1965 is elevated in the taxonomic rank to an independent species, *Zygospira multicostata* n. sp.

Class Rynchonellata Williams et al. (1996)

Order Atrypida Rzhonsnitskaya (1960)

Family Anazygidae Davidson (1882)

Subfamily Anazyginae Davidson (1882)

Genus *Zygospira* Hall (1862)

Type species. — Producta (Atrypa) modesta Say in Hall, 1847 Katian, Cincinnati, OH and Nashville, TN regions.

Diagnosis. — Small biconvex shells. Outline subcircular or elliptical. Surface sharply plicated with fine or strong ribs. Ventral valves often have an accentuated median costa, fewer ribs, and elevated marginal ridges from the sulcus. Dorsal valves composed of double radiating ribs, and a deep median costa. Concentric growth lines are usually

Table 5. Specimens examined for species that do not require taxonomic revision. * Indicates non-type specimens.

Species	Museum	Catalog number	Type
C. anticostiensis	USNM	PAL 94413a	*
	USNM	PAL 94413b	*
	CMNH	22638a	*
	CMNH	22538b	*
C. arcana	Willians (1962)	BB 26733	Holotype
C. headi	USNM	PAL 87052	Plesiotype
	USNM	PAL 87052	Plesiotype
	Copper (1977)	GS 45398	*
	FMNH	PE 89339	*
	CMNH	95342	*
	CMNH	89904	*
	CMNH	89538	*
	CMNH	6182	*
	FMNH	PE 89341a	*
	FMNH	PE 89341b	*
Z. cincinnatiensis	CMNH	PE 9509	*
	CMNH	28127	*
	CMNH	69136	*

Table 5 Continued

Z. cincinnatiensis	CMNH	19064	*
	CMNH	18946	*
Z. concentrica	CMNH	19027a	*
	CMNH	19027b	*
	CMNH	33583	*
	CMNH	18969	*
Z. kentuckiensis	USNM	PAL 511871	Plesiotype
	USNM	PAL 511872	Plesiotype
	USNM	PAL 97596	Plesiotype
	USNM	PAL 9748a	*
	USNM	PAL 9748b	*
	CMNH	19062a	*
	CMNH	19062b	*
	CMNH	54470a	*
	CMNH	54470b	*
	CMNH	33663a	*
	CMNH	33663b	*
Z. modesta	USNM	PAL 40485	Plesiotype
	USNM	PAL 418150	Plesiotype

Table 5 Continued

Z. modesta	USNM	PAL 418149	Plesiotype
	USNM	ACC 175438a	*
	USNM	ACC 175438b	*
	USNM	PAL 1.22F1	*
	USNM	PAL 1356a	Lectotype
	Foerste (1910)	1356-1	*
	FMNH	6460	*
	FMNH	1496	*
	CMNH	64207a	*
	CMNH	64207b	*
	CMNH	69130a	*
	CMNH	69130b	*
Z. recurvirostra	USNM	PAL 87057	Plesiotype
	USNM	PAL 97609	Plesiotype
	USNM	PAL 78460	Holotype
	USNM	PAL 24869	*
	USNM	PAL 24871	*
	USNM	PAL 124826	Plesiotype
	USNM	PAL 705.3	Holotype
	FMNH	P9509	*

Table 5 Continued

Z. resupinata			
	USNM	PAL 2.6G5c	*
	USNM	PAL 2.6G5c	*
	USNM	ACC 306219	*
	USNM	ACC 306219	*
	USNM	PAL 175438	*
	USNM	PAL 175438	*
	SUI	1874	Holotype
	SUI	1873	Paratype
Z. sulcata	USNM	PAL 145059	Paratype
	USNM	PAL 145059	Paratype
	USNM	PAL 145059	Paratype

absent. Distinct and curved beak, often with an acute angle from the ventral shell. Strong to weak fold and sulcus, resulting in a wide commissure. Commissure shape varies. Acute dorsal apical area, narrow and prominent ventral umbo, associated with a small, and triangular delthyrium. Crura are oppositely long, extending anteriorly to the shell in a dorsally oriented spiralia. The number and shape of whorls vary, and the presence of dental cavities is observed.

Occurrence. — Early Late Ordovician (Sandbian 2 – Katian 4 stages), mostly abundant in the strata of central to eastern North America. In the United States, *Zygospira* is abundant and diverse in rocks from the Katian 2 to Katian 3 stages (Edenian to Maysvillian stages in North American nomenclature).

Description. — Maximum average length of 7.05 mm, width of 7.27, and height of 4.43 mm. Quadrate (W > L) to elliptical (L > W) shells, circular outline, with marginal plications. Costae always present, average of 22.07 ventral, and 21.48 dorsal costae. Curved, short or long beaks (average size of 2.16 mm). Pedicle foramens are always open and exposed. When fold and sulcus are strong, ventral valve is risen on the two lateral sides, forming a distinct progression, seen in most species (average length of 1.28 mm on the righthand side). Jugum dorsally positioned, with variable shape (e.g., D or V-shaped), spiralia whorls variable ranging from 1 to 10.

Other species. — *Anazyga calhounensis* Fenton and Fenton, 1922 type's horizon and locality unknown, non-types from the Kimmswick Limestone in Batchtown, IL, U.S.; *Zygospira circularis* Cooper, 1956 from the upper Carters Formation, Franklin, TN, U.S.,

and Saturday Mountain Formation, Lemhi Range, ID, U.S.; *Zygospira lebanonensis* Cooper, 1956 from the Lebanon Formation, Shelbyville, TN, U.S., and Saturday Mountain Formation, Lemhi Range, ID, U.S.; *Zygospira aff. putilla* Ross, 1959 = *Zygosprira idahoensis* n. sp. from the Saturday Mountain Formation in Lemhi Range, ID, U.S.; *Atrypa recurvirostra* Hall, 1847 from the Trenton Group, MN, NJ, NY, and VA, U.S., Red River Formation, MT, U.S., and Cynthiana Formation, KY, U.S.; *Zygospira variabilis* Fenton and Fenton, 1922 from the Plattin and Black River formations, KY, U.S.; *Zygospira cincinnatiensis* James in Meek, 1873 from the Hudson River Group, Kope, Fairview (Fairmount Member), and Mt. Auburn formations in Cincinnati, OH, U.S.; *Zygospira concentrica* Ulrich, 1879, from the Kope, Lorraine, and Bellevue formations in Cincinnati, OH, U.S.; *Zygospira kentuckiensis* Nettelroth, 1889 from the Waynesville Formation in Jefferson, Marion, and Oldham counties, KY, U.S., Reedsville Formation near Ewing, VA, U.S., and Manitoulin Island in Canada; *Zygospira modesta* Hall, 1847 from the Hudson River Group, Fairmount and Corryville formations in Cincinnati, OH, U.S., Liberty Formation in Oxford, OH, U.S., Arnheim Formation in Nashville, TN and Waynesville, OH, U.S., and Whitewater Formation in South Gate, IN, U.S.; *Zygospira resupinata multicostata* Howe, 1965 = *Zygospira multicostata* n. sp. from the Montoya Group, El Paso, TX, U.S.; *Zygospira resupinata* Wang, 1949 from the Maquoketa Formation, Jackson County, IA, U.S., Elkhorn Formation, in Hamburg, IN, and Eaton, OH, U.S.; *Zygospira sulcata* Howe, 1965 from the Montoya Group, El Paso, TX, U.S. *Zygospira uphami* from the Galena Group in Weisebach's Dam, Spring Valley, and Wykoff and Fountain, MN, U.S.; and *Zygospira hicksi* Cowper Reed, 1905 from the Slade Formation, Haverfordwest, Wales.

Remarks. — Zygospira was proposed by Hall (1862) and externally defined as "shell bivalve, equilateral, inequivalve, surface plicate in the typical species; a sinus in the dorsal valve", with the typical form being *Zygospira modesta*. In relation to its internal morphology, *Zygospira* was compared to being similar to *Atrypa*, another atrypid genus, that had a similar loop arrangement. *Anazyga* was proposed as a distinct genus by Davidson (1883) based on its smaller size, oval outline, and the whorls being positioned in the same direction as observed in *Zygospira*. However, shortly thereafter, Hall and Clarke (1894) noted that the morphological features of *Zygospira*, mostly related to the jugum position supported synonymizing *Anazyga* with the older *Zygospira* (Hall and Clarke, 1894; Sproat and McLeod, 2023). Eighty years later, uncertainties overlying Anazygidae came back into debate. Copper (1977) restored the *Anazyga* Davidson, 1882 as a discrete genus based on size, the direction of the spiralia, and rib appearance. Copper (1977) reassigned basal zygospirinid forms to *Anazyga* Davidson 1883, claiming that the two genera differ by *Zygospira* externally "having coarser ribs, more strongly carinated shells, with differentiated mid and lateral ribs, and planoconvex-ventribiconvex shells". Williams et al. (1996) analyzed zygospirinid specimens, and showed that biconvexity, and accentuated costae are predominant in both *Anazyga* and *Zygospira*, and argued, that these features should not be used to distinguish the two genera.

Sproat and McLeod (2023) recently recharacterized *Zygospira* based on its coarse external ribs and its mediodorsally directed spiralia based on internal data from the Treatise on Invertebrate Paleontology (Copper, 2002). Both the studies of Copper (1977) and Sproat and McLeod (2023) constrained the genus *Zygospira* to comprise stratigraphically younger species. However, these species do not optimize as clades in

the phylogenetic analyses, which suggests the two genera are not discrete historical entities.

Copper (1977) also pointed to differences in internal morphology of the type species of *Anazyga* and *Zygospira* as having a larger number of whorls and the jugum being positioned postero-dorsally. Nonetheless, the availability of internal data is not enough to show a phylogenetic signal, separating the clades (see 2.5 Discussion). Thus, although the type species of *Anazyga recurvirostra* and *Zygospira modesta* show distinct jugal processes, the variability seen within *Zygospira* itself (Hall and Clarke, 1894; Howe, 1965; Sproat and McLeod, 2023), and external morphological features indicate that both genera may be variations of the same lineage. Notably, neither genus optimizes as a clade within the best supported phylogenetic reconstruction and attempts to force the species into monophyletic groups reflecting historical species associations are much more poorly supported. Consequently, my analyses strongly support synonymy of *Anazyga* with *Zygospira*, and I propose the transfer of all valid species previously attributed to *Anazyga* to the genus *Zygospira.*

Zygospira multicostata new species

Figure 5, 1–5

1965 *Zygospira resupinata multicostata* Howe, p. 653, pl. 81, figs. 1–8.

1997 *Zygospira resupinata multicostata* Jin et al., p. 40, pl. 30, figs. 1–21.

Type specimens. — Holotype: USNM PAL 145054; Paratypes: USNM PAL 145055, USNM PAL 145056, and USNM PAL 145057 from the Aleman Limestone of the Late

Ordovician Montoya Group (Katian 2 Stage: Cincinnatian, Edenian), Hueco Mountains, El Paso, Texas, U.S.

Diagnosis. — Elliptical, biconvex, parasulcate, gently folded shells. Numerous strong ribs, presence of double ribs, and ventral accentuated median costae. Remarkable resupination on the dorsal and ventral shells, i.e., ventral folding and dorsal sulcation. Short and curved beak. Small delthyrium, and palintrope area, mostly covered by the curved, accentuated umbo.

Occurrence. — Aleman Limestone (Katian 2) of the Montoya Group in the Hueco and Franklin mountains, New Mexico, U.S.; Surprise Creek (Katian 3, Maysvillian Stage) and Caution Creek (Katian 4, early Richmondian Stage) formations, in Ontario, Canada.

Description. — Average length of 7.05 mm, width of 6.75, and height of 4.74 mm. Costae numerous, average dorsal costae number of 27.73, and ventral of 28.73. Costae originating anterior to the umbo. In the dorsal valve, deep median costae and double ribs are often observed. The ventral valve has accentuated median costae and very gentle sulcus. Shell resupinate. Internal characters largely unknown.

Etymology. — Following the original description (Howe, 1965), the subspecific name *multicostata* comes from Latin. Relying on the species' abundant number of costae, the prefix "multi" meaning "many" and the adjective "costatus" meaning "ribbed".

Remarks.— *Zygospira multicostata* is distinguishable from *Zygospira resupinata* Wang, 1949 by its larger number of ventral and dorsal costae (27-28 to 16-19, respectively), greater resupination, larger size, and thicker shells as discussed in Howe (1965) and

Sproat and McLeod (2023). When compared to the two zygospirinids from the Cincinnati basin, *Zygospira modesta* and *Z. kentuckiensis*, *Z. multicostata* shows gentler fold and sulcus, resupination, and more ribs (>25). Jin et al. (1997) noted that Canadian forms of the species are more elongate and have a larger number of ribs (25–35). *Z. multicostata* is placed within *Zygospira* based on its plicated shells, small size, double-ribbed costae, and distinct apical region. Based on one single specimen, Sproat and McLeod (2023) noted that *Z. multicostata*'s calcified lophophore has a dorsomedial directionality, consistent with *Zygospira* (Hall, 1847; Davidson, 1882).

Zygospira idahoensis new species

Figure 6, 1-5

1913 *Atrypa putilla* Savage, p. 85, pl IV, fig. 25.

1959 *Zygospira aff. putilla* Ross Jr., p. 457, pl. 56, figs 11–12.

Type specimens. — Holotype: USNM PAL 133263 (figured), from the Saturday Formation, Lemhi Range, Idaho, U.S.

Occurrence. — Sandbian, Late Ordovician (Mohawkian Series) in the United States. Hudson River Group in Missouri, U.S.; Saturday Mountain Formation (Sandbian 2) in Lemhi Range, Idaho, U.S.

Additional Materials. — USNM PAL 133262, USNM PAL 133263.

Description. — Average length of 3.7 mm, width of 3.31, and height of 1.94 mm. Biconvex, elongate shells, average number of costae is 14 in the ventral valve and 12 in the dorsal valve. Strong and distinct costae radiating anterior to the umbo, lack of

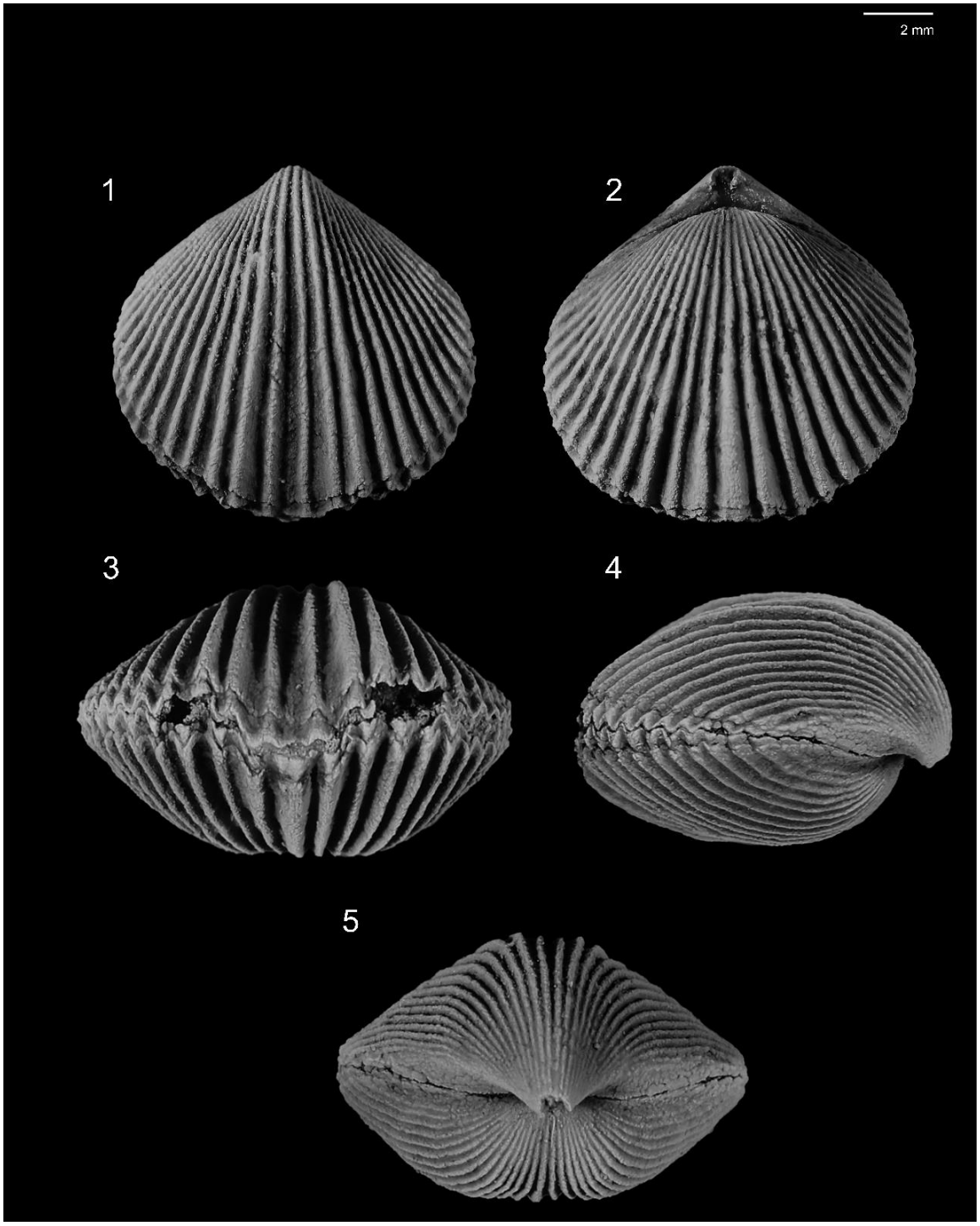

Figure 5. Holotype of *Zygospira multicostata* (USNM PAL 145054). (1) Dorsal, (2) ventral, (3) commissure, (4) lateral, and (5) hinge line views.

concentric ornamentation. Prominent curved umbo, projecting in a 55° angle from the dorsal shell.

Remarks.— In their original description of *Zygospira putilla*, Hall and Clarke (1894) recognized the specimens' morphological similarities with the genus *Zygospira*, mainly relying on the plications on the valves and the posteriorly directed spiralia, and erected the Silurian zygospirinid species *Zygospira putilla*. Amsden (1974) synonymized *Zygospira putilla* and *Atrypa praemarginalis* into one species, *Eospirigerina putilla* due to ontogenetic evidence and overall shell size. *Eospirigenina* is a member of the subfamily Spirigerininae, which is not closely related to the Anazyginae, which includes *Zygospira* (Baarli et al., 2022). Thus *Z. putilla* is excluded from the monophyletic concept of *Zygospira* developed herein. The specimens examined by Amsden (1974) and Ross (1959) from the Edgewood Formation are in fact, eospirigerinid forms (see Plates 18 figs 1a-1j and 19 figs. 1a-1h in Amsden (1974)) and members of a clade exclusive of the Anazygidae.

However, Ross (1959) also identified *Z. putilla*-like specimens from the Saturday Mountain Formation (Sandbian 2 Stage) as atypical *Z. putilla* specimens. These atypical specimens were identified as *Zygospira aff. Z. putilla* Hall and Clarke, 1894. Morphological affinities shared between the collected specimens and *Zygospira recurvirostra*, *Z. circularis*, and *Z. lebanonensis* were addressed.

Ross' *Zygospira aff. Z. putilla* specimens differ from typical *Z. putilla* forms by their unusual elongate outline, small size, strong ribs, lack of concentric ornamentation, the presence of double-ribbed valves, and its occurrence in Late Ordovician (Mohawkian) strata. The non-identified specimens collected by Ross (1959) were submitted to a

Bayesian phylogenetic analysis (this study) and are considered as a sister taxon to *Zygospira multicostata* and *Zygospira modesta*. *Zygospira aff. Z. putilla* differs from eospirigerinids by not having radial growth lines, its small length and width sizes (3 mm – 5 mm), and an older stratigraphic range (Sandbian 2) than the Spirigerininae clade (Baarli et al., 2022). Thus, I accept Ross's *Zygospira aff. Z. putilla* as a valid *Zygospira* species, and therefore, the name *Zygospira idahoensis* is proposed for this taxon.

Zygospira calhounensis Fenton and Fenton, 1922

Figure 6, 6–10

1922 *Zygospira calhouensis* Fenton and Fenton, p. 76, pl. 2, figs. 4–6.

1977 *Anazyga calhouensis* Copper, p. 305.

Type specimens. — Cotype: WM 27457; Paratype: WM 27458, from Calhoun County, Illinois, U.S.

Diagnosis. — Shell size varying in length and width from 4 to 6 mm, oval outline (length > width), no growth lines, no evident median costae or distinct rib, medium to fine parallel ribs originating near the umbo. Concave umbo projecting on top of the ventral valve, round delthyrium, distinct palintrope area. Weak fold and sulcus, ventral valve almost flat, with no clear contrast between sulcus and the remainder of in the ventral valve. Shell anteriorly wider, very rotund commissure opening.

Occurrence. — Maysvillian, Late Ordovician (Cincinnatian Series, Katian Stage) in the United States. Non-type specimens collected from the Kimmswick Limestone (Katian 2 Stage) in Batchtown, Illinois, U.S.

Additional Materials. — Figured plesiotype: FMNH UC20757.

Description. — Average length of 5.04 mm, width of 4.57, and height of 3.68. Elliptical (or oval) shell, unisulcate commissure shape, deflections in the commissure (zigzag-shaped). Average number of costae in the ventral valve is 18.25 and dorsal is 17. Medium fine ribs originating near the umbo, overall biconvex valves. Absence of apparent growth lines, high angled umbo, with round delthyrium opening. No evident median costae, absence of double ribbing. Weak fold and sulcus. Sulcus in the ventral valve very weak, no progression observed in the ventral valve. Internal characters are unknown.

Remarks. — Although similar in rib orientation and appearance, *Zygospira calhounensis* is distinguished from *Z. circularis* by the overall outline, which is more long than wide, and by the rotundity of the commissure area (see Figure 6, 3-8). The commissure deflection is not influenced by the folding but is, nonetheless, significantly wider than the rest of the shell.

Zygospira circularis Cooper, 1956

Figure 6, 11–14

1956 *Zygospira circularis* Cooper, p. 670, pl. 141C, figs. 18–21.

1977 *Anazyga circularis* Copper, p. 305.

Type specimens. — USNM PAL 111374a (holotype) from the Carters Formation in Tennessee, U.S.; USNM PAL 133267 and 133268 (plesiotypes) from the Saturday Mountain Formation, Idaho, U.S.

Diagnosis. — Shell size varying in length and width, semi-circular atrypid shell, very short in height (depth), inconspicuous ribs, ventral and dorsal valves abundant in the number of ribs, ribs spacing distance is continuous throughout the valves. No apparent median costae, uniform ribs in size and appearance. Gentle dorsal fold, and weak sulcation, almost flattened ventrally and no extension of the degree of the sulcus progression in the ventral valve.

Occurrence. — Sandbian and Katian stages, Late Ordovician in the United States. Specimens found in the Carters Formation (Katian 1) in Tennessee, U.S (holotypes) and in the Cynthiana Formation (Sandbian 2) in Idaho, U.S (plesiotypes).

Description. — Dorsi-biconvex semi-circular to quadratic shells ranging from 3.0 to 4.5 mm in length and width. An average of 22 distinctive but not prominent ribs on the dorsal and ventral valves. Absence in growth lines, weak fold and sulcus originating anterior to the umbo, parasulcate deflected (zigzag-shaped) commissure opening, ventrally flattened shells, with anterior and posterior fold deflection of 0.80 and 0.10 mm, respectively. Small, low-angled umbo, barely covering the dorsal valve. Internal characters are unknown.

Remarks. — The diagnosis was based on a USNM plesiotype specimen with a broken umbo. Therefore, observations made by Cooper (1956) about umbo's angle and projection cannot be verified but can be accessed in Ross (1959). *Anazyga circularis* differs from other zygospirinids by its almost completely circular outline, the lack of a median costae, and the uniformly spaced ribs in both the dorsal and ventral valves. In the

original description, Cooper (1956) differentiates *A. circularis* as "resembling *A. variabilis* Fenton and Fenton but differs in its more rounded outline and indistinctness of the fold and sulcus". However, *A. circularis* is not as rotund as *A. variabilis*, its ribs are numerous, not as strong, and distinct, and the umbo is not as well developed and projected. *Anazyga variabilis*, otherwise, has a more typical *Zygospira* shape, with stronger and well-spaced ribs, and fold and sulcus. Ross (1959) describes *A. circularis* as being similar to *Z. resupinata* Wang, 1949 which has clear distinctions in their rib's rotundness and fold and sulcus progression. *Anazyga circularis* has a typical morphology (outline, overall ribs' morphology, and size) observed in basal zygospirinids, such as *Z. sulcata* Howe, 1965 and *Z. concentrica* Ulrich, 1879 from the Upham Limestone in NM and the Kope Formation in OH, respectively.

Zygospira hicksi Cowper Reed, 1905

Not figured

1905 *Zygospira hicksi* Cowper Reed, p. 452, pl. 23, figs. 17–19.

1977 *Catazyga hicksi* Copper, p. 312.

Type specimens. — 20, SMCU A30861 (paralectotype), 21, SMCU A30862 (lectotype) from the Slade and Redhill formations in Cuckoo Grove Lane, Haverfordwest, Wales.

Diagnosis. — Overall larger, slightly folded shells. Elliptical outline, simple radiating ribs, double ribs absent, weak deep median costae, growth lines present. Short teeth, adductors divided by median ridge. Brachidia morphology unknown.

Occurrence. — Katian Stage, Late Ordovician in Wales. Specimens found in the Slade and Redhill formations (Katian 4) in Cuckoo Grove Lane, Haverfordwest, Wales.

Description. — Average length and width of 10 mm, respectively. 25-30 ribs, short, curved beak.

Remarks. — Zygospira hicksi was erected by Cowper Reed (1905), who noted its circular outline and the numerous fine ribs. *Zygospira hicksi* was the second known atrypid brachiopod in the Ordovician exposures in Britain. Cowper Reed (1905) identified overall outline similarities with *Zygospira* (Catazyga) *headi* var. *angelica*. *Zygospira hicksi* however, differs from this early catazygid by bearing fewer ribs, and having a more quadratic outline. Similar to *Z. kentuckiensis*, *Z. hicksi* is a larger zygospirinid with numerous ribs.

Zygospira lebanonensis Cooper, 1956

Figure 6, 15–19

1892 *Hallina saffordi* Winchell and Schuchert, p. 292, pl. 34, figs. 55–58.

1894 *Zygospira saffordi* Hall and Clarke, p. 151, pl. 84, figs. 36–38.

1956 *Zygospira lebanonensis* Cooper, p. 671, pl. 142C, figs. 11–15.

1977 *Anazyga lebanonensis* Copper, p. 306.

Type specimens. — USNM PAL 111377a (holotype) from the Lebanon Formation in Tennessee, U.S.; USNM PAL 133270 (plesiotype) from the Saturday Mountain Formation in Lemhi Range, Idaho, U.S.

Diagnosis. — Overall small shell, variable length, and width. Rectangular to semi-circular and biconvex valves. Ventral and dorsal valves are characterized by having strong costae separated by deep marginal valleys. Small umbo and palintrope area. Strong ventral sulcation originating anterior to the delthyrium (approximately 2/3 of the valve), containing three deep median costae and deformation progressing approximately 1 mm from the sulcus.

Occurrence. — Whiterockian (Middle Ordovician), and Sandbian (Late Ordovician - Mohawkian Series) stages in the United States. Lebanon Limestone (Sandbian 1) at Shelbyville, Tennessee, U.S.; Moccasin Formation in Tennessee, U.S.; Camp Nelson Formation in Kentucky, U.S.; Barnhart Formation in Missouri, U.S.; Cynthiana Formation (Sandbian 2) in Lemhi Range, Idaho, U.S.

Additional Materials. — Plesiotypes: USNM PAL 133269, USNM PAL 133270.

Description. — Average length of 4.2 mm, width of 4.2 mm, and height of 2.4 mm. Parasulcate zigzagged commissure opening, no evident accentuated median costa and growth lines in either valve.

Remarks.— Zygospira lebanonensis was first recognized by Winchell and Schuchert (1892) as a terebratulid species, rather than an atrypid, although the authors highlighted the external morphological similarities between *Z. lebanonensis* and *Z. recurvirostra* (former *Anazyga recurvirostra*). In Hall and Clarke (1894), the interior of *Z. lebanonensis* was examined, and similarities with zygospirinids were identified including

the development of spiral cones and lophophore's loops and an inward inclination of the apices, which are very typical of *Zygospira*.

Zygospira uphami Winchell and Schuchert, 1892
Not figured

1892 *Zygospira uphami* Winchell and Schuchert, p. 291.

1895 *Zygospira uphami* Winchell and Schuchert, p. 468, pl. 34, figs. 45–48.

1977 *Catazyga uphami* Copper, p. 312.

Type specimens. — Neotype: MGS 8227 from Galena Formation, Weisebach Dam, Spring Valley, Minnesota.

Diagnosis. — Large, pentagonal, biconvex shells. Strong and numerous ribs, radiating anteriorly to the umbo and extending to the anterior margins, concentric ornamentation, and double ribs sometimes present, absent accentuated or deep median costae. Weak fold and sulcus, thick umbo.

Occurrence. — Sandbian 2 and Katian 1, Late Ordovician (Mohawkian Series). Present in the fine-grained horizons in the Galena Group (Edenian) in Weisebach Dam, Spring Valley, and Wykoff and Fountain, Minnesota, U.S.

Description. — Average length of 7.8 mm, width of 7.1, and height of 4.7 mm. Biconvex to dorsibiconvex, pentagonal shells, average number of costae in the ventral valve of 36.2 and dorsal of 37.5. Dorsal costae radiating near the umbo. Parasulcate zigzagged commissure opening. Thick and curved umbo (average size of 2.4 mm), partially covering the ventral valve (dorsally apsacline). Internal characters are unknown.

Remarks.— Copper (1977) reassigned *Zygospira uphami* Winchell and Schuchert, 1892 to *Catazyga* without further reasoning. *Catazyga uphami*'s internal morphology was not able to be assessed herein and was not described by either Copper (1977) or Winchell and Schuchert (1892, 1895). Therefore, the phylogenetic placement of *Catazyga uphami* was evaluated in using Bayesian phylogenetic inference in this study, and the most robust results indicate a placement within *Zygospira* not *Catazyga*. *Zygospira uphami* distinguished from *Catazyga*-form species by its smaller size, numerous, but more accentuated costae, stronger fold in the dorsal valve, lack of concentric ornament, and double ribs. These morphological attributes, and the evolutionary placement of *Z. uphami* as a sister taxon to *Z. calhounensis* and *Z. resupinata* suggest that *Z. uphami* is a zygospirinid.

Zygospira variabilis Fenton and Fenton, 1922

Figure 6, 20–24

1922 *Zygospira variabilis Fenton and Fenton*, p. 75–76, pl 2, figs. 7–9.

1977 *Anazyga variabilis* Copper, p. 305.

Type specimens. — WM 27861 (holotype); USNM PAL 111387a (plesiotype) from the Plattin Formation, St. Genevieve County, Missouri, U.S.

Diagnosis. — Thick, robust in height, rectangular, and biconvex shells. Poorly developed fold and sulcus. Sulcus on the ventral valve separated by two accentuated lateral ridges. Strong ribs originating near the umbo. Absence of growth lines. Very distinct apsacline dorsal valve, resulting in a large, high-angled prominent umbo.

Occurrence. — Sandbian, Late Ordovician (Mohawkian Series) in the United States. Plattin Formation in Kentucky and Missouri, U.S; Black River Formation in Kentucky, U.S.

Additional Materials. — USNM PAL 111387a-b, USNM PAL 111388a-b

Description. — Average length of 5.3 mm, width of 5.6 mm, and height of 3.6 mm. Biconvex, rectangular shells, average number of costae in the ventral valve of 15.5 and dorsal of 17. Dorsal costae radiating near the umbo. Parasulcate zigzagged commissure opening. Sharp and curved umbo (average size of 1.7 mm), partially covering the ventral valve (dorsally apsacline). Internal characters are unknown.

Remarks. — As noted by Fenton and Fenton (1922), *Zygospira variabilis* can be distinguished from *Z. recurvirostra* by its overall greater size but lower thickness. *Zygospira variabilis* has a different costae configuration with stronger and fewer ribs in both valves. Analysis of internal morphology of a silicified specimen (USNM PAL 111387d) indicates a resemblance of the spiral stems of the lophophore of *Z. variabilis* with those documented from *Z. modesta* Hall, 1862 and *Z. recurvirostra* Davidson, 1882. In this case, both stems are parallel to each other for a short distance before the loops, which were not identifiable as preserved.

Subfamily Catazyginae Copper, 1977

Genus *Catazyga* Hall and Clarke, 1894

Type species. — Athyris headi Billings, 1862, p. 147.

Diagnosis. — Moderate to large, elongate, fine-ribbed anazygids. Biconvex, thick (in height) shells. Numerous ribs, rarely bifurcating double ribs, concentric ornamentation frequently present at the margins. Rectinomarginate to unisulcate zig-zagged commissure openings. Weak fold and sulcus, lack of distinct deep or accentuated median costae. Thick umbo, projecting upwards and covering most of the ventral valve. Discrete pedicle openings. Deep, thick adductor area, small central teeth socket cavities. Narrow and poorly defined diductor muscles area. Posteriorly oriented jugum directly inclined toward whorls apices, three to ten whorls.

Occurrence. — Early to mid-Late Ordovician (Sandbian 2 to Katian 4). The oldest specimens are found in Sandbian 2 to Katian 1 exposures in Wales and Scotland. In North America, *Catazyga* is more abundant and commonly found in exposures from the Katian 4 Stage (Richmondian) in the eastern basins, such as the Cincinnati Arch and in the Anticosti Island, Canada.

Description. — Average length of 14 mm, width of 13 mm, and height of 8 mm. Elliptical (L > W) to pentagonal (L > W) biconvex shells, subcircular outline, without plications. Costae and concentric growth lines always present, average number of 31, and 32 ventral and dorsal costae, respectively. Thick, short beaks (average size of 4.5 mm). Pedicle foramen small, but always open. Weak fold and sulcus, weak sulcus progression in the ventral valve.

Other species. — *Zygospira anticostiensis* Billings, 1862 from the Hudson River Formation in Anticosti Island, Quebec, Canada; *Catazyga arcana* Williams, 1962 from

the Kiln Mudstone in the Craighead Formation in Ayrshire, Girvan district, Scotland; *Catazyga cartieri* Cooper and Kindle, 1936 from the Whitehead Formation in Percé, Quebec; *Athryis headi* Billings, 1862 from the Pontgravé River Formation in Bécancour, Quebec, Canada, and from the Waynesville Formation in Madison, and Weisburg, IN, U.S., Oxford, Woodville, Waynesville, and Blanchester, OH, U.S.; *Athyris headi borealis* Billings, 1862 from the Hudson River Formation in Lake St. John, Quebec, Canada; *Catazyga headi filistriata* Sproule, 1936 from the Cobourg Formation, Georgian Bay, Ontario, Canada; *Catazyga homeospiroides* Ross and Dutro, 1966 from the Jones Ridge Formation near the Tatonduk River, Alaska, U.S.

Remarks. — *Catazyga* was erected by Hall and Clarke (1894) based on its rotundity, weak fold and sulcus, and its great number of costae. Internally, *Catazyga* is distinguished from *Zygospira* by having a posteriorly oriented lophophore, with 3 to 10 whorls. Copper (1977) described more details of *Catazyga* muscles and teeth structures; the genus is recognized by having a broad adductor muscle area, and irregular, small, teeth cavities.

Catazyga homeospiroides Ross and Dutro, 1966

Figure 7, 1–5

1966 *Catazyga homeospiroides* Ross and Dutro, p. 8, pl. 2, figs. 8,11, and 13.

1977 *Catazyga homeospiroides* Copper, p. 315.

Holotype. — USNM PAL 14532 from the Jones Ridge Formation in Alaska, U.S.

Diagnosis. — Thick, elliptical biconvex shells, protruding umbo, and well-defined delthyrium. Poor developed fold and sulcus, with a slight sulcus progression at the ventral valve. Distinct and well-spaced costae radiating anterior to the umbo, occasional presence of growth lines. Rectimarginate and marginally deflected anterior commissure.

Occurrence. — Katian 1 Stage, Late Ordovician (Edenian, Cincinnatian Series) in the United States. Trenton Formation in Alaska, U.S.

Materials. — Holotype: SNM145327; Paratypes: USNM PAL 145331, and USNM PAL 145329.

Description. — Overall large specimens, average length of 11.8 mm, width of 11.0 mm and height of 8.20 mm. Elliptical shells, average number of costae in the ventral valve of 13 and 19.5 strong ribs in the dorsal valve. Growth lines occasionally present, absence of double ribs and median costae. Delthyrium is very distinct, with a 55° angle. Interior morphology unknown.

Remarks. — In the original description, Ross and Dutro (1966) were hesitant to unambiguously place *Catazyga homeospiroides* within the *Catazyga*. Copper (1977) further indicated that the placement requires confirmation. Based on these analyses, the higher number of costae (>10), rotundity, poor development of the fold and sulcus, and ovoid outline present in the analyzed specimens are consistent with the placement of this species within the genus *Catazyga*.

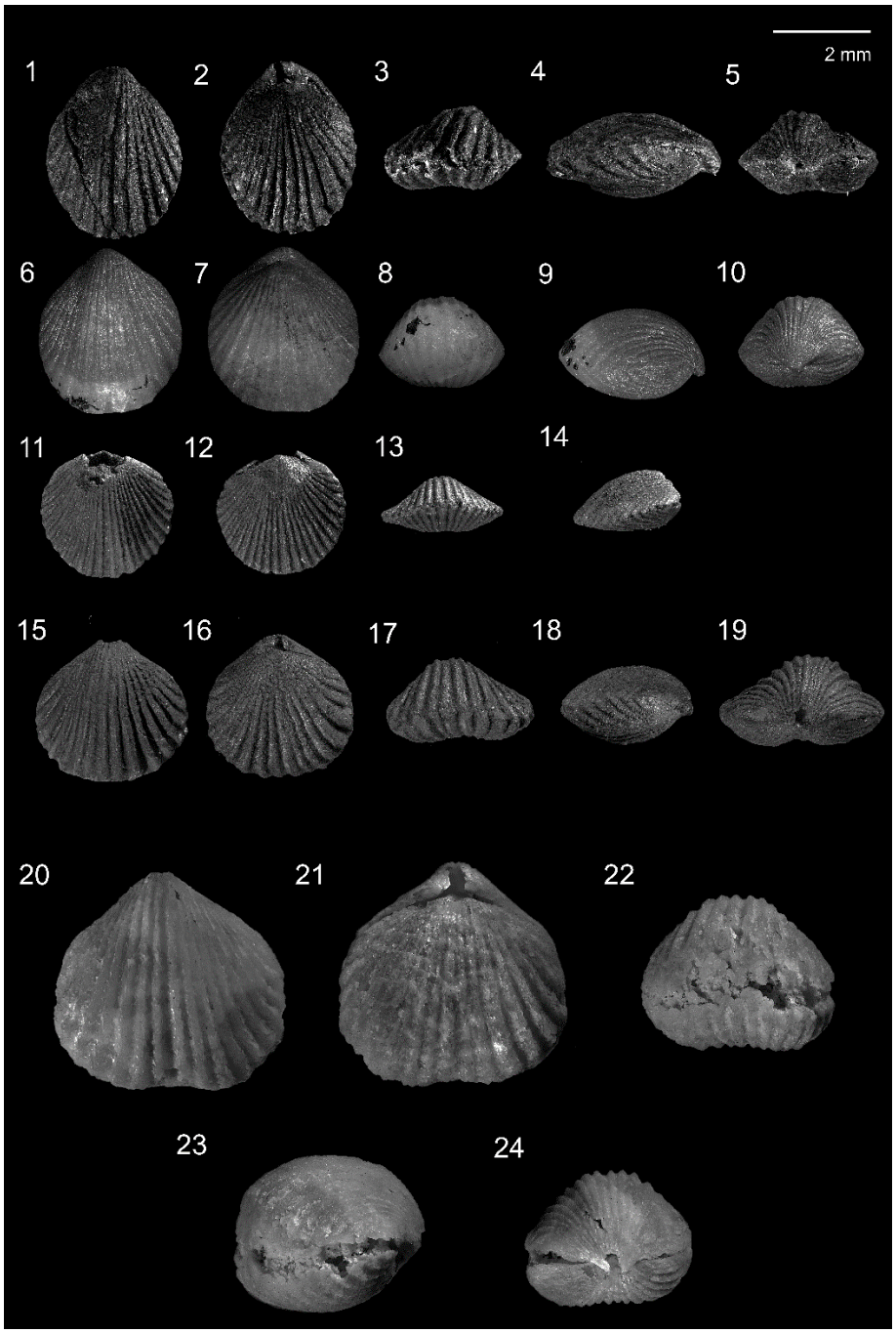

Figure 6. *Zygospira*. Dorsal, ventral, commissure, lateral and hinge line views are shown for all figured specimens, except for *Zygospira circularis*, that lacks the hinge line view. 1–5 *Zygospira idahoensis* (Holotype) USNM PAL 133263; 6-10 *Zygospira calhouensis* (non-type) FMNH UC20757; 11-14 *Zygospira circularis* (Plesiotype) USNM PAL 133268; 15-19 *Zygospira lebanonensis* (Plesiotype) USNM PAL 133270; 20–24 *Zygospira variabilis* (Plesiotype) USNM PAL 111387a.

Overall, *C. homeospiroides* is a typical *Catazyga* form, but with coarser costae as a derived trait. Moreover, the species can be distinguished from other Catazyginae forms by its coarser costae, weak fold but a gentle sulcus progression in the ventral valve, a larger but not curved umbo, and its extreme biconvexity. Ross and Dutro (1966) noted that *Catazyga homeospiroides* resembles in outline and number of growth lines a related species, *C. cartieri*. However, the costae in *C. homeospiroides* are coarser. *Catazyga arcana*, another related species from the Scoto-Avalonia terrane (Girvan) differs by having a highly convex ventral shell, whereas *C. homeospiroides* is characterized by its biconvexity. Finally, Ross and Dutro (1966) compared *C. homeospiroides* to the typical Catazyginae form, *C. headi*, which can be differentiated by finer costae and a more rotund outline.

Catazyga cartieri Cooper and Kindle, 1936

Figure 8, 1–5

1936 *Catazyga cartieri* Cooper and Kindle, p. 359, pl. 52, figs. 8–13, 18.

1977 *Catazyga cartieri* Copper, p. 315.

Type specimens — USNM PAL 91786a-e (holotypes); USNM PAL 91786a (paratype) from the Whitehead Formation in Percé, Quebec, Canada.

Diagnosis. — Biconvex, elliptical shells. Numerous fine costae originating near to the short, thick umbo. Absence of growth lines, and median costae. Short delthyrium. Rectimarginate commissure opening. Fold and sulcus typically absent, when present, slightly protuberant at the dorsal valve.

Occurrence. — Katian 1 Stage, Late Ordovician (Edenian in the Cincinnatian Series) in Canada. Whitehead Formation, north-west Percé, Gaspé Peninsula, Quebec, Canada.

Description. — Average length of 16.6 mm, width of 15.8, and height of 10.3 mm. Average number of fine costae in the ventral valve of 30.5 and of 32 in the dorsal valve, lack of double ribs, and growth lines. High angled umbo (59°), and average umbo size of 5.0 mm.

Remarks. — As noted by Cooper and Kindle (1936), *Catazyga cartieri* differs from other Catazyginae forms by its sharp umbo and convex valves. *C. cartieri* shows a unique rotundity in its outline and profile, costae are evenly and homogenously distributed throughout the valves.

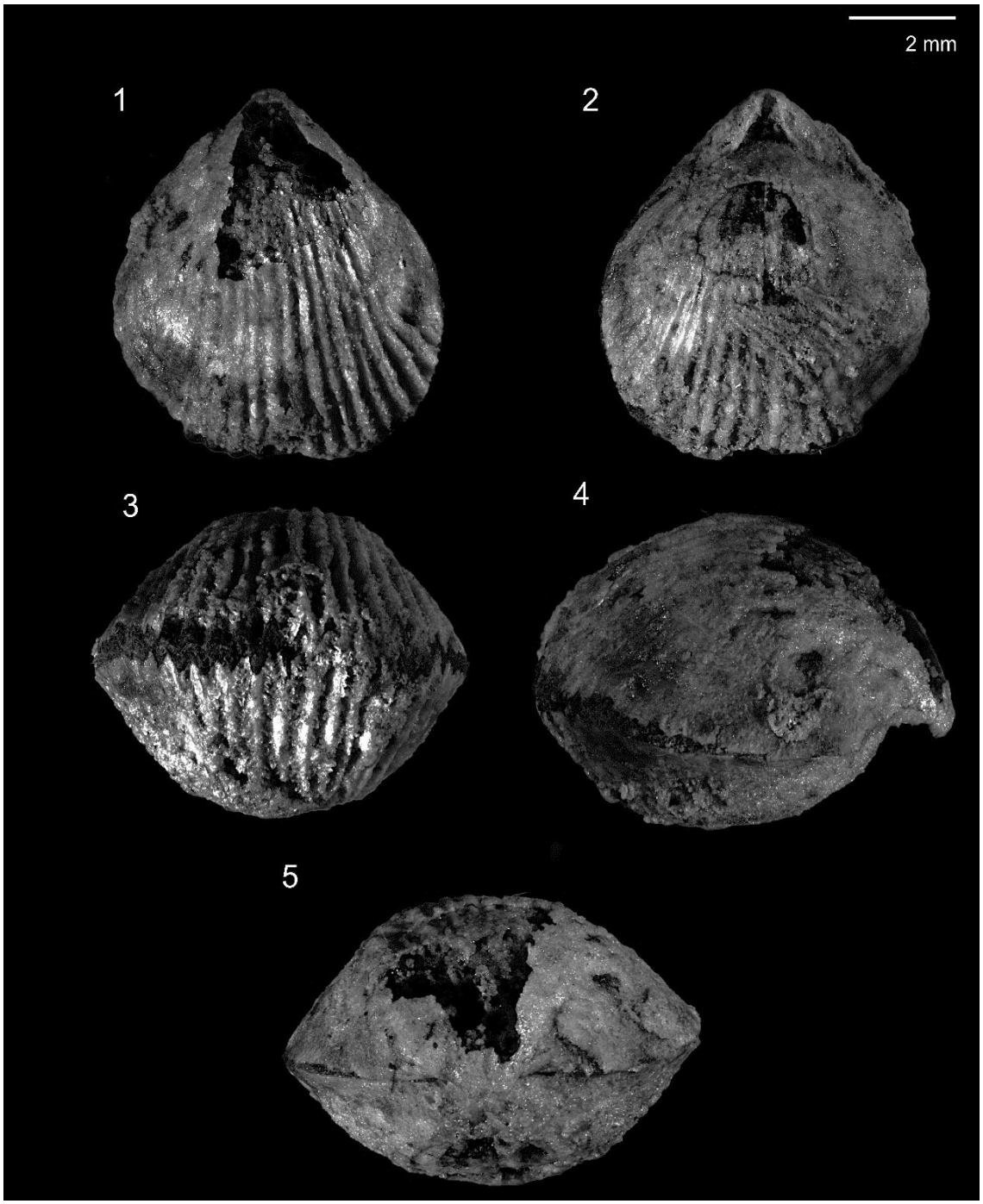

Figure 7. Holotype of *Catazyga homeospiroides* (USNM PAL 145327). (1) Dorsal, (2) ventral, (3) commissure, (4) lateral and (5) hinge line views.

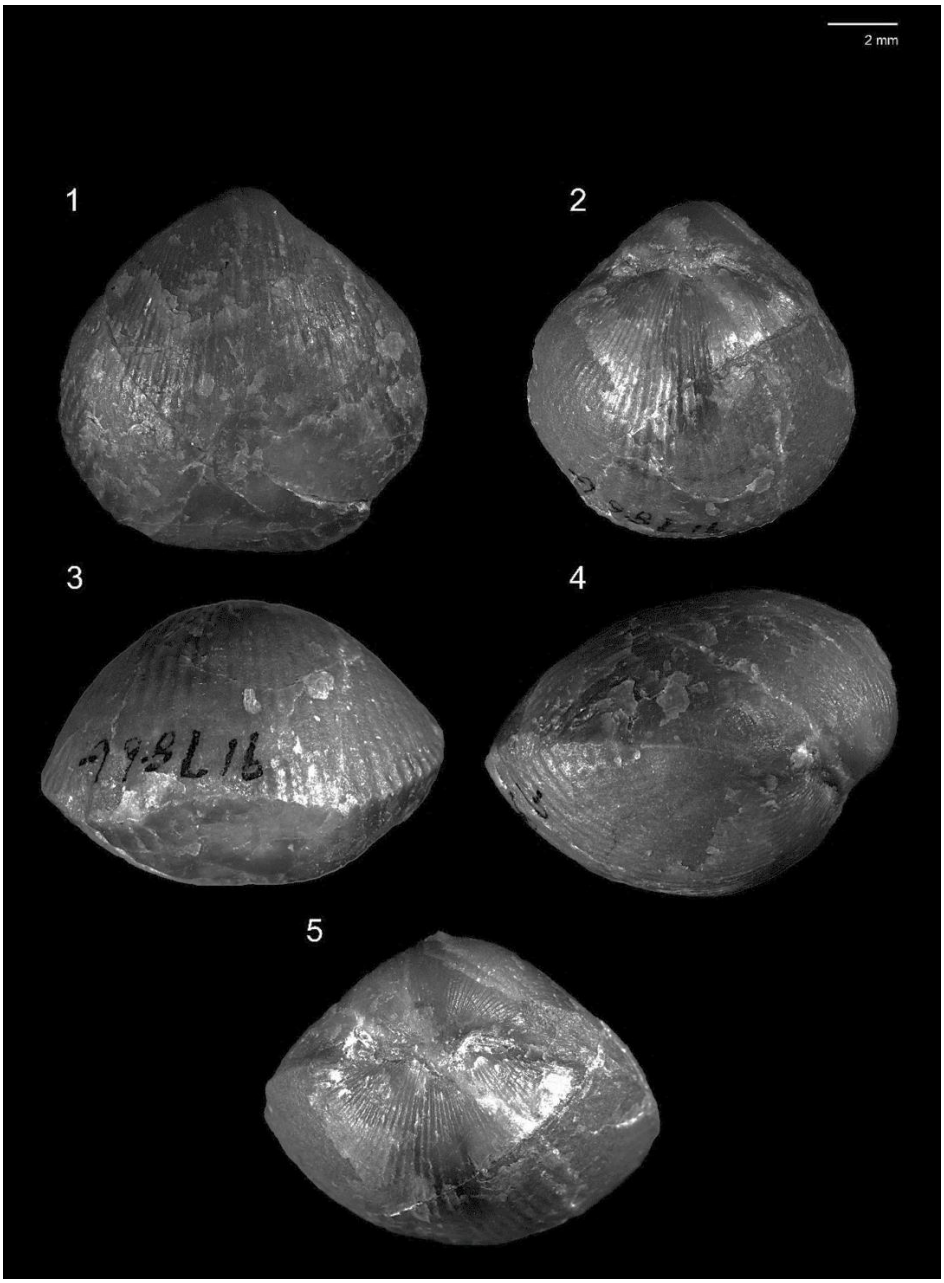

Figure 8. Holotype of *Catazyga cartieri* (USNM PAL 91786E). (1) Dorsal, (2) ventral, (3) commissure, (4) lateral and (5) hinge line views.

2.4 Results

The inferred MCC tree is given in **Figure 9** (posterior probability mean: –328.71, and ESS: 582). From the set of trees, the tree characterized by the highest posterior probability and best mixing was the one constructed with only external traits and constrained topologies to include monophyletic Catazyginae with exception of the two transferred species, *Zygospira hicksi* and *Z. uphami* (scenario 3). In all four scenarios (**Figure 9**; **Figures A1-A3**), the Bayesian framework recovered paraphyly shared among the subfamilies Anazyginae and Catazyginae. In the first scenario (internal + external characters, no taxonomic constraints), the estimated topology was similar to **Figure 9**: Anazyginae includes two distinct clades, and Catazyginae contains all previously assigned *Catazyga* species + *Zygospira kentuckiensis* (posterior probability: -327.56; **Figure A1**). The second scenario (external characters only, no taxonomic constraints) recovered Anazyginae and Catazyginae, with distinctions within Anazyginae in relation to **Figure 9** (posterior probability: –318.77). In this scenario, the position of *Zygospira recurvirostra* changed to sister taxon to the derived zygospirinids. *Zygospira hicksi* + *Zygospira resupinata* + *Zygospira calhounensis* was estimated as a polytomous clade (**Figure A2**). The fourth scenario (external characters only, constrained to monophytic traditional general) recovered the lowest posterior probability (–342.19) among all runs, and internal relationships observed in previous scenarios were not maintained (**Figure A3**). In all unconstrained scenarios, recovered clades included a mix of species previously assigned to *Anazyga* and *Zygospira*. Therefore, the validity of *Anazyga* as a discrete monophyletic entity is not supported. Consequently, the best supported

systematic interpretation transfers *Anazyga* species to *Zygospira*, as indicated in **Figure 10**.

The predicted highest posterior density (95% HPD) for the clade's origination was during the Late Sandbian Stage, around 453.48 Mya. The origin of both subfamilies was estimated to have occurred in the Katian Stage Slice 1 with the Anazyginae group is estimated to have originated 452.68 Mya, slightly before the Catazyginae estimate of 452.25 Mya. The predicted diversification rate for the entire family was relatively low (mean: 0.16, ESS: 411), whereas the turnover rate was higher (mean: 0.82, ESS: 292).

Skyline model (posterior probability mean: –64.67, ESS: 4176) results predicted higher speciation and extinction rates for intermediate stage slices (Katian 2 and Katian 3). Katian 4 exhibited the lowest speciation and extinction rates, indicating a decline in speciation within the clade (**Table 6).** Biodiversity (the counted number of lineages) was estimated to be the highest at Katian 3 and early Katian 4. Boxplots with the estimated rates are shown in **Figure 11** and raw values are shown in **Table 6**.

2.5 Discussion

2.5.1 Recognition of clades

Phylogenetic analysis resolved the genera into two clades which coincide with the two subfamilies proposed by Davidson (1882), Copper (1977), and Baarli et al. (2022): (1) Catazyginae (**Figure 10a**), encompassing a monophyletic group of *Catazyga* species, and (2) Anazyginae (**Figure 10b**), including the species historically assigned to *Anazyga* and *Zygospira* plus two species formerly assigned to *Catazyga, Catazyga hicksi*, and *C. uphami*. Catazyginae group comprises all other known *Catazyga* species, and is supported by fine ribbed, biconvex, pentagonal shells.

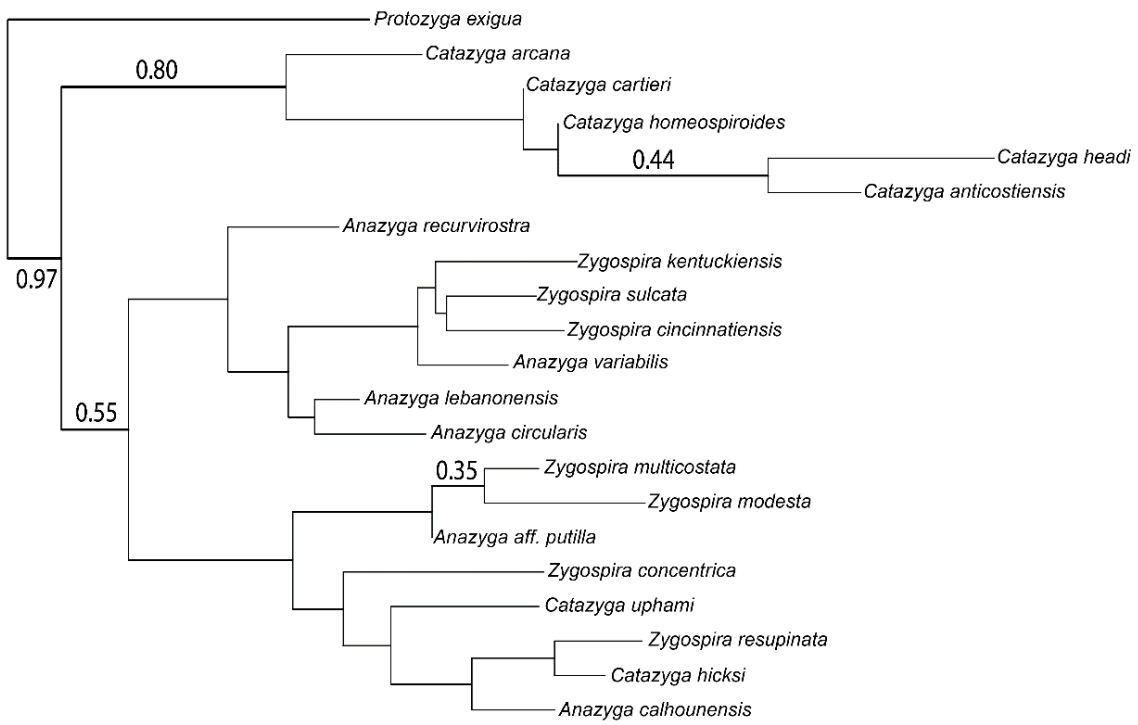

Figure 9. MCC tree Bayesian phylogeny estimated using external data and with the monophyletic Catazyga constraint for the subfamily Anazygidae under the fossilized birth-death model in the Late Ordovician (Cincinnatian: Katian). Posterior probability: -328.71. Branch widths are equivalent to their posterior probability, the highest posterior probabilities (i.e., higher than 0.40) are labeled. Taxonomic nomenclature correlates with the second column on **Table 1**.

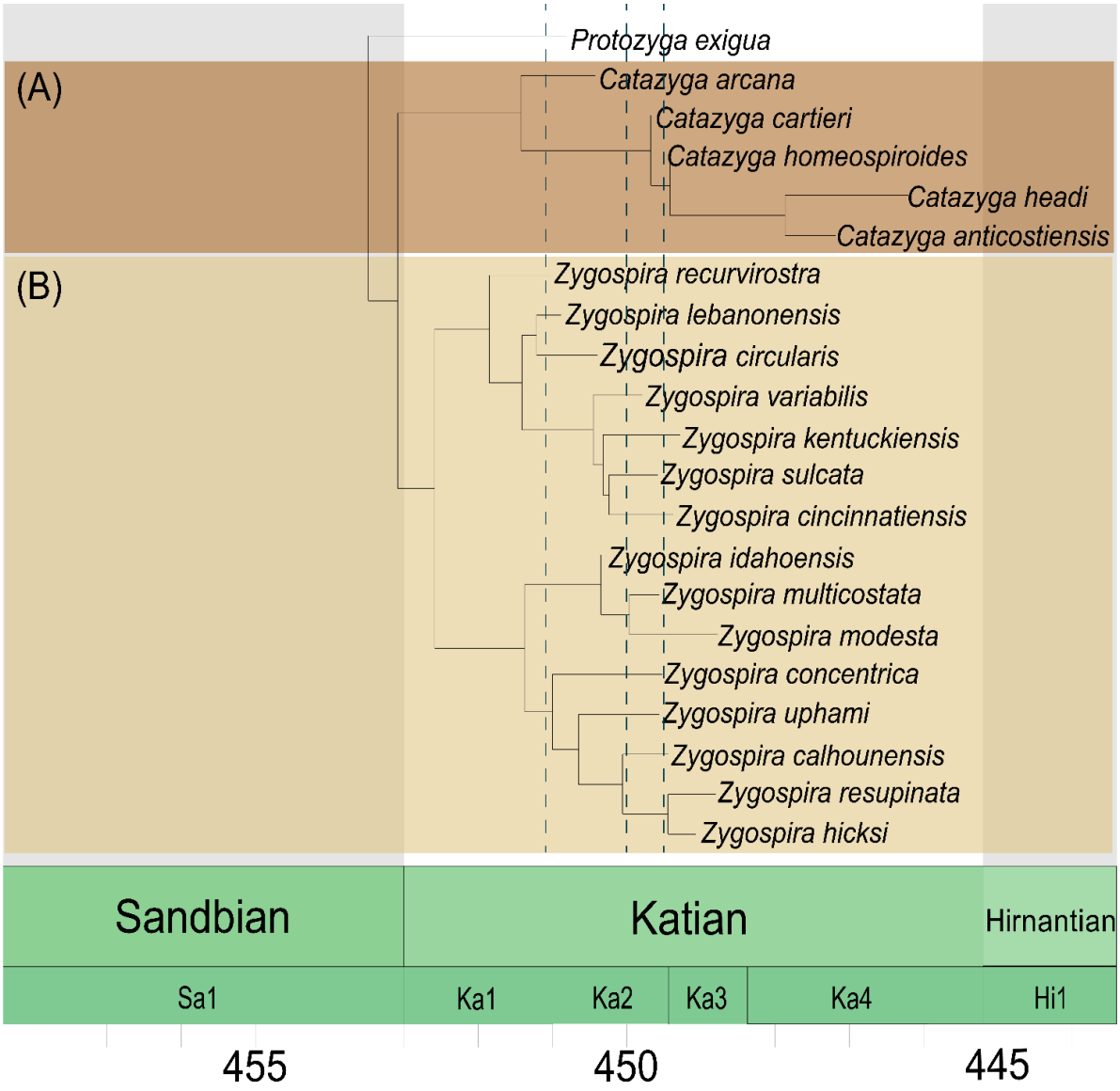

Figure 10. Updated time-calibrated phylogeny of the Anazygidae based on results of Bayesian phylogenetic analysis. Evolutionary relationships and branch lengths are scaled to geologic time. Taxonomic assignments reflect the revisions proposed herein. X-axis reflects units of time in millions of years (Myr). (A) represents the Catazyginae group, and (B) represents the Anazyginae group. Taxonomic nomenclature correlates with the third column on **Table 1**.

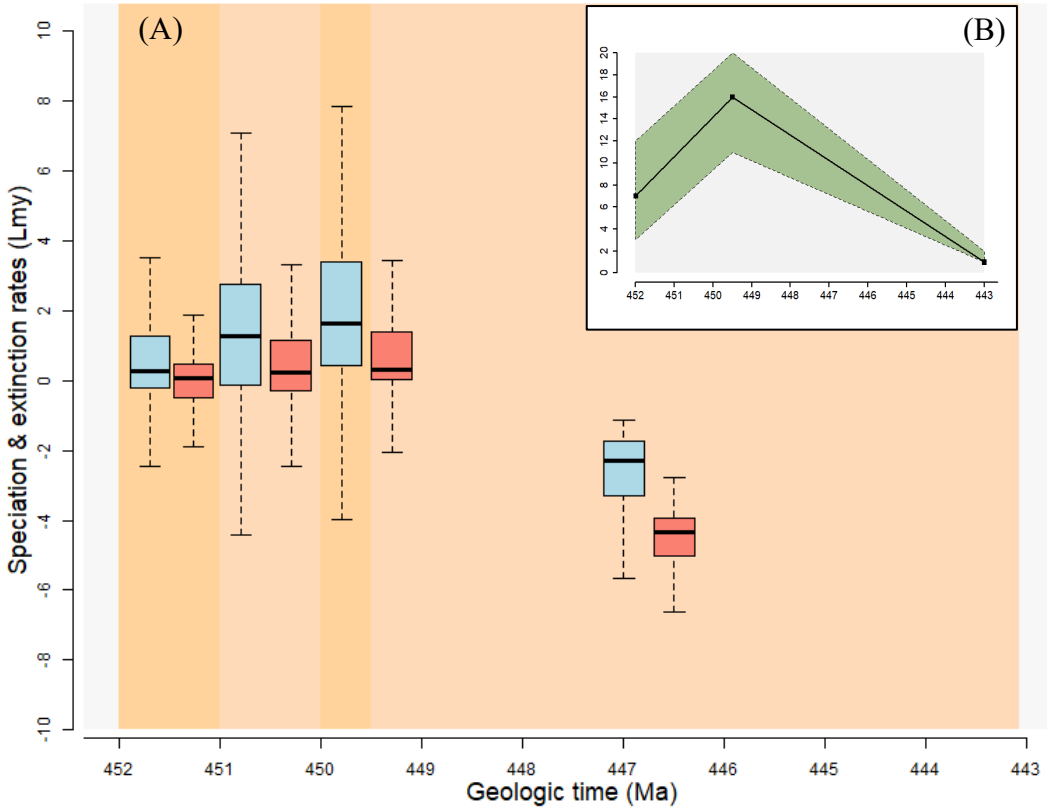

Figure 11. (A) Boxplot of estimated birth (speciation) and death (extinction) rates in lineages per million years (Lmy). Speciation rates are shown in blue boxes, and extinction rates in red. Thicker horizontal lines indicate median values. The four analyzed time intervals are highlighted by the tan and light tan rectangles. 452–451 Ma (Chatfieldian, Sandbian 2-Katian 1); 451–450 (Katian 2, Edenian); 450–449.7 (Katian 3, Maysvillian); 449.7–443 (Katian 4-Hirnantian, Richmondian and Gamachian). (B) Diversity through time, counts represent the number of branches (lineages).

Table 6. Estimated Skyline median speciation and extinction rates for the four analyzed time intervals.

Estimated rates	Interval 1	Interval 2	Interval 3	Interval 4
Median speciation rate	0.291	1.280	1.639	–2.27
Median extinction rate	0.053	0.245	0.320	–4.349
Median preservation rate	0.002	0.016	0.22	–0.90

For all the analyzed phylogenetic scenarios, Catazyginae was grouped distinctively apart from Anazyginae. Furthermore, the external only + *Catazyga* constraint tree was the best supported statistically (**Figure 9**). Anazyginae includes both *Anazyga* and *Zygospira* species that have strong costae, plicated outline, and prominent fold and sulcus. In all analyzed scenarios, the group was largely monophyletic (**Figure 9**; **Figure A1-A3**). In the most probable scenario, two sister groups were recovered within Anazyginae, one including the type species of *Anazyga*, *A. recurvirostra*, and the other one including the type species of *Zygospira*, *Z. modesta* (**Figure 9**). However, both clades within Anazyginae included a mix of species assigned to both *Anazyga* and *Zygospira* rendering both genera polyphyletic as recently circumscribed. Therefore, a systematic revision is proposed in which *Anazyga* is synonymized with *Zygospira*. Prior phylogenetic (Baarli et al., 2022) and early systematic studies (Hall, 1862; Hall and Clarke, 1894; Copper, 1977) also expressed concerns about the validity of *Anazyga* and *Zygospira* as discrete evolutionary entities. The FBD model suggests that some species previously assigned to *Anazyga* may be ancestral to later forms of *Zygospira*, as predicted by Copper (1977).

The overlapping evolutionary signal within the Anazyginae subfamily is interpreted as a response to the typical external anatomy shared by all anazyginid species *Zygospira*, related to the size, folding, and striae in the shells. However, some species previously assigned to *Anazyga* shares internal traits with catazyginid species, specifically directionally of the jugum in the lophophore (Hall and Clarke, 1894; Copper, 1977). This internal similarity would likely represent the pleisiomorphic condition of the Anazygidae in general as it is expressed in the oldest members of both subfamilies

(**Figure 9-10**). The close and sometimes overlapping relationship among the three traditional genera indicates that the division of the family into three monophyletic genera is not supported by evolutionary relationships among the species.

The incorporation of internal traits in the phylogeny does not improve resolution of the evolutionary relationships in the group (**Figure A1-A3**). Instead, tree support is reduced (posterior probability: –327.56) and resolution declines. In fact, one noticeable outcome is the positioning of *Zygospira kentuckiensis* among the Catazyginae clade, an outcome highly inconsistent with overall shell morphology that appears to be primarily influenced by the larger size of the shell. When internal traits are excluded from the data matrix, the analysis favors a more resolved phylogenetic tree (**Figure A2**). In the latter case, the monophyly in Catazyginae is still maintained (posterior probability: –318.77). Taking that into account, our preferred phylogenetic tree includes a clade constraint in Catazyginae, which consists of five *Catazyga* species: *C. arcana*, *C. cartieri*, *C. homeospiroides*, *C. anticostiensis*, and *C. headi*. The clade excludes *Zygospira kentuckiensis*, suggesting that even when excluding internal traits, external anatomy size has a higher evolutionary influence in the groupings (average length: 11.8 mm). Two *Catazyga* species, *Catazyga hicksi* and *Catazyga uphami* are also not included in Catazyginae; these two species were in fact, first described as *Zygospira* spp. (Winchell and Schuchert, 1892; Cowper Reed, 1905). Hence, they are transferred to *Zygospira* herein.

2.5.2 Evolutionary patterns

Clade origination is predicted to have occurred around 453 Mya during the Late Sandbian Age (**Figure 10**). The results indicate that anazygids underwent a basal division into the two subfamilies during the early Katian. Within the Anazyginae, the clade including *Zygospira recurvirostra* diversified first, becoming more abundant in the Katian 1 and Katian 2 Stage Slices (Chatfieldian to Edenian). The clade including *Zygospira modesta* diversified mainly during the Katian 2 Slices (Edenian to basal Maysvillian). The Catazyginae were less diverse, but cladogenetic events extended from the late Chatfieldian through Richmondian (Stage Slices Katian 1 through 4). *Catazyga* and *Zygospira* were abundant forming shell pavements across the basins at specific horizons (Copper, 1977; Harper et al., 2017), such as those observed by Bretsky (1969) and Copper (1982).

Anazygid speciation and extinction rates indicate a biodiversification event during the middle Katian Stage, followed by a decline in both speciation and extinction rates (**Figure 11**). These rates reached their maximum during the Maysvillian (Katian 3), causing a biodiversity accumulation by the early late Katian (**Figure 11**). The diversity decline observed during the Richmondian and later (Katian 4 and Hirnantian Stage) is explained by a decline in speciation rates; reducing the number of originations that lead to the clade's downfall (**Table 6**; **Figure 11**). The radiation of *Zygospira* and *Catazyga* is found to have reached its peak during the Katian 3 Stage (**Figure 10; Figure 11**). This finding is coordinated with higher speciation rates present at the last peak of diversification of the Great Ordovician Biodiversification Event (GOBE) before the diversity decline by the late Katian (Rasmussen et al., 2019). Anazygid biodiversification

is often discussed (Copper, 1977, 2001; Sproat and McLeod, 2023) and these results provide additional evidence of their rapid but brief radiation after the GOBE conforms to the diversification patterns predicted by earlier studies (Copper, 1977, 2001; Harper et al., 2017).

2.5.3 Model implications

The proposed phylogeny contradicts a temporal stratification among species within *Anazyga* and *Zygospira* that was previously suggested (Davidson, 1882; Hall and Clarke, 1894; Copper, 1977, 2001; Sproat and McLeod, 2023). Instead, *Zygospira* is reconstructed as a diverse clade with an ancestor-descendent relationship among species previously assigned to *Anazyga,* such as *Z. resupinata* and other zygospirinids. Anazygid species are predominantly present from the Late Sandbian to early Katian Stage, and *Catazyga* is the only genus that persists throughout and beyond Katian 4 (**Figure 10**).

When applying tip-dating methods, uncertainties in the models are expected (Barido-Sottani et al., 2020; Wright et al., 2021). Discrepancies among the models and the stratigraphic record are usually associated with mismatches between the age data and the assumed priors. The FBD analysis was conducted through a log-normal relaxed clock model. Of the 21 atrypid species analyzed, all of them showed a satisfactory modeled stratigraphic range relative to their known stratigraphic duration (see Hopkins et al. (2018) for discussion). The exception is *Zygospira modesta* which presented a shorter range than expected. Contrary to what the total evidence calibration shows, this species is present in most of the Richmodian (Katian 4) of the United States. In **Figure 10,** however, its range is shown to be up to the Katian 3 Stage only (~449.96 Mya). The tip's 95% HPD showed to have a 2.14-million range, from 448.33 to 450.47 Mya. A younger

range would be more reasonable, considering the age data input (**Table 4**). The relatively older placement of these middle Katian 4 species is associated with the clock model application, which has shown calibration conflict with a small set of phenotypical data (as explained by Gavryushkina and Zhang, 2020). Although there is uncertainty in the clades' age, probabilistic models should not be disregarded solely on this basis. Clock models, when incorporated in fossilized birth-death models, can still provide robust information on ancestral states, diversification patterns, and origination age (Gavryushkina and Zhang, 2020).

Anazygids have historically been classified by considering their external morphology (such as shell size, outline, beak size and angle, and costae appearance) and their stratigraphic range in the early Paleozoic. Unfortunately, data for internal morphology of anazygid species are scarce, obstructing the incorporation of brachidia into phylogenetic analyses. Here, I propose an external-character-only phylogenetic framework to explain the taxonomic relationships often explained in previous studies. My results indicate that the family's current taxonomic status does not reflect phylogenetic relationships, and that the previously distinct genus *Anazyga* should be once again synonymized with *Zygospira*. The FBD phylogenetic tree presented here explains the origination and the ancestor-descendant relationships within Anazyginae. Although the clade is supported by stratigraphical and dating relationships, clades should not be based only on occurrences' succession, but rather on morphological similarities and evolutionary evidence.

2.6 Conclusions

Anazygidae was an essential and diverse clade in the Late Ordovician, and its species played an important role in ecological communities. Indeed, there are no stratigraphic units among the Edenian to Richmondian strata of the Cincinnati region in which this clade is absent. The increase in diversification and speciation right at the end of the GOBE suggest that anazygids might have been one of the last clades to benefit from the environmental cooling and increase in oxygenation at the interval (Rasmussen et al., 2019; Stigall et al., 2019). The two main genera within this revised classification, *Zygospira* and *Catazyga* are monophyletic groups. However, species within the former genus concepts of *Anazyga* and *Zygospira* do not segregate as clades. Therefore, all species previously assigned to these genera are reassigned to *Zygospira.* Some species previously ascribed to *Anazyga,* such as *Z. calhounensis,* include more plesiomorphic features. Overall, *Catazyga* is reconstructed as a monophyletic genus, spanning almost the entirely of the Late Ordovician. Although the phylogenetic trees with the highest posterior probability were the ones without internal traits, adding internal characters for all studied taxa when anazygid brachiopods in future studies may result in a more detailed and finer scaled framework. In addition to difficulty imposed by the small size, many shared traits among members of the clade such as the loop position, overall shape of the spirals, and valve outline are extremely variable (Hall and Clarke, 1894). This makes it more complex to fully reconstruct systematic relationships with confidence. Nevertheless, phylogenetic estimation of evolutionary relationships is the first step to the understanding of how ecological and biogeographical factors might have impacted the apparent evolutionary convergence in the clade.

CHAPTER 3: ASSESSING BIOGEOGRAPHIC AND SPECIATION PATTERNS WITHIN THE LATE ORDOVICIAN BRACHIOPOD FAMILY ANAZYGIDAE (ATRYPIDA)

Abstract

The Late Ordovician was a period of substantial environmental change. The co-evolution of Earth systems changes involving tectonic uplift and eustasy and biotic changes, such as dispersal and speciation, are recorded in the Late Ordovician in Laurentia. Notably, the final stages of the Ordovician Radiation include the origination, diversification, and extinction of the widespread brachiopod family Anazygidae. In this study, the Anazygidae are examined as a focal group for understanding the dispersal pathways of minute brachiopods within eight sedimentary basins. Stochastic analysis applied to the Bayesian phylogenetic tree for anazygid species using BioGeoBEARS facilitated prediction of basin-to-basin dispersal events and speciation modes within the clade. Three algorithms were implemented, Dispersal-extinction-cladogenesis (DEC), DIVALIKE, and BayArea-like. Additionally, the founder-event effect was included in each model run to account for hopping or jump dispersal (+J parameter). The DEC+J parameter was the most strongly supported model (Posterior probability: -54.82, AICc: 115). Results provide a framework to identify intra and extracratonic dispersal events and indicate a dispersal trend from the more northerly basins toward the southern-most basins in Laurentia. Dispersal within the group was found to be explained by hopping dispersal events, with marginal-Laurentian islands acting as "stepping stones" to intracratonic species. Anazygidae originated from an ancestral vicariance event, and most subsequent speciation events occurred via dispersal (total of 14 distinct episodes). Dispersal is linked to connectivity and isolation pulses between the mid-continent and southern basins related to episodic tectonic events and regional sea level changes. These results indicate that Anazygidae followed dispersal pathways similar to those previously observed in other brachiopod groups, and that diversification was affected by increase in dispersal capacity across different Laurentian basins.

3.1 Introduction

In the Late Ordovician, Anazygidae originated and dispersed throughout the basins in Laurentia and associated islands (e.g., Alaska, and Scoto-Avalonia) (Davidson, 1882; Copper, 1977, 2001; Sproat and McLeod, 2023). The family's speciation and related diversification during the Ordovician has been attributed to tectonic changes that influenced basins' connectivity, sedimentary regime, depositional settings, and sea level (Copper, 1977; Sproat and McLeod, 2023). Although such relationships have been posited, they have not been directly tested. Dispersal pathways and speciation events are poorly understood during anazygid evolution and have never been quantitatively

assessed. In this study, I examine the tempo and mode of potential dispersal pathways and speciation events for two anazygid genera in the Late Ordovician (Katian Stage) using a probabilistic assessment of evolutionary biogeography conditioned on the phylogeny developed in **Chapter 2**.

3.1.1 Geologic Setting

The Upper Ordovician strata (458 Ma–443 Ma) of Laurentia record intense biodiversity and sedimentological changes (McLaughlin and Stigall, 2023). Throughout this period, Laurentia was located in subtropical latitudes at 20–25°S (Cocks and Torsvik, 2021). The tropical environment and the subsequent inundation in these areas created a vast carbonate platform covered by epicontinental seas (Holland and Patzkowsky, 1998; Patzkowsky and Holland, 2007). Consequently, Laurentia hosted extensive benthic communities composed of brachiopods, bryozoans, echinoderms, trilobites, mollusks, and corals (Cocks and Torsvik, 2021).

During the Late Ordovician, collision of eastern Laurentia and island arcs produced the Taconic (second) tectophase of the Taconic Orogeny and converted this margin from a passive margin to a convergent boundary. This tectonic event is recorded by a thick accumulation of mixed carbonate-siliciclastic sediment and the presence of soft-sediment deformation resulting from seismic events (Quinlan and Beaumont, 1984; Patzkowsky and Holland, 1997; Holland and Patzkowsky, 1998). Intense tectonic loading resulted in the forming of a retro-arc foreland basin, which caused subsequent arching in adjacent areas, including the Nashville Dome and the Cincinnati Arch (Quinlan and Beaumont, 1984). Cycles of tectonic loading and unloading facilitated the rise and fall of

intracratonic arches, which created barriers to and connections for dispersal, respectively. Tectonic impacts also facilitated environmental changes, such as shifts in ocean currents and interbasinal connections. These environmental shifts have previously been shown to affect biogeographic patterns and dispersion among brachiopod species during this interval (Lam et al., 2018). Therefore, the exposed sedimentary layers and the abundance of marine invertebrates such as brachiopods and bryozoans in the eastern United States provide an ideal data source for assessing evolutionary, biogeographic, and paleoecologic patterns at broader timescales.

3.1.2 Evolutionary Framework

Prior analyses have identified general patterns related to speciation rates and dispersal and vicariance events during the Late Ordovician (Stigall et al., 2017; Harper et al., 2017; Rasmussen et al., 2019). More specifically, the final phases of the Ordovician Radiation occur in the early stages of the Late Ordovician (Rasmussen et al., 2019). The brachiopod order Atrypida is not an exception; it is a cosmopolitan order that originated in the Middle Ordovician along with other major brachiopod groups (Harper et al., 2017). Within the order, Anazygidae is a widespread family, occurring mostly in Upper Ordovician rocks in the United States (Copper, 1977; Sproat and McLeod, 2023; see **Chapter 2**). Members of the family, specifically *Catazyga headi,* are recognized to be invaders during the Richmondian Invasion in the Cincinnati Basin (Stigall et al., 2019; Purcell and Stigall, 2021; Forsythe and Stigall, 2023). Although this basic framework of distribution and exemplar of dispersal is well known, no evolutionarily-informed analysis has been conducted on the biogeographical patterns and no species-level analyses have

been conducted to adequately evaluate speciation processes within the family. In this study, the phylogeny developed in **Chapter 2** is used to reconstruct biogeographic dynamics by combining a phylogenetic framework, geographic distribution, and temporal scale data within the phylogenetic biogeographic software package BioGeoBEARS (Matzke, 2013).

Although the incorporated phylogeny does not encompass all the known anazygid species (see **Chapter 1**), the dense sampling of species within a combination of different geographical basins and morphological traits makes it possible to holistically assess evolutionary relationships within the clade. Previous analyses have used a similar approach and shown that evolutionary trends can be obtained by combining phylogenetic and biogeographic approaches (Lam et al., 2018, 2021; Bauer, 2021).

The BioGeoBEARS framework allows the explicit incorporation and assessment of different speciation modes within a probabilistic analysis. Geographic location of a speciation event is an inherited trait, constrained by the geographic distribution of the ancestral population (Wiens, 2004). However, the speciation process is also controlled by geographic and ecological parameters (Wiens, 2004). Allopatric speciation comprises two modes, vicariance and dispersal. Vicariance occurs when a geographic barrier fragments a population, resulting in the range contraction of a population followed by subsequent differentiation of these populations into new species (Benton and Pearson, 2001; Wiens, 2004; Stigall, 2014). On the other hand, dispersal occurs when a limited number of organisms migrate to another geographic region (range expansion) and subsequently differentiate to form new species. An additional speciation mode that will be implemented in the biogeographical framework is sympatric speciation, which takes

place when speciation occurs within the same geographic range as the ancestor population due to differences in reproductive timing. Within sympatry, the geographic range of ancestor and daughter species are stable over time.

This study provides the first species-level biogeographical framework for anazygids in the Late Ordovician. By incorporating a dated Bayesian phylogeny, dispersal, and colonization patterns among and within basins during this period are constrained and related to Earth systems events including tectophases of the Taconic orogeny, oceanographic changes, and development and closure of dispersal corridors among basins.

3.2 Material and Methods

Speciation processes were reconstructed within a phylogenetic biogeographic analysis using BioGeoBEARS (Matzke, 2013). Data inputs required for this program include a Bayesian phylogeny for the focal clade along with geographic and temporal occurrence data for each taxon.

3.2.1 Phylogenetic framework

BioGeoBEARS requires a fully bifurcated Bayesian phylogenetic tree. Here, I used the tree presented in **Chapter 2** (**Figure 9**), which was constructed under the fossilized birth-death model (FBD), as the input for the biogeographical analysis in a NEXUS file. The FBD tree was generated in BEAST2.5 v2.7.6 (Bouckaert et al., 2019; see **Chapter 2**), using a log-normal clock for character evolution. Its posterior probability mean was -328.71, and no polytomies were observed. Since chronostratigraphic data are

already available in the time calibrated FBD estimation, no additional chronostratigraphic information was required as an input for BioGeoBEARS.

3.2.2 Geographic areas and species occurrence data

Included taxa were assigned to discrete geographic regions based on their known distributions for analysis. Biogeographic regions were defined based on geographic barriers present during the Late Ordovician and follows the framework employed by previous phylogenetic biogeographic studies of Late Ordovician taxa in Laurentia (Lam et al., 2018, 2021). Here, eight geographic regions were included which were first defined based on the outcrop exposures in the states and provinces in the United States and Canada. These are: Western Mid-Continent (W), which includes exposures in the states of Idaho, New Mexico, and Texas; Upper Mississippi Valley (U), comprising exposures in Illinois, Iowa, Minnesota, and Missouri; Appalachian Basins, which includes all of the states within the Appalachians mountain range, and Equatorial Laurentia (E), which includes Anticosti Island, and Quebec. In addition, Alaska (A) and Scoto-Avalonia (O) were included at a paleocontinental level since there are fewer number of species found in the entire paleocontinents. Basins within North America were further subdivided by considering also differences in tectonic flexure, sediment influx, and age. This final classification allowed the differentiation of the Appalachian Basin into the Northern Appalachian Basin (N), comprising the Cincinnati area, Indiana, and northern Kentucky; the Southern Appalachian Basin (S), which includes Nashville, and southern Kentucky; and the Proximal Foreland basin (F), which includes the states of New Jersey, New York, and Virginia (**Figure 12**).

Species occurrences in the eight areas (**Figure 12**) were obtained from the Paleobiology DataBase (www.paleodb.org), IDigBio databases (www.idigbio.org), primary literature, and museum specimens (see **Chapter 2**). Species' presence (1) or absence (0) was coded for each individual basin in a binary format in a text file (**Table A2**).

3.2.3 Model development

Speciation patterns were reconstructed using BioGeoBEARS (BioGeography with Bayesian (and likelihood) Evolutionary Analysis with R Scripts) (Matzke, 2013). This is an R package that applies probabilistic inference methods in phylogenetic biogeographic analyses (Matzke, 2013; Lam et al., 2018). BioGeoBEARS requires two main datasets: (1) a Bayesian phylogeny; and (2) a binary text file containing biogeographic regions in which the species' occurrences are found. The algorithm uses user-informed data to predict the most likely speciation scenarios (i.e., dispersal and vicariance) under different biogeographical models. Here, I applied the standard biogeographical models: Dispersal-extinction-cladogenesis (DEC) (Ree and Smith, 2008); DIVALIKE (Ronquist, 1997); and BayArea-like (Landis et al., 2013). Each of these models incorporates different geographical assumptions regarding clades' ancestry and each has been shown to adequately describe biogeographical patterns of brachiopods (Lam et al., 2018).

The models applied to this dataset incorporate different maximum likelihood models to a known phylogenetic topology for the clade. Although statistical analyses are implemented and posterior probability values are assessed, models do not exist without error. Therefore, all three biogeographical models were compared on the basis of their

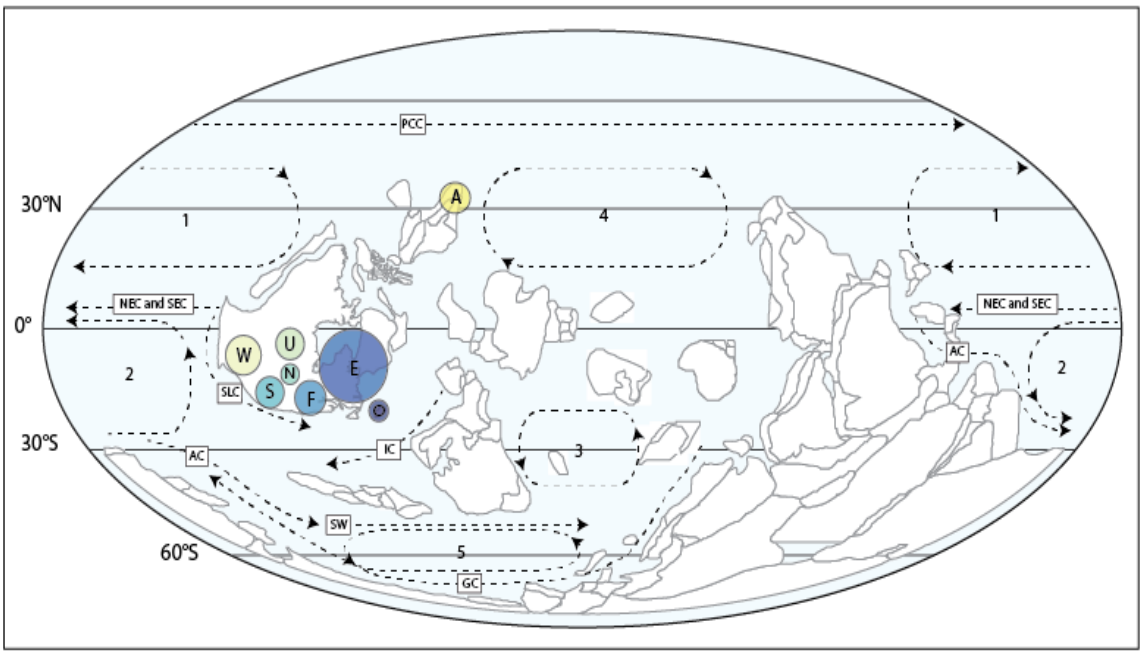

Figure 12. Late Ordovician paleogeographic map with focal basins indicated. A, Alaska; W, Western Mid-Continent; U, Upper Mississippi Valley; N, Northern Appalachian basin; S, Southern Appalachian basin; F, Proximal Foreland basin; E, Equatorial Laurentia; O, Scoto-Avalonia. Arrows and dashed lines indicate reconstructed oceanic gyres labelled from 1 to 5. 1, north Panthalassic convergence; 2, south Panthalassic convergence; 3, south Paleo-Tethys convergence; 4, north Paleo-Tethys convergence; and 5, Rheic convergence. Oceanic currents are abbreviated. NEC, north equatorial current; SEC, south equatorial current; IC, Iapetus Current; SLC, southern Laurentia Current; AC, Antarctica Current; SW, southern westerlies; and GC, Gondwanan westerlies. Paleogeographic map modified after Kolata et al., 2001; Lam and Stigall, 2015; and Lam et al., 2018, 2021.

AIC values, and the model with the lowest recovered AIC is here proposed as the best supported explanation for biogeographical history of the genera.

Considering the two allopatric speciation modes (i.e., vicariance and dispersal) that are detectable in the fossil record and the multiple assumptions concerning ecological and morphological patterns that are often made, I compared all three available models in the package. Here, I assumed that allopatric speciation is always morphologically distinguishable, and, therefore, is recorded within the phylogenetic framework. I also assume that the geographical heritage of daughter lineages is preserved in the fossil record.

Dispersal-extinction-cladogenesis (DEC) is a maximum likelihood-based method which predicts subset sympatry and narrow vicariance at cladogenesis (Ree and Smith, 2008; Matzke, 2013). In the past, the DEC model has proven to be computationally inefficient when applied to datasets with more than 10 biogeographical areas (Landis et al., 2013), because it applies matrix exponentiation to estimate geographical ranges (also referred here as potential states) at the tree's tips. In a larger dataset, the number of potential states (n) a species can occupy is equal to 2^n - 1, therefore, in a study with 10 geographical areas, the probable geographic range would be $2^{10} – 1 = 1{,}023$ (Ree and Smith, 2008; Landis et al., 2013). However, DEC is still appliable to the presented dataset since there are only eight basins analyzed (**Figure 12**). Speciation under the DEC model assumes that each event will generate only two daughter lineages. This results in a nonidentical biogeographical model, in which daughter lineage 1 will always inherit one single geographical area and daughter lineage 2 will inherit part or the total ancestor range (Ree and Smith, 2008).

The DIVALIKE model mimics the parsimony-oriented dispersal-vicariance analysis in a maximum likelihood framework (Matzke, 2013). DIVALIKE is useful to assume equal probability of basin combinations, which is effective when the connectivity of basins is not clearly known (Ronquist, 1997; Ronquist and Sanmartín, 2011). Moreover, DIVALIKE considers all speciation events as potentially vicariance-driven. The lack of power present in the model results in the estimation of widespread vicariance in internal nodes and dispersal events in terminal branches. One method to avoid the tendency of the DIVALIKE model to favor vicariance in internal nodes is to add a maximum number of geographic areas a species can occupy. To address this concern, I set the maximum number of occupied areas by a species to four.

Lastly, BayArea-like is Bayesian-based method, which incorporates the likelihood of species' geographical range evolution through a data augmentation process (Landis et al., 2013). The difference from the latter two is that BayArea-like incorporates Markov Chain Monte Carlo (MCMC) models to estimate potential states (n), in probabilistic framework similar to the ones incorporated in Bayesian phylogenetic models in discrete datasets (Landis et al., 2013). Therefore, the incorporation of complex models allows the estimation of a larger number of biogeographical areas while applying less computational cost (Landis et al., 2013). To test and compare the three different maximum likelihood approaches, I added BayArea-like to the analysis to look for the best suited biogeographical model. Moreover, BayArea-like better describes widespread sympatric patterns (Matzke, 2013; Landis et al., 2013).

An additional tool available within BioGeoBEARS and applied in this study is the +J (i.e., jump dispersal) parameter. This applies the founder-event speciation concept into

the model. This +J parameter is important for this study, considering that the initial gene pool that forms a population created by allopatry matters the most for the new population's evolutionary history, especially in island species (Matzke, 2013). When considering a continent with multiple basins, isolated basins can be treated as islands, and the posterior colonization of these areas is controlled by which members of the population are the colonizers. The +J parameter has already been shown to significantly impact brachiopod phylogeny (Lam et al., 2018). Therefore, each of the three models (DEC, DIVALIKE, and BayArea-like) was computed with and without a +J parameter, resulting in six total biogeographic models.

Lastly, I counted the number of allopatric speciation events in the final selected model, considering dispersal (A -> B) and vicariance (A -> A, A') to develop a summary of speciation processes for the clade.

3.3 Results

Among the six models, the biogeographical model that best described anazygids biogeography was the DEC model + J parameter (**Figure 13**). Dispersal, extinction, jump dispersal, and corrected Akaike Information Criterion for all six models are provided on **Table 7**. Corrected AIC (or AICc) is the preferred parameter used for model selection for this dataset. AICc operates similarly to the traditional AIC, but its applicability is better suited to small sample sizes (Hurvich and Tsai, 1989). In a biogeographical analysis, the sample size is the number of species (in this case 20 anazygid species). Lower AICc scores indicate better model fit. Jump dispersal models have a better model fit than the standard models alone. The model's preference for a founder-event speciation means that

dispersal events across basins where colonization of areas outside the ancestors' geographic range (for example, ABCD -> ABCD, E) is often observed in the clade.

The initial differentiation of the subfamilies Anazyginae and Catazyginae occurred via vicariance events that set the stage for geographically discrete evolution of these clades for much of their evolutionary history. Vicariance is inferred during the early evolution of the Anazyginae related to the separation of the Laurentian interior and marginal basins (**Figure 14**). Ancestrally, the Anazyginae (*Zygospira* lineage) as restricted to intracratonic basins (e.g., Western Mid-Continent, Upper Mississippi Valley, and Northern Appalachian basins), whereas the Catazyginae (*Catazyga* lineage) evolved on the continental margins (**Figure 13**). Two additional vicariance events in the Mohawkian Stage separated the subclades within *Zygospira* to Appalachian basin areas versus Western Mid-Continent areas. Results further suggest a primarily intracratonic evolution for the Anazyginae subfamily, with subsequent expansion to the southern-most basins and proximal islands such as the ones observed for *Zygospira hicksi* (Scoto-Avalonia lineage) and *Zygospira modesta*, and *Z. kentuckiensis* (Northern and Southern Appalachians). In total, 11 dispersal episodes and three vicariance event are observed within the Anazyginae (**Figure 14a**).

In Catazyginae, an initial vicariance event along the continental margin (Scoto-Avalonia islands) established the clade (**Figure 14b**). Subsequently, dispersal events among the two outer-Laurentia areas were reconstructed, from Equatorial Laurentia to the northern most basin (Alaska) and from Equatorial Laurentia to the Southern Appalachian basin. A general progression is apparent within the evolution of *Catazyga*, from Scoto-Avalonia to Equatorial Laurentia to other regions.

Table 7. Comparison of BioGeoBEARS models and models fit statistics in the analysis. Log-likelihood values for each individual model (LnL); Dispersal rates along each branch (d); Extinction rates along each branch (e); Relative weight of jump dispersal, i.e., the +J parameter (j); Akaike Information Criterion (AIC); and corrected Akaike Information Criterion (AICc).

Model	LnL	D	e	J	AIC	AICc
DEC	-62.68	0.055	0.019	0	129.36	130.1
DEC+J	**-54.82**	**0.030**	**1.0^{-12}**	**0.12**	**115.63**	**117.1**
DIVALIKE	-61.56	0.072	1.0^{-12}	0	127.11	127.8
DIVALIKE+J	-56.43	0.043	1.0^{-12}	0.072	118.85	120.4
BAYAREALIKE	-75.17	0.093	0.73	0	154.33	155
BAYAREALIKE+J	-59.33	0.025	1.0^{-7}	0.16	124.65	126.2

A migration event from Equatorial Laurentia resulted in the origination of the only Catazyginae lineage ever found in Alaska, *Catazyga homeospiroides*. The ancestor node also produced descendants in the Equatorial Laurentia and Northern Appalachian basins, *Catazyga anticostiensis* and *Catazyga headi*, respectively. All reconstructed speciation events within the Catazyginae are related to dispersal. In total, three dispersal events are predicted for the subfamily, and no vicariance is observed (**Figure 14b**).

Overall, dispersal was the most frequent speciation mode (total counts: 14) among anazygid taxa during the Late Ordovician. In contrast, vicariance was only predicted four times (**Figure 14**), and all of these events occurred in the Chatfieldian Stage (i.e., Katian Stage Slice 1). The division between the Catazyginae and Anazyginae is reconstructed as due to vicariance, dating approximately 453 Mya (**Figure 14**). This event consisted of the separation of intracratonic lineages (e.g., Southern Appalachia, Northern Appalachia, Foreland basin, Western Mid-Continent) from the Scoto-Avalonia lineages.

3.4 Discussion

Speciation events and evolutionary trends can be linked to tectonic, climatic, oceanographic, and other environmental changes. In the eastern Laurentia, the effects of the Taconic Orogeny on marine communities are well studied, and evidence of interactions between geological and biogeographic data has been previously identified for other clades (Howe, 1988; Patzkowsky and Holland, 1997; Stigall et al., 2017; Lam et al., 2018, 2021; Bauer, 2021). Although the implementation of biogeographical models explains the most probable speciation history of the group, BioGeoBEARS does not consider environmental changes or their impacts on speciation events. However, the

coincidental timing of dispersal events and documented environmental changes during the early Late Ordovician (i.e., from the late Sandbian to the early Katian or Chatfieldian to Edenian Ages) indicates that a link between speciation patterns and basin uplifting/subsidence and intracratonic currents should be explored.

From the upper Middle Ordovician to the lower Late Ordovician, the eastern margin of Laurentia was environmentally unstable (Holland and Patzkowsky, 1998; Brett et al., 2020; McLaughlin and Stigall, 2023). Through tectonic activity, during the Taconic Orogeny, the shallow ocean that was covering most of Laurentia at the time was constantly affected by changes in clastic composition, basinal depth, oceanographic changes, and biotic immigration events (or BIMEs *sensu* Stigall et al. (2017)). The Taconic orogeny is divided into two tectophases; however, only the latter is properly timed to have impacted anazygid evolution. The Taconic tectophase II spanned between 452–450 Mya and increased cool water deposition in the peripheral bulge of the Appalachians Mountains (Ettensohn, 2010; Macdonald et al., 2017; McLaughlin and Stigall, 2023). Kolata et al. (2001) showed that the Sebree Trough, a shallow regional geological feature, extending from west Tennessee to the tri-state area (i.e., Ohio, Kentucky, and Indiana) was developed at the time. The Sebree Trough exhibits variability in width, being wider in the south (Tennessee and Alabama) and thinning towards Ohio. As suggested in previous studies (Kolata et al., 2001; Sohrabi and Jin, 2013; Lam and Stigall, 2015; Jenkins and Holland, 2016; Sproat and McLeod, 2023), this geomorphological characteristic could have influenced the number and frequency of dispersal events between the northeastern-most basins (e.g., South and North

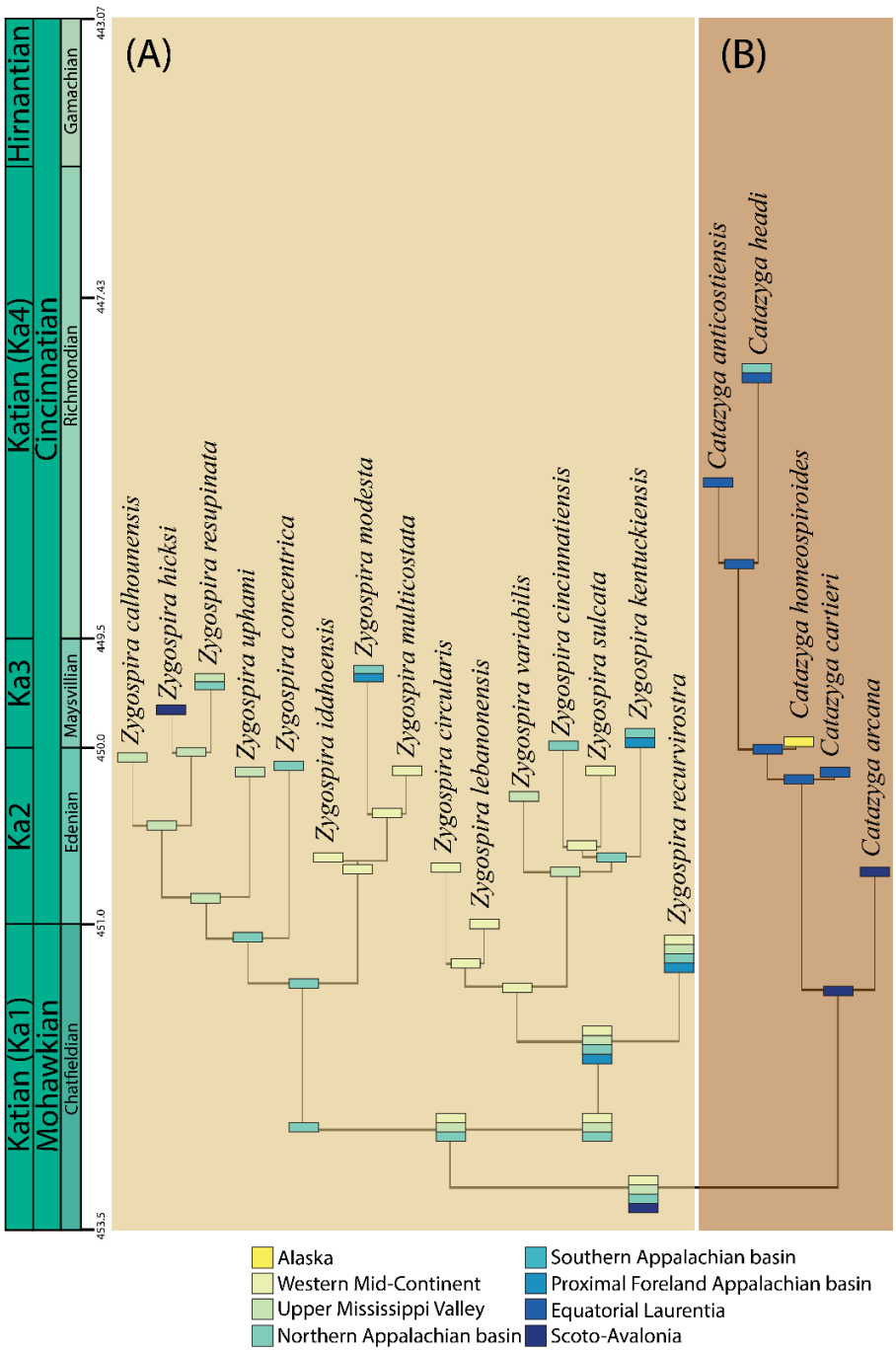

Figure 13. Biogeographical framework under the DEC+J model on BioGeoBEARS (Matzke, 2013). (A) Highlighting the Anazyginae subfamily, (B) Catazyginae subfamily. Basins names and colors correlate with the ones presented in **Figure 12**.

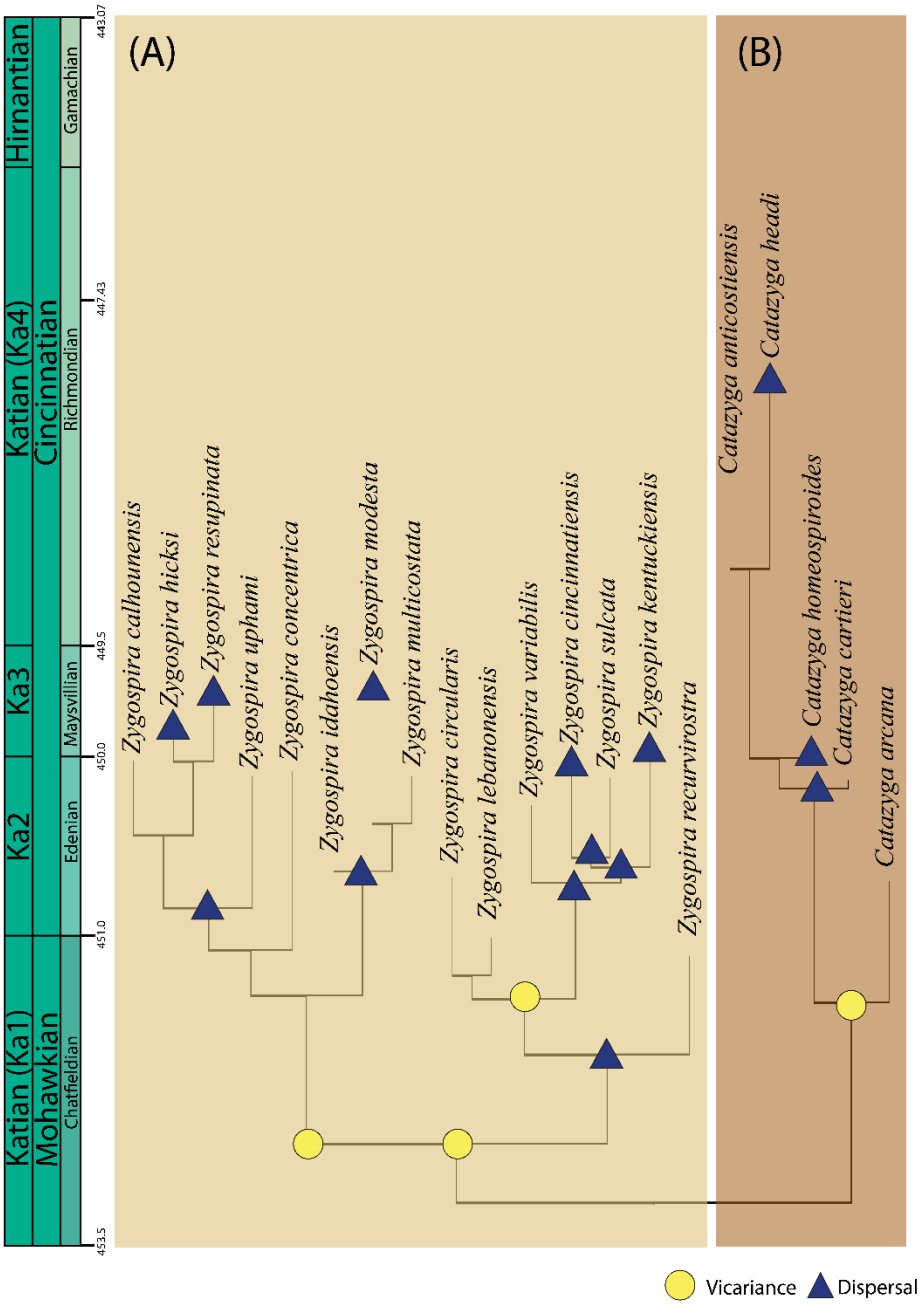

Figure 14. Cladogenetic speciation events estimated under the DEC+J model using BioGeoBEARS (Matzke, 2013). (A) Anazyginae, (B) Catazyginae subfamily.

Appalachian) and the mid-west of Laurentia (Upper Mississippi Valley, and Western Mid-Continent), due to geographical proximity (see **Figure 12**).

Recently, Sproat and McLeod (2023) hypothesized that the Cincinnati anazygid fauna (e.g., *Zygospira modesta*, *Z. kentuckiensis*, and *Z. cincinnatiensis*) might have used this geomorphological feature as a dispersal pathway between the interior basins in Laurentia, resulting in a later diversification in the Cincinnati basin (Northern Appalachian basin, see **Figure 12**). Moreover, Sproat and McLeod (2023) argued that speciation within the Cincinnati anazygid fauna can be explained by sympatric speciation events, rather than allopatric speciation, because of the lack of geographic barriers between North American basins. Sympatric speciation requires niche partitioning and differentiation in niche exploitation by different groups, since it involves biological isolation within a population in the same geographic space (Gavrilets, 2003; Wani, 2011). In the Cincinnati fauna, this distinction is attributed to differences in shell sizes, such as between the larger *Zygospira kentuckiensis* and the smaller *Zygospira modesta* (Sproat and McLeod, 2023). Although described in rare cases in the fossil record (Wani, 2011; Lam et al., 2018; Bauer, 2021), sympatric speciation is not reflected on species' geographic distribution. My findings indicate that sympatric speciation (i.e., speciation within the same geographic area) is observed in the clade (**Figure 14**, see the nodes without symbols). However, sympatric speciation events are genetic isolation episodes within populations, which are not accurately detectable in a higher scale probabilistic approach (this study). Therefore, the Cincinnati fauna resulted from dispersal (*Zygospira resupinata*, *Z. modesta*, and *Z. kentuckiensis*) and vicariance (*Zygospira cincinnatiensis*), rather than sympatric speciation events.

Results of this study support a higher number of allopatric speciation events via dispersal between the western and northeastern basins with a subsequent dispersal to northeast basins. This pattern occurs during the evolution of *Zygospira kentuckiensis* and *Zygospira modesta*, in which migration from western Laurentia is followed by dispersal to the Northern Appalachian basin, and then later dispersal into the Southern Appalachian basin (**Figure 14**). This migration pattern during upper Edenian and Maysvillian time supports previously interpreted ephemeral migration events in the early Katian, preceding the Richmondian Invasion for marine fauna (Stigall and Fine, 2019).

Allopatric speciation events observed at this time can also be explained by changes in oceanic currents (Lam and Stigall, 2015; Lam et al., 2018, 2021; Bauer, 2021). Intracratonic currents during the lower Cincinnatian Series support dispersal pathways during the Edenian and Maysvillian (Lam and Stigall, 2015). Results of this study suggest that Anazygidae followed the same larval pathways reconstructed by Lam and Stigall (2015). These include interchanges between the mid-continent and the Upper Mississippi Valley as well as the mid-continent and the Southern Appalachian basin during early Katian (Edenian) time. Subsequently, during Katian 3 (Maysvillian) time, dispersal pathways operated from the Western Mid-Continent to the Northern, and Southern Appalachian basins, specifically from more equatorial to more temperate basins. Dispersal also occurred between Equatorial Laurentia and Alaska.

Dispersal within the two anazygid groups was found to be associated with the founder-speciation effect, with shallow marine basins acting as biogeographical islands. The island-hopping effect in the marine paleontological record (Congreve and Lieberman, 2008), supports that descendent subpopulations utilized basins as stepping-

stone areas of migration, until the final colonization. This effect is seen in other Paleozoic marine clades, such as trilobites (Congreve and Lieberman, 2008; Lam et al., 2018; Monti et al., 2023), and brachiopods (Villas et al., 2015; Lam et al., 2018). This dispersal pattern explains long-distance migrations, such as the ones observed from Laurentia to Alaska, and Scoto-Avalonia (**Figure 13**).

Besides the dispersal pathways from western Laurentia to eastern Laurentia, anazygid evolution includes dispersal events between paleocontinents. These affinities relate to Ordovician island arcs that are now part of modern Scotland and Wales (Cowper Reed, 1905; Williams, 1962). Two species are found in these paleocontinents, *Catazyga arcana* and *Zygospira hicksi*. Although endemic to the Scoto-Avalonia geographical area (**Figure 13**), morphological and chronostratigraphic data do not support direct shared ancestry between these two species (see **Chapter 2**), which indicates separate evolutionary pathways. *Catazyga arcana* is here reconstructed as an ancestral form of Catazyginae and a remnant or refugial species of the Scoto-Avalonia basin following the vicariance event that originated Anazygidae (**Figure 14b**). Jenkins and Holland (2016) documented how western marine community compositions became more ecologically and biogeographically similar to the Northern and Southern Appalachian basins by the Late Ordovician. These similarities provide evidence of possible evolutionary ancestry shared between these basins.

Anazygid diversity declined during the mid and late Katian (Richmondian). Speciation rates declined relative to extinction rates, and the clade became extinct by approximately 447 Mya (**Chapter 2**). The decrease in atrypid species at this time is recorded in previously published biodiversity curves (Harper et al., 2013), and the

reconstructed phylogeny further reflects this trend (see **Chapter 2**). The extinction of anazygids as a clade is here hypothesized to be a consequence of the Late Katian crisis interval (Stigall et al., 2017; Rasmussen et al., 2019; **Chapter 2**) that preceded the Late Ordovician Mass Extinction (LOME). The reason for this downfall is attributed to the fact that new species were not forming. Dispersal events are observed in the fauna during the Richmondian Invasion in Laurentia, and faunal exchange between continents is recorded, but these are primarily range expansions and do not give rise to new species (Harper et al., 2013; Lam et al., 2018, Stigall et al., 2017; Rasmussen et al., 2019; **Chapter 2**).

Hence, the reconstructed evolutionary biogeography of the Anazygidae appears to follow similar dispersal patterns observed in other brachiopod clades in similar analyses (Lam et al., 2018) and to paleoecological analyses focused on *Zygospira* and the former *Anazyga* (Jenkins and Holland, 2016). Through the usage of anazygids brachiopods in biogeographical framework, this study shows that major trends in speciation and biodiversity were followed by the broadly distributed family.

3.5 Conclusions

The biogeographic evolution of the Anazygidae recovered herein is consistent with the model proposed by Stigall et al. (2017), which states that biodiversity is built by alternating allopatric processes, more specifically, between dispersal events (i.e., Biotic Immigration Events or BIMEs) and vicariance events (**Figure 14**). The tools applied in this study are probabilistic assessments based on the fossil record and previous phylogenies (see **Chapter 2**), which indicates that uncertainty should be regarded when

assessing biogeographical models. Despite that, probabilistic models should not be entirely overlooked from paleontological studies since they provide holistic assessments on species' biogeography and evolutionary history. Here, based on statistical inference, this is the first biogeographical analysis for Anazygidae (Atrypida).

The evolutionary biogeography of the Late Ordovician brachiopod family Anazygidae is characterized by:

(1) Directionality in dispersal events. Dispersal from the more centrally located basins (Upper Mississippi Valley, Western Midcontinent, and Northern Appalachian basin) to southeastern and marginal areas of Laurentia was observed during the middle Katian (Edenian and Maysvillian), and corroborated by sea level, intracratonic currents, and previous biogeographical studies (Lam et al., 2018, 2021).

(2) Ancestral and biogeographical relatedness with proximal island arcs (e.g., Scotland). This finding is supported by previous biogeography-based studies, incorporating other brachiopod faunas (Sohrabi and Jin, 2013; Jenkins and Holland, 2016; Sproat and Jin, 2017). Anazygid diversification and dispersal is synchronized with tectonic separation between the Appalachians and Scotland, which reflects the phylogenetic affinities among species.

(3) A decline in biodiversity by the mid-Katian in Laurentia, resulting from extinction pulses preceding the LOME. At that time, biodiversity in the Ordovician was already in decline, although dispersal and colonization of new geographic ranges occurred, speciation, i.e., the process by which new species are formed, is reduced.

CHAPTER 4: CONCLUSIONS

Species-level Bayesian phylogeny recovered two monophyletic groups within Anazygidae: Anazyginae (*Anazyga* + *Zygospira*) and Catazyginae (*Catazyga*). The study presented in **Chapter 2** tests previously hypothesized evolutionary relationships for the clade, which stated that the stratigraphically older previously assigned *Anazyga* species are the ancestors of *Zygospira* and *Catazyga* species (Copper, 1977). The results indicate that morphological features of the external and the known internal variations within the subfamily Anazyginae are shared among *Anazyga* and *Zygospira*. Although some species previously attributed to *Anazyga* are stratigraphically older than *Zygospira*, the set of species classically attributed to *Anazyga* do not constitute a clade. Therefore, *Anazyga* is interpreted as a junior synonym of *Zygospira* herein which agrees with Hall and Clarke (1894). Therefore, all species recently attributed to *Anazyga,* and two species recently attributed to *Catazyga* are now combined into a monophyletic *Zygospira* concept.

A key question in atrypid systematics is the relative importance of internal versus external characteristics for classification and phylogeny reconstruction. This question was tested by running multiple analyses that included or excluded internal characteristics. For this clade, the inclusion of internal characters reduced phylogenetic signal and output resolution. This likely results from an extremely low percent of valid species that contain diagnosable interiors. The lack of constraint on internal characters for the great majority of species renders use of these characters prohibitive. Internal characters may be useful for future revisions as more data becomes available.

Evolutionary rate analyses indicate that the Anazygidae originated during the Sandbian 2 Stage (453 Mya) and attained maximum diversification rate and standing

diversity during Katian 3 (Maysvillian) time. These observations are compatible with basinal-level ecological studies (Candela, 2015; Jenkins and Holland, 2016), that indicate an increase in species-level biodiversity for *Zygospira* during the early Katian. In the Late Ordovician, high-level diversity patterns relate to higher sea levels, which promoted allopatric speciation via dispersal (see **Chapter 3**). Anazygidae diversity declined in the latest Katian, which overlaps with major abiotic and biotic changes, such as the Richmondian Invasion (450 Ma) in the Cincinnati basin in eastern Laurentia (Holland, 1997; Stigall, 2019; Forsythe and Stigall, 2023), and the environmental changes preceding the Late Ordovician Mass Extinction, such as lower sea levels and temperatures (**Figure 15**).

The applied biogeographic framework presented in **Chapter 3** shows that dispersal was the most common speciation mode observed for Anazygidae during the Late Ordovician. Dispersal directionality was also observed, with Anazyginae experiencing a southern-oriented migration. More specifically, 57% of the dispersal episodes within Anazyginae were directed from midwestern basins to southern Laurentian basins. This dispersal pathway among the Laurentian basins is attributed to be a consequence of intracratonic ocean currents (Lam et al., 2018) and the effects of the Sebree Trough (Kolata et al., 2001), which allowed oscillating connectivity between southern and midwestern Laurentia. This pathway was probably utilized by other clades (Lam et al., 2018, 2021), considering that similarities in community structures are observed (Sohrabi and Jin, 2013; Jenkins and Holland, 2016). Probabilistic analytical methods estimate that the anazygid subfamilies originated from a vicariance event, this episode is synchronous with the Taconic tectophase 2 during the Sandbian 2 (Mohawkian

Stage in the North American nomenclature, Ettensohn, 1994; Candela, 2015). This event is followed by multiple dispersal episodes during the early Katian, which are synchronous with higher sea levels.

The presented phylogenetic and biogeographic probabilistic models provide a novel framework for interpreting anazygids' evolutionary history during the Late Ordovician. Nonetheless, it is important to distinguish probabilistic models from empirical datasets, and although these models show satisfactory posterior probability, future incorporation of new data will enhance model fit and power. The biogeographic and phylogenetic patterns of anazygid taxa have long been discussed in the literature (Copper, 1977, 2001; Sproat and McLeod, 2023), but dispersal and vicariance models have never been used to holistically access the clade's diversification during the Ordovician. This study elucidates previously assumed patterns of dispersal and evolutionary inheritance shared among the analyzed taxa, and presents new perspectives into the relationship between biotic evolution of the Anazygidae and environmental and tectonic changes.

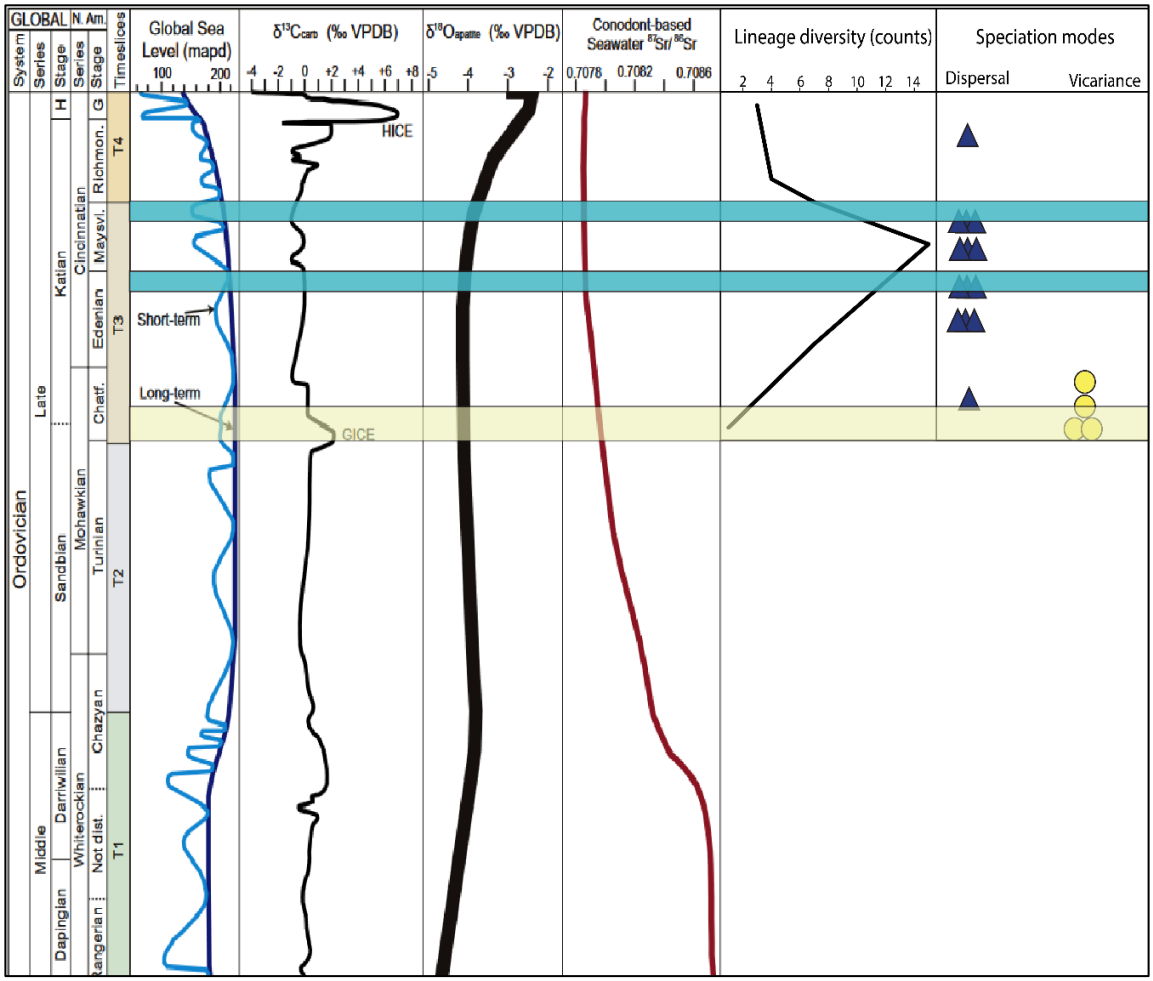

Figure 15. Chronostratigraphic Ordovician chart, from left to right: (1) Global sea level in meters above present-day sea level; (2) $\delta^{13}C$ from Bergström et al. (2009); (3) $\delta^{18}O$ apatite curve from Trotter et al. (2008); (4) Seawater strontium values from Edwards et al. (2015); (5) Diversity curve for Anazygidae (number of lineages counted); and (6) Counts of allopatric speciation events. The Taconic tectopulse is highlighted in light yellow, and episodes of high sea-levels are highlighted in blue. Modified from Lam et al. (2018).

REFERENCES

Amsden, T.W., 1974, Late Ordovician and Early Silurian articulate brachiopods from Oklahoma southwestern Illinois, and eastern Missouri: Oklahoma Geological Survey, v. 119.

Baarli, B.G., Huang, B., and Maroja, L.S., 2022, Phylogeny of the Ordovician and Silurian members of the order Atrypida: Journal of Systematic Palaeontology, v. 20, p. 2145920, doi:10.1080/14772019.2022.2145920.

Barido-Sottani, J., Pohle, A., de Baets, K., Murdock, D., and Warnock, R.C.M., 2023, Putting the F into FBD analysis: tree constraints or morphological data? Palaeontology, v. 66, doi:https://doi.org/10.1111/pala.12679.

Barido-Sottani, J., Van Tiel, N.M.A., Hopkins, M.J., Wright, D.F., Stadler, T., and Warnock, R.C.M., 2020, Ignoring fossil age uncertainty leads to inaccurate topology and divergence time estimates in time calibrated tree inference: Frontiers in Ecology and Evolution, v. 8, p. 183, doi:10.3389/fevo.2020.00183.

Bauer, J.E., 2021, Paleobiogeography, paleoecology, diversity, and speciation patterns in the Eublastoidea (Blastozoa: Echinodermata): Paleobiology, v. 47, p. 221–235, doi:10.1017/pab.2020.27.

Bauer, J.E., and Stigall, A.L., 2016, A combined morphometric and phylogenetic revision of the Late Ordovician brachiopod genera *Eochonetes* and *Thaerodonta*: Journal of Paleontology, v. 90, p. 888–909, doi:10.1017/jpa.2016.56.

Benton, M.J., and Pearson, P.N., 2001, Speciation in the fossil record: Trends in Ecology & Evolution, v. 16, p. 405–411, doi:10.1016/S0169-5347(01)02149-8.

Bergström, S.M., Chen, X., Gutiérrez-Marco, J.C., and Dronov, A., 2009, The new chronostratigraphic classification of the Ordovician System and its relations to major regional series and stages and to δ^{13} C chemostratigraphy: Lethaia, v. 42, p. 97–107, doi:10.1111/j.1502-3931.2008.00136.x.

Billings, E., 1862, New species of fossils from different parts of the Lower, Middle, and Upper Silurian rocks of Canada, *in* Paleozoic fossils, Montreal, Geological Survey of Canada, 4, v. 1, p. 96–168.

Blakey, R., 2013, North American paleogeographic maps: Colorado Plateau Geosystems, Inc., https://deeptimemaps.com/ (accessed May 2024).

Bouckaert, R. et al., 2019, BEAST 2.5: An advanced software platform for Bayesian evolutionary analysis (M. Pertea, Ed.): PLOS Computational Biology, v. 15, p. e1006650, doi:10.1371/journal.pcbi.1006650.

Bretsky, P.W., 1969, Central Appalachian Late Ordovician Communities: Geological Society of America Bulletin, v. 80, p. 193.

Brett, C.E., Aucoin, C.D., Dattilo, B.F., Freeman, R.L., Hartshorn, K.R., McLaughlin, P.I., and Schwalbach, C.E., 2020, Revised sequence stratigraphy of the upper Katian Stage (Cincinnatian) strata in the Cincinnati Arch reference area: Geological and paleontological implications: Palaeogeography, Palaeoclimatology, Palaeoecology, v. 540, p. 109483, doi:10.1016/j.palaeo.2019.109483.

Brunton, H., Cocks, L.R.M., and Long, S.L. (Eds.), 2001, Radiations and extinctions of atrypide brachiopods: Ordovician–Devonian, *in* Brachiopods, CRC Press, p. 215–225, doi:10.1201/9780203210437-29.

Candela, Y., 2015, Evolution of Laurentian brachiopod faunas during the Ordovician Phanerozoic sea level maximum: Earth-Science Reviews, v. 141, p. 27–44, doi:10.1016/j.earscirev.2014.11.012.

Cocks, L.R.M., and Torsvik, T.H., 2021, Ordovician palaeogeography and climate change: Gondwana Research, v. 100, p. 53–72, doi:10.1016/j.gr.2020.09.008.

Congreve, C.R., and Lieberman, B.S., 2008, Phylogenetic and biogeographic analysis of Ordovician homalonotid trilobites: The Open Paleontology Journal, v. 1, p. 24–32, doi:10.2174/1874425700801010024.

Cooper, G.A., 1956, Chazyan and related brachiopods: Smithsonian Miscellaneous Collections, v. 127.

Cooper, G.A., and Kindle, C.H., 1936, New brachiopods and trilobites from the Upper Ordovician of Percé, Quebec: Journal of Paleontology, v. 10, p. 348–372.

Copper, P., 2002, Atrypida, *in* Treatise on Invertebrate Paleontology, Part H: Brachiopoda, Boulder, The Geological Society of America and the University of Kansas, Rhynchonelliformea, v. 4, p. H1377–H1474.

Copper, P., 1982, Early Silurian Atrypoids from Manitoulin Island and Bruce Peninsula, Ontario: Journal of Paleontology, v. 56, p. 680–702.

Copper, P., 1986, Evolution of the earliest smooth spire-bearing atrypoids (Brachiopoda: Lissatrypidae, Ordovician - Silurian): Palaeontology, v. 29, p. 827–867.

Copper, P., 2001, Radiations and extinctions of atrypide brachiopods: Ordovician-Devonian, *in* Brachiopods, p. 460, https://doi.org/10.1201/9780203210437.

Copper, P., 1977, Zygospira and some related Ordovician and Silurian atrypoid brachiopods: Palaeontology, v. 20, p. 295–335.

Cowper Reed, F.R., 1905, New Fossils from the Haverfordwest District: Geological Magazine, v. 2, doi:10.1017/S0016756800128377.

Davidson, T., 1882, A Monograph of the British Fossil Brachiopoda. Vol. V. Part I. Devonian and Silurian Supplements. Pages 1–134; Plates I–VII: Monographs of the Palaeontographical Society, v. 36, p. 1–134, doi:10.1080/02693445.1882.12027975.

Edwards, C.T., Saltzman, M.R., Leslie, S.A., Bergström, S.M., Sedlacek, A.R.C., Howard, A., Bauer, J.A., Sweet, W.C., and Young, S.A., 2015, Strontium isotope (87Sr/86Sr) stratigraphy of Ordovician bulk carbonate: Implications for preservation of primary seawater values: Geological Society of America Bulletin, v. 127, p. 1275–1289, doi:10.1130/B31149.1.

Ettensohn, F.R., 2010, Origin of Late Ordovician (mid-Mohawkian) temperate-water conditions on southeastern Laurentia: Glacial or tectonic?, *in* The Ordovician Earth System, Geological Society of America, doi:10.1130/2010.2466(11).

Ettensohn, F.R., 1994, Tectonic Control on Formation and Cyclicity of Major Appalachian Uncoformities and Associated Stratigraphic Sequences, *in* Tectonic and Eustatic Controls on Sedimentary Cycles, SEPM Society for Sedimentary Geology, v. 4, https://doi.org/10.2110/csp.94.04.

Fenton, C.L., and Fenton, M.A., 1922, Some Black River brachiopods from the Mississippi Valley: v. 29.

Finnegan, S., Rasmussen, C.M.Ø., and Harper, D.A.T., 2016, Biogeographic and bathymetric determinants of brachiopod extinction and survival during the Late Ordovician Mass Extinction: Proceedings of the Royal Society B: Biological Sciences, v. 283, p. 20160007, doi:10.1098/rspb.2016.0007.

Foerste, A.F., 1910, Preliminary notes on Cincinnatian and Lexington Fossils of Ohio, Indiana, Kentucky and Tennessee: Scientific Laboratories Bulletin, v. 16, p. 17–100.

Foote, M., 2000, Origination and extinction components of taxonomic diversity: General problems: Paleobiology, v. 26, p. 74–102.

Forsythe, I.J., and Stigall, A.L., 2023, Insights for modern invasion ecology from biotic changes of the Clarksville Phase of the Richmondian Invasion (Ordovician, Katian): Paleobiology, v. 49, p. 493–508, doi:10.1017/pab.2022.45.

Gavrilets, S., 2003, Models of speciation: What have we learned in 40 years? Evolution, v. 57, p. 2197–2215, doi:10.1111/j.0014-3820.2003.tb00233.x.

Gavryushkina, A., and Zhang, C., 2020, Total-evidence dating and the fossilized birth-death model, *in* The Molecular Evolutionary Clock: Theory and Practice, Sydney, Australia, Springer Cham, p. 175–193.

Goldman, D., Sadler, P.M., Leslie, S.A., Melchin, M.J., Agterberg, F.P., and Gradstein, F.M., 2020, The Ordovician Period, *in* Geologic Time Scale 2020, Elsevier, p. 631–694, doi:10.1016/B978-0-12-824360-2.00020-6.

Goloboff, P.A., Mattoni, C.I., and Quinteros, A.S., 2006, Continuous characters analyzed as such: Cladistics, v. 22, p. 589–601, doi:10.1111/j.1096-0031.2006.00122.x.

Hall, 1862, Observations upon a new genus of Brachiopoda: Fifteenth Report on the Cabinet of Natural History, v. 15, p. 154–155.

Hall, J., 1847, Palaeontology of New York: Containing Descriptions of the Organic Remains of the Lower Division of the New York System (Equivalent to the Lower Silurian rocks of Europe): Albany, New York, Paleontological Society, v. 1, 338 p.

Hall, J., and Clarke, J.M., 1894, Palaeontology: An introduction to the study of the genera of Paleozoic Brachiopoda: Albany, New York, Geological Survey of the State of New York Part II, v. 3.

Harper, D.A.T., Lefebvre, B., Percival, I.G., and Servais, T., 2023, A Global Synthesis of the Ordovician System: London, Geological Society, Special Publications 532, v. 1.

Harper, D.A.T., Popov, L.E., and Holmer, L.E., 2017, Brachiopods: origin and early history (A. Smith, Ed.): Palaeontology, v. 60, p. 609–631, doi:10.1111/pala.12307.

Harper, D.A.T., Rasmussen, C.M.Ø., Liljeroth, M., Blodgett, R.B., Candela, Y., Jin, J., Percival, I.G., Rong, J., Villas, E., and Zhan, R., 2013, Chapter 11 Biodiversity, biogeography and phylogeography of Ordovician rhynchonelliform brachiopods: Geological Society, London, Memoirs, v. 38, p. 127–144, doi:10.1144/M38.11.

Heled, J., and Bouckaert, R.R., 2013, Looking for trees in the forest: summary tree from posterior samples: BMC Evolutionary Biology, v. 13, p. 221, doi:10.1186/1471-2148-13-221.

Ho, S.Y.W., and Phillips, M.J., 2009, Accounting for calibration uncertainty in phylogenetic estimation of evolutionary divergence times: Systematic Biology, v. 58, p. 367–380, doi:10.1093/sysbio/syp035.

Holland, S.M., 1997, Using time/environment analyssi to recognize faunal events in the Upper Ordovician of the Cincinnati Arch, *in* Paleontological events: stratigraphic,

ecological, and evolutionary implications, New York, Columbia University Press, p. 309–334.

Holland, S.M., and Patzkowsky, M.E., 1998, Sequence stratigraphy and relative sea-level history of the Middle and Upper Ordovician of the Nashville Dome, Tennessee: Journal of Sedimentary Research, v. 68, p. 684–699, doi:https://doi.org/10.2110/jsr.68.684.

Hopkins, M.J., Bapst, D.W., Simpson, C., and Warnock, R.C.M., 2018, The inseparability of sampling and time and its influence on attempts to unify the molecular and fossil records: Paleobiology, v. 44, p. 561–574, doi:10.1017/pab.2018.27.

Howe, H.J., 1988, Articulate brachiopods from the Richmondian of Tennessee: Journal of Paleontology, v. 62, p. 204–218, doi:10.1017/S002233600002984X.

Howe, H.J., 1965, Plectambonitacea, Strophomenacea, and Atrypacea from the Montoya Group (Ordovician) of Trans-Pecos Texas: Journal of Paleontology, v. 39, p. 647–656.

Hurvich, C.M., and Tsai, C.-L., 1989, Regression and time series model selection in small samples: Biometrika, v. 76, p. 297–307.

Jenkins, C.E., and Holland, S.M., 2016, Continental-scale biogeographic variation: provinces versus gradients in the Upper Ordovician of Laurentia: Paleobiology, v. 42, p. 410–425, doi:10.1017/pab.2015.56.

Jin, J., Caldwell, W.G.E., and Norford, B.S., 1997, Late Ordovician brachiopods and biostratigraphy of the Hudson Bay Lowlands, northern Manitoba and Ontario: 513, 513 p., doi:10.4095/208903.

Jin, J., Harper, D.A.T., Cocks, L.R.M., McCausland, P.J.A., Rasmussen, C.M.O., and Sheehan, P.M., 2013, Precisely locating the Ordovician equator in Laurentia: Geology, v. 41, p. 107–110, doi:10.1130/G33688.1.

Kolata, D.R., Huff, W.D., and Bergström, S.M., 2001, The Ordovician Sebree Trough: An oceanic passage to the Midcontinent United States: Geological Society of America Bulletin, v. 113, p. 1067–1078, doi:10.1130/0016-7606(2001)113<1067:TOSTAO>2.0.CO;2.

Kröger, B., 2018, Changes in the latitudinal diversity gradient during the Great Ordovician Biodiversification Event: Geology, v. 46, p. 127–130, doi:10.1130/G39587.1.

Lam, A.R., Sheffield, S.L., and Matzke, N.J., 2021, Estimating dispersal and evolutionary dynamics in diploporan blastozoans (Echinodermata) across the great Ordovician

biodiversification event: Paleobiology, v. 47, p. 198–220, doi:10.1017/pab.2020.24.

Lam, A.R., and Stigall, A.L., 2015, Pathways and mechanisms of Late Ordovician (Katian) faunal migrations of Laurentia and Baltica: Estonian Journal of Earth Sciences, v. 64, p. 62, doi:10.3176/earth.2015.11.

Lam, A.R., Stigall, A.L., and Matzke, N.J., 2018, Dispersal in the Ordovician: Speciation patterns and paleobiogeographic analyses of brachiopods and trilobites: Palaeogeography, Palaeoclimatology, Palaeoecology, v. 489, p. 147–165, doi:10.1016/j.palaeo.2017.10.006.

Landis, M.J., Matzke, N.J., Moore, B.R., and Huelsenbeck, J.P., 2013, Bayesian analysis of biogeography when the number of areas is large: Systematic Biology, v. 62, p. 789–804, doi:10.1093/sysbio/syt040.

Lewis, P.O., 2001, A likelihood approach to estimating phylogeny from discrete morphological character data: Systematic Biology, v. 50, p. 913–925, doi:10.1080/106351501753462876.

Macdonald, F.A., Karabinos, P.M., Crowley, J.L., Hodgin, E.B., Crockford, P.W., and Delano, J.W., 2017, Bridging the gap between the foreland and hinterland II: Geochronology and tectonic setting of Ordovician magmatism and basin formation on the Laurentian margin of New England and Newfoundland: American Journal of Science, v. 317, p. 555–596, doi:10.2475/05.2017.02.

Matzke, N.J., 2013, Probabilistic historical biogeography: new models for founder-event speciation, imperfect detection, and fossils allow improved accuracy and model-testing: Frontiers of Biogeography, v. 5, p. 242–248.

McLaughlin, P.I., and Stigall, A.L., 2023, Ordovician of the conterminous United States: Geological Society, London, Special Publications, v. 533, p. 93–113, doi:10.1144/SP533-2022-198.

Meek, F.B., 1873, Report of the Geological Survey of Ohio: Geology and Palaeontology, *in* Nevins and Meyers, Palaeontology Part II, v. 1, p. 399.

Monti, D.S., Confalonieri, V.A., and Tortello, M.F., 2023, The Central Andean Basin as a dispersal centre: Biogeographic patterns of olenid trilobites during the late Cambrian – Early Ordovician: Palaeogeography, Palaeoclimatology, Palaeoecology, v. 618, p. 111519, doi:10.1016/j.palaeo.2023.111519.

Nascimento, F.F., Reis, M.D., and Yang, Z., 2017, A biologist's guide to Bayesian phylogenetic analysis: Nature Ecology & Evolution, v. 1, p. 1446–1454, doi:10.1038/s41559-017-0280-x.

Nettelroth, H.C.E., 1889, Kentucky Fossil Shells: A Monograph of the Fossil Shells of the Silurian and Devonian Rocks of Kentucky: Frankfort, Kentucky, E. Polk Johnson, Public Printer and Binder, 245 p.

Parins-Fukuchi, C., 2018, Use of continuous traits can improve morphological phylogenetics: Systematic Biology, v. 67, p. 328–339, doi:10.1093/sysbio/syx072.

Patzkowsky, M.E., and Holland, S.M., 1999, Biofacies replacement in a sequence stratigraphic framework: Middle and Upper Ordovician of the Nashville Dome, Tennessee, USA: PALAIOS, v. 14, p. 301, doi:10.2307/3515459.

Patzkowsky, M.E., and Holland, S.M., 2007, Diversity partitioning of a Late Ordovician marine biotic invasion: controls on diversity in regional ecosystems: Paleobiology, v. 33, p. 295–309, doi:10.1666/06078.1.

Patzkowsky, M.E., and Holland, S.M., 1997, Patterns of turnover in Middle and Upper Ordovician brachiopods of the eastern United States: a test of coordinated stasis: Paleobiology, v. 23, p. 420–443, doi:10.1017/S0094837300019825.

Purcell, C.K.Q., and Stigall, A.L., 2021, Ecological niche evolution, speciation, and feedback loops: Investigating factors promoting niche evolution in Ordovician brachiopods of eastern Laurentia: Palaeogeography, Palaeoclimatology, Palaeoecology, v. 578, p. 110555, doi:10.1016/j.palaeo.2021.110555.

Quinlan, G.M., and Beaumont, C., 1984, Appalachian thrusting, lithospheric flexure, and the Paleozoic stratigraphy of the Eastern Interior of North America: Canadian Journal of Earth Sciences, v. 21, p. 973–996, doi:10.1139/e84-103.

Rae, T.C., 1998, The logical basis for the use of continuous characters in phylogenetic systematics: Cladistics, v. 14, p. 221–228.

Rambaut, A., Drummond, A.J., Xie, D., Baele, G., and Suchard, M.A., 2018, Posterior summarisation in Bayesian phylogenetics using Tracer 1.7: Systematic Biology, v. 67, p. 901–904, doi:https://doi.org/10.1093/sysbio/syy032.

Rasmussen, C.M.Ø., Kröger, B., Nielsen, M.L., and Colmenar, J., 2019, Cascading trend of Early Paleozoic marine radiations paused by Late Ordovician extinctions: Proceedings of the National Academy of Sciences, v. 116, p. 7207–7213, doi:10.1073/pnas.1821123116.

Ree, R.H., and Smith, S.A., 2008, Maximum Likelihood Inference of Geographic Range Evolution by Dispersal, Local Extinction, and Cladogenesis (A. Baker, Ed.): Systematic Biology, v. 57, p. 4–14, doi:10.1080/10635150701883881.

Ronquist, F., 1997, Dispersal-Vicariance Analysis: A new approach to the quantification of historical biogeography: Systematic Biology, v. 46, p. 195–203.

Ronquist, F., Klopfstein, S., Vilhelmsen, L., Schulmeister, S., Murray, D.L., and Rasnitsyn, A.P., 2012, A total-evidence approach to dating with fossils, applied to the early radiation of the Hymenoptera: Systematic Biology, v. 61, p. 973–999, doi:10.1093/sysbio/sys058.

Ronquist, F., and Sanmartín, I., 2011, Phylogenetic methods in biogeography: Annual Review of Ecology, Evolution, and Systematics, v. 42, p. 441–464, doi:10.1146/annurev-ecolsys-102209-144710.

Ross, R.J., 1959, Brachiopod fauna of Saturday Mountain Formation, southern Lemhi Range, Idaho: United States Department of the Interior, Geological Survey, p. 441–459.

Ross, R.J., and Dutro, J.T., 1966, Silicified Ordovician brachiopods from east-central Alaska: Smithsonian Miscellaneous Collections, v. 149.

Rzhonsnitskaya, M.A., 1960, Otryad Rhynchonellida i Atrypida, *in* Osnovy paleontologoii. Mshanki, Brakhiopody, Moscow, Akademiya Nauk SSSR, p. 257–264.

Sepkoski, J.J., 1981, A factor analytic description of the Phanerozoic marine fossil record: Paleobiology, v. 7, p. 36–53, doi:10.1017/S0094837300003778.

Servais, T., and Harper, D.A.T., 2018, The Great Ordovician Biodiversification Event (GOBE): definition, concept and duration: Lethaia, v. 51, p. 151–164, doi:10.1111/let.12259.

Servais, T., Harper, D.A.T., Lefebvre, B., and Percival, I.G., 2023, A Global Synthesis of the Ordovician System: London, Geological Society, Special Publications 533, v. 2.

Sohrabi, A., and Jin, J., 2013, Global palaeobiogeography of brachiopod faunas during the early Katian (Late Ordovician) greenhouse episode: Palaeogeography, Palaeoclimatology, Palaeoecology, v. 389, p. 78–86, doi:10.1016/j.palaeo.2013.02.027.

Sproat, C.D., and Jin, J., 2017, Paleobiogeography of the early Late Ordovician "Trentonian" (latest Sandbian to middle Katian) brachiopod fauna during a major marine transgression and colonization of the epicontinental seas in Laurentia: Palaeogeography, Palaeoclimatology, Palaeoecology, v. 487, p. 105–117, doi:10.1016/j.palaeo.2017.07.041.

Sproat, C.D., and McLeod, J.S.A., 2023, Sympatric speciation driving evolution of Late Ordovician brachiopod *Zygospira* in eastern North America: Journal of Paleontology, v. 97, p. 292–317, doi:10.1017/jpa.2022.102.

Sproule, J.C., 1936, A study of the Cobourg Formation: Geological Survey of Canada Memoir, v. 202, p. 93–111.

Stadler, T., 2010, Sampling-through-time in birth–death trees: Journal of Theoretical Biology, v. 267, p. 396–404, doi:10.1016/j.jtbi.2010.09.010.

Stadler, T., Gavryushkina, A., Warnock, R.C.M., Drummond, A.J., and Heath, T.A., 2018, The fossilized birth-death model for the analysis of stratigraphic range data under different speciation modes: Journal of Theoretical Biology, v. 447, p. 41–55, doi:10.1016/j.jtbi.2018.03.005.

Stadler, T., Kühnert, D., Bonhoeffer, S., and Drummond, A.J., 2013, Birth–death skyline plot reveals temporal changes of epidemic spread in HIV and hepatitis C virus (HCV): Proceedings of the National Academy of Sciences, v. 110, p. 228–233, doi:10.1073/pnas.1207965110.

Stigall, A.L., 2019, The Invasion Hierarchy: Ecological and evolutionary consequences of invasions in the fossil record: Annual Review of Ecology, Evolution, and Systematics, v. 50, p. 355–380, doi:10.1146/annurev-ecolsys-110617-062638.

Stigall, A.L., 2014, When and how do species achieve niche stability over long time scales? Ecography, v. 37, p. 1123–1132, doi:10.1111/ecog.00719.

Stigall, A.L., Bauer, J.E., Lam, A.R., and Wright, D.F., 2017, Biotic immigration events, speciation, and the accumulation of biodiversity in the fossil record: Global and Planetary Change, v. 148, p. 242–257, doi:10.1016/j.gloplacha.2016.12.008.

Stigall, A.L., Edwards, C.T., Freeman, R.L., and Rasmussen, C.M.Ø., 2019, Coordinated biotic and abiotic change during the Great Ordovician Biodiversification Event: Darriwilian assembly of early Paleozoic building blocks: Palaeogeography, Palaeoclimatology, Palaeoecology, v. 530, p. 249–270, doi:10.1016/j.palaeo.2019.05.034.

Stigall, A.L., and Fine, R., 2019, Contrasting ecosystem impacts of biotic invasions in the Type Cincinnatian Series (Late Ordovician, Katian): Palaeoworld, v. 28, p. 166–172, doi:10.1016/j.palwor.2018.04.004.

Stigall Rode, A.L., 2005, The application of geographic information systems to paleobiogeography: Implications for the study of invasions and mass extinctions: The Paleontological Society Papers, v. 11, p. 77–88, doi:10.1017/S108933260000125X.

Trotter, J.A., Williams, I.S., Barnes, C.R., Lécuyer, C., and Nicoll, R.S., 2008, Did cooling oceans trigger Ordovician biodiversification? Evidence from conodont thermometry: Science, v. 321, p. 550–554, doi:10.1126/science.1155814.

Ulrich, E.O., 1879, New genera and species of fossils from the lower Silurian about Cincinnati: Journal of the Cincinnati Society of Natural History, v. 2, p. 8–30.

Villas, E., Colmenar, J., and Gutiérrez-Marco, J.C., 2015, Late Ordovician brachiopods from Peru and their palaeobiogeographical relationships (F. Alvarez, Ed.): Palaeontology, v. 58, p. 455–487, doi:10.1111/pala.12152.

Wang, Y., 1949, Maquoketa Brachiopoda of Iowa: Geological Society of America Memoir, v. 42, p. 55.

Wani, R., 2011, Sympatric speciation drove the macroevolution of fossil cephalopods: Geology, v. 39, p. 1079–1082, doi:10.1130/G32317.1.

Wiens, J.J., 2004, Speciation and ecology revisited: Phylogenetic niche conservatism and the origin of species: Evolution, v. 58, p. 193–197, doi:10.1111/j.0014-3820.2004.tb01586.x.

Williams, A., 1962, The Barr and Lower Ardmillan Series (Caradoc) of the Girvan District, South-West Ayrshire, with descriptions of the Brachiopoda: London, The Geological Society of London, v. 3, 267 p.

Williams, A., Carlson, S.J., Brunton, C.H.C., and Holmer, L.E., 1996, A Supra-Ordinal Classification of the Brachiopoda: Philosophical Transactions: Biological Sciences, v. 351, p. 1171–1193, doi:doi.org/10.1098/rstb.1996.0101.

Winchell, N.H., and Schuchert, C., 1892, Preliminary descriptions of new Brachiopoda from the Trenton and Hudson River groups of Minnesota: The American Geologist, v. 9, p. 285–294.

Winchell, N.H., and Schuchert, C., 1895, The Lower Silurian Brachiopoda of Minnesota, *in* Paleontology, Minneapolis, Geological Natural History Survey of Minnesota, 1, v. 3.

Wright, A., 2019, A systematist's guide to estimating Bayesian phylogenies from morphological data: Insect Systematics and Diversity, v. 3, doi:https://doi.org/10.1093/isd/ixz006.

Wright, D.F., and Stigall, A.L., 2013, Geologic drivers of Late Ordovician faunal change in Laurentia: Investigating links between tectonics, speciation, and biotic invasions (R. J. Butler, Ed.): PLoS ONE, v. 8, p. e68353, doi:10.1371/journal.pone.0068353.

Wright, D.F., and Stigall, A.L., 2014, Species-level phylogenetic revision of the Ordovician orthide brachiopod *Glyptorthis* from North America: Journal of Systematic Palaeontology, v. 12, p. 893–906, doi:10.1080/14772019.2013.839584.

Wright, A., Wagner, P.J., and Wright, D.F., 2021, Testing Character Evolution Models in Phylogenetic Paleobiology: A case study with Cambrian echinoderms: Elements of Paleontology, doi:10.1017/9781009049016.

APPENDICES

Table A1. Measurement data for specimens collected from museum and literature sources. The used taxonomic nomenclature relates to the second column on **Table 1**. Coded characters relate to the character states presented on **Table 2**. Columns enumerated from 0 to 36: (1) Specimen museum number (codes related to the ones presented on **Chapter 2**); (2) Type category; (3) Maximum length in mm; (4) Maximum width in mm; (5) Maximum height in mm; (6) Length/width ratio; (7) Outline; (8) Number of ribs (ventral valve); (9) Number of ribs (dorsal valve); (10) Concentric ornament; (11) Ribs appearance; (12) Profile; (13) Beak angle; (14) Beak size in mm; (15) Position fold/sulcus; (16) Apical angle; (17) Hinge line angle; (18) Accentuated median costae; (19) Sinuosity of the anterior commissure; (20) Anterior deflection in mm; (21) Posterior deflection in mm; (22) Deep median costae; (23) Deflections in the anterior commissure; (24) Double ribs; (25) Degree of progression of the sulcus in mm; (26) Accentuated median rib (ventral); (27) Sulcus and fold appearance; (28) Ribs spacing; (29) Deflection rate (anterior); (30) Deflection rate (posterior); (31) Number of whorls; (32) Jugum position; (33) Cardinal processes; (34) Teeth; (35) Jugum shape; and (36) Hinge plates.

ID	1	2	3	4	5	6	7	8	9	10	11	12	13	14	15	16	17	18	19	20	21	22	23	24	25	26	27	28	29	30	31	32	33	34	35	36
Zygospira modesta 1	**USNM40485**	Plesiotype	5.89	5.9	2.98	0.99	0	15	16	0	1	0	40	1.18	2	70	20	0	2	1.45	1.4	0	1	1	3.16	0	1	2.7	1.53	1.58	?	?	?	?	?	?
Zygospira modesta 2	**USNM418150**	Plesiotype	4.25	4.22	2.12	1.007	0	19	18	0	1	0	30	0.94	2	65	45	0	2	1.74	1.58	0	1	1	1.62	0	1	4.2	0.38	0.54	?	?	?	?	?	?
Zygospira modesta 3	**USNM418148**	Plesiotype	5.89	6.13	3.65	0.96	1	18	16	0	1	0	40	1.4	2	53	45	0	2	1.74	1.58	0	1	1	2.76	0	1	2.6	1.91	2.07	?	?	?	?	?	?
Zygospira modesta 4	**ACC175438**	Non-type	6.6	6.91	3.32	0.95	1	18	18	0	1	0	60	0.86	2	40	43	0	1	1.39	1.83	1	1	1	2.17	0	1	2.6	1.93	1.49	?	?	?	?	?	?
Zygospira modesta 5	**ACC175438**	Non-type	6.31	6.47	2.69	0.97	1	15	16	0	1	0	40	1.18	2	42	30	0	1	2.47	2.05	1	1	1	1.62	0	0	2.4	0.22	0.64	?	?	?	?	?	?
Zygospira modesta 6	**USNM1.22 F1**	Non-type	8.38	9	4.95	0.93	1	19	17	0	1	0	40	2.03	2	40	44	0	1	3.08	3.59	1	1	1	2.73	0	1	1.8	1.87	1.36	?	?	?	?	?	?
Zygospira modesta 7	**USNM1356 A**	Lectotype	7.2	8.1	3.9	0.88	1	?	?	?	1	0	?	?	?	?	?	?	?	?	?	?	?	?	?	?	?	?	?	?	5	2	0	2	1	?
Zygospira modesta 8	**13561**	Non-type	7.8	9.2	4.1	0.84	1	?	18	?	1	?	?	?	1	?	?	0	?	?	?	1	?	1	?	1	?	?	?	?	?	?	?	?	?	?
Zygospira modesta 9	**P6460**	Non-type	?	?	?	?	?	16	18	0	1	?	?	?	2	?	?	0	?	?	?	?	?	?	0	?	0	1	?	?	?	?	?	?	?	?
Zygospira modesta 10	**P1496**	Non-type	?	?	?	?	?	21	?	0	1	?	?	?	?	?	?	?	?	?	?	?	?	?	?	0	1	?	?	?	?	?	?	?	?	?

Table A1 Continued

ID	1	2	3	4	5	6	7	8	9	10	11	12	13	14	15	16	17	18	19	20	21	22	23	24	25	26	27	28	29	30	31	32	33	34	35	36
Zygospira modesta 11	**CMNH64207a**	Non-type	7.29	8.47	3.87	0.861	1	15	14	0	1	2	53	2	2	43	34	0	5	1.29	1.67	1	1	1	2.83	0	1	1.6	2.58	2.2	?	?	?	?	?	?
Zygospira modesta 12	**CMNH64207b**	Non-type	5.82	6.84	3.1	0.851	1	16	14	0	1	0	45	1.07	1	33	48	0	5	1.21	1.69	1	1	1	2.5	0	1	2.0	1.89	1.41	?	?	?	?	?	?
Zygospira modesta 13	**CMNH69130a**	Non-type	7.14	7.79	4.31	0.917	1	19	18	0	1	0	62	1.15	2	43	40	0	0	1.42	1.68	1	1	1	2.64	0	1	2.3	2.89	2.63	?	?	?	?	?	?
Zygospira modesta 14	**CMNH69130b**	Non-type	6.35	6.97	3.01	0.911	1	19	19	0	1	0	56	1.34	1	36	39	0	5	1.54	1.59	1	1	1	2.28	0	1	2.7	1.47	1.42	?	?	?	?	?	?
Zygospira sulcata 1	**USNM145059**	Paratype	6.4	7.11	4.21	0.9	1	25	20	0	1	0	50	1.8	1	56	41	0	1	1.77	2.48	0	1	0	2.42	0	1	2.8	2.44	1.73	?	?	?	?	?	?
Zygospira sulcata 2	**USNM145059**	Paratype	6.17	6.24	3.86	0.989	1	24	21	0	1	0	41	2	1	50	55	0	0	2.54	2.28	0	1	0	1.26	0	1	3.3	1.32	1.58	?	?	?	?	?	?
Zygospira sulcata 3	**USNM145059**	Paratype	6.37	6.52	4.32	0.977	1	?	?	0	1	0	45	1.86	1	57	65	0	0	2.34	2.35	0	1	0	2.24	0	1	?	1.98	1.97	?	?	?	?	?	?
Zygospira sulcata 4	**NA**	NA	5.67	5.7	5.1	0.995	3	27	26	0	1	0	58.53	1.59	2	39.71	18.93	1	3	1.56	2.68	1	?	1	0	1	?	4.5	3.54	2.42	?	?	?	?	?	?
Zygospira resupinata 1	**USNM2.6G5c**	Non-type	5.2	4.6	2.56	1.13	3	15	17	0	1	2	47	1.27	2	53	40	0	0	1.5	1.67	0	1	0	1.21	0	0	3.6	1.06	0.89	?	?	?	?	?	?
Zygospira resupinata 2	**USNM2.6G5c**	Non-type	3.52	3.5	2.31	1.006	3	?	?	0	1	2	40	0.77	2	50	49	0	0	1.2	1.26	0	1	0	1	0	0	?	1.11	1.05	?	?	?	?	?	?
Zygospira resupinata 3	**ACC306219**	Non-type	5.64	5.48	3.9	1.02	3	13	16	0	1	2	50	2.4	2	40	42	0	0	2.5	3.19	0	1	0	1.55	0	0	2.9	1.4	0.71	?	?	?	?	?	?
Zygospira resupinata 4	**ACC306219**	Non-type	4.19	4.28	2.1	0.979	2	15	16	0	1	2	50	0.8	2	55	35	0	0	1.08	1.55	0	1	0	1.45	0	0	3.738	1.02	0.55	?	?	?	?	?	?
Zygospira resupinata 5	**USNM175438**	Non-type	5.08	4.65	2.51	1.092	3	18	21	0	1	0	50	1.23	2	55	51	0	0	1.56	1.88	0	1	0	1.44	0	0	4.516	0.95	0.63	?	?	?	?	?	?
Zygospira resupinata 6	**USNM175438**	Non-type	4.57	4.02	2.1	1.137	3	15	19	0	1	0	49	1.88	2	52	47	0	0	1.28	1.48	0	1	0	1.7	0	0	4.726	0.82	0.62	?	?	?	?	?	?
Zygospira resupinata 7	**SUI1874**	Holotype	7.27	7.13	4.03	1.02	3	23	25	0	1	0	61	1.49	1	53	39	0	2	1.76	1.75	0	1	0	2.23	0	0	3.506	2.27	2.28	?	?	?	?	?	?
Zygospira resupinata 8	**SUI1873**	Paratype	5.07	5.24	2.89	0.968	3	19	19	0	1	0	42	1.03	1	57	44	0	2	1.29	1.3	1	1	0	0.5	0	0	3.626	1.6	1.59	?	?	?	?	?	?
Zygospira cincinnatiensis 1	**N/A**	Non-type	6.13	7.65	4.63	0.801	1	6	10	1	1	1	55	2.43	1	40	25	0	1	3	3.3	1	1	0	2.29	0	1	1.307	1.63	1.33	?	?	?	?	?	?
Zygospira cincinnatiensis 2	**N/A**	Non-type	6.32	7.04	3.45	0.898	1	11	13	0	1	1	50	2.21	1	40	33	0	1	2.96	2.36	1	1	0	2.53	0	1	1.847	0.49	1.09	?	?	?	?	?	?

Table A1 Continued

ID	1	2	3	4	5	6	7	8	9	10	11	12	13	14	15	16	17	18	19	20	21	22	23	24	25	26	27	28	29	30	31	32	33	34	35	36
Zygospira cincinnatiensis 3	**P9509**	Non-type	?	?	?	?	1	14	16	0	1	?	?	?	2	?	?	0	?	?	?	1	?	0	?	0	1	?	?	?	?	?	?	?	?	?
Zygospira cincinnatiensis 4	**CMNH28127**	Non-type	8.94	10.02	4.19	0.892	1	14	14	0	1	2	57	3.1	1	60	53	0	4	1.63	2.51	1	1	1	2.39	1	1	1.39	2.56	1.68	?	?	?	?	?	?	?
Zygospira cincinnatiensis 5	**CMNH69136**	Non-type	10.33	11.81	5.18	0.875	1	12	12	0	1	0	35	2.43	1	38	40	0	4	3.19	2.78	1	1	1	2.97	1	1	1.01	1.99	2.4	?	?	?	?	?	?	?
Zygospira cincinnatiensis 6	**CMNH19064**	Non-type	6.81	8.6	3.59	0.792	1	17	15	0	1	2	61	2.52	2	36	40	0	5	1.95	2.48	1	1	0	2.74	1	1	1.74	1.64	1.11	?	?	?	?	?	?	?
Zygospira cincinnatiensis 7	**CMNH18946**	Non-type	13.13	14.86	8.29	0.884	1	16	14	0	1	0	65	1.67	1	41	37	0	5	2.69	2.31	1	1	0	3.08	1	1	0.94	5.6	5.98	?	?	?	?	?	?	?
Zygospira kentuckiensis 1	**USNM511871**	Plesiotype	16.48	18.07	11.13	0.912	1	20	21	0	1	0	45	5.15	1	32	33	0	1	5.6	6.38	1	1	0	6.74	0	1	1.16	5.53	4.75	?	?	?	?	?	?	?
Zygospira kentuckiensis 2	**USNM511872**	Plesiotype	12.13	16.86	8.3	0.719	1	24	23	0	1	0	42	4.52	1	35	32	0	1	4.7	4.55	1	1	0	4.82	0	1	1.36	3.6	3.75	?	?	?	?	?	?	?
Zygospira kentuckiensis 3	**USNM97596**	Plesiotype	8.69	10.28	4.71	0.845	1	20	19	0	1	0	50	3.81	1	45	40	0	1	2.26	3.25	1	1	0	2.89	0	1	1.84	2.45	1.46	?	?	?	?	?	?	?
Zygospira kentuckiensis 4	**USNM9748**	Non-type	13.04	14.73	7.79	0.885	1	19	20	0	1	1	65	4.48	2	45	35	0	1	4.34	5.06	0	1	0	5.42	0	1	1.35	3.45	2.73	?	?	?	?	?	?	?
Zygospira kentuckiensis 5	**USNM9748**	Non-type	12.27	13.66	8.07	0.898	1	22	20	0	1	1	60	4.31	2	46	55	0	1	4.12	4.84	0	1	0	3.78	0	1	1.46	3.95	3.23	?	?	?	?	?	?	?
Zygospira kentuckiensis 6	**CMNH19062a**	Non-type	13.41	15.54	7.55	0.863	1	22	21	1	1	0	49	4.08	2	44	39	0	5	4.2	5.53	0	1	0	4.55	0	1	1.35	3.35	2.02	?	?	?	?	?	?	?
Zygospira kentuckiensis 7	**CMNH19062b**	Non-type	13.13	14.86	8.29	0.884	2	18	16	1	1	0	60	5.4	1	44	44	0	5	4.8	6.2	0	1	0	4.45	0	1	1.07	3.49	2.09	?	?	?	?	?	?	?
Zygospira kentuckiensis 8	**CMNH54470a**	Non-type	10.2	12.03	6.21	0.848	2	21	20	1	1	0	58	2.79	2	54	53	0	0	2.79	4.04	0	1	0	3.88	0	0	1.66	3.42	2.17	?	?	?	?	?	?	?
Zygospira kentuckiensis 9	**CMNH54470b**	Non-type	7.91	8.93	4.57	0.886	2	22	21	1	1	0	46	2.28	2	28	41	0	0	1.98	2.59	0	1	0	3.09	0	0	2.35	2.59	1.98	?	?	?	?	?	?	?
Zygospira kentuckiensis 10	**CMNH33663a**	Non-type	11.23	11.99	6.23	0.937	1	18	21	1	1	0	37	4.69	2	48	46	0	5	3.75	3.43	1	1	0	?	0	0	1.75	2.48	2.8	?	?	?	?	?	?	?
Zygospira kentuckiensis 11	**CMNH33663b**	Non-type	11.59	12.69	6.48	0.913	1	17	22	0	1	0	67	3.19	2	47	47	0	5	3.24	3.68	1	1	0	?	0	0	1.73	3.24	2.8	?	?	?	?	?	?	?
Zygospira concentrica 1	**CMNH19027a**	Non-type	7.1	7.51	4.06	0.945	2	2	6	1	0	0	60	2.24	2	33	30	0	4	1.7	2.26	1	0	0	?	0	1	0.79	2.36	1.8	?	?	?	?	?	?	?
Zygospira concentrica 2	**CMNH19027b**	Non-type	5.92	6.87	3.53	0.862	2	3	3	1	0	0	55	1.51	2	47	45	0	4	2.29	2.55	0	0	0	?	0	1	0.43	1.24	0.98	?	?	?	?	?	?	?
Zygospira concentrica 3	**CMNH33583**	Non-type	7.23	6.97	3.57	1.037	3	3	2	1	0	0	52	2.51	1	46	34	0	4	2.05	1.97	1	0	0	?	1	1	0.28	1.52	1.6	?	?	?	?	?	?	?
Zygospira concentrica 4	**CMNH18969**	Non-type	7.47	10.41	3.96	0.718	2	21	11	1	0	0	56	2.03	1	47	35	0	4	2.63	1.65	1	0	0	?	0	1	1.05	1.33	2.31	?	?	?	?	?	?	?
Zygospira resupinata multicostata 1	**NA**	Non-type	7.37	7.63	2.99	0.966	3	29	28	0	1	0	66.08	2.79	2	38.72	15.05	1	1	3.73	3.2	1	?	1	?	1	?	3.67	-0.74	-0.21	?	?	?	?	?	?	?
Zygospira resupinata multicostata 2	**NA**	Non-type	7.89	8.12	5.67	0.972	3	33	32	0	1	0	?	?	2	37.78	14.96	1	1	3.46	3.66	1	?	1	?	1	?	3.94	2.21	2.01	?	?	?	?	?	?	?
Zygospira resupinata multicostata 3	**NA**	Non-type	7.05	6.27	5.43	1.124	3	27	26	0	1	0	?	?	2	40.84	15.54	1	1	3.52	3.07	1	?	1	?	1	?	4.14	1.91	2.36	?	?	?	?	?	?	?
Zygospira resupinata multicostata 4	**NA**	Non-type	8.08	7.83	5.73	1.032	3	29	28	0	1	0	72.07	3.29	2	33.39	17.87	1	1	3.41	3.47	1	?	1	?	1	?	3.57	2.32	2.26	?	?	?	?	?	?	?

Table A1 Continued

ID	1	2	3	4	5	6	7	8	9	10	11	12	13	14	15	16	17	18	19	20	21	22	23	24	25	26	27	28	29	30	31	32	33	34	35	36
Zygospira resupinata multicostata 5	**NA**	Non-type	6.91	7.37	5.63	0.938	3	29	28	0	1	0	?	?	2	38.98	20.4	1	1	3.32	3.07	1	?	1	?	1	?	3.79	2.31	2.56	?	?	?	?	?	?
Zygospira resupinata multicostata 6	**NA**	Non-type	7.6	7.49	5.37	1.015	3	29	28	0	1	0	?	?	2	37.45	21.78	1	1	3.11	3.62	1	?	1	?	1	?	3.73	2.26	1.75	?	?	?	?	?	?
Zygospira resupinata multicostata 7	**NA**	Non-type	8.28	7.58	5.19	1.092	3	29	28	0	1	0	60.03	3.03	2	39.83	15.19	1	1	3.19	3.98	1	?	1	?	1	?	3.69	2	1.21	?	?	?	?	?	?
Zygospira resupinata multicostata 8	**NA**	Non-type	7.5	7.33	5.44	1.023	3	32	31	0	1	0	53.56	2.93	2	40.9	15.7	1	1	2.79	3.24	1	?	1	?	1	?	4.22	2.65	2.2	?	?	?	?	?	?
Zygospira resupinata multicostata 9	**NA**	Non-type	8.15	7.44	5.67	1.095	3	27	26	0	1	0	?	?	2	42.41	15.98	1	1	2.98	3.52	1	?	1	?	1	?	3.49	2.69	2.15	?	?	?	?	?	?
Zygospira resupinata multicostata 10	**NA**	Non-type	7.21	6.99	4.96	1.031	3	29	28	0	1	0	?	?	2	40.25	15.96	1	1	1.93	3.29	1	?	1	?	1	?	4.00	3.03	1.67	?	?	?	?	?	?
Zygospira resupinata multicostata 11	**NA**	Non-type	7.81	8.34	5.37	0.936	3	27	26	0	1	0	58.12	3.04	2	39.29	15.01	1	1	3.2	3.73	1	?	1	?	1	?	3.11	2.17	1.64	?	?	?	?	?	?
Zygospira resupinata multicostata 12	**NA**	Non-type	6.29	6.77	4.29	0.929	3	33	32	0	1	0	66.54	2.13	2	35.27	14.02	1	1	2.68	2.83	1	?	1	?	1	?	4.72	1.61	1.46	?	?	?	?	?	?
Zygospira resupinata multicostata 13	**NA**	Non-type	7.04	7.47	4.77	0.942	3	29	28	0	1	0	?	?	2	35.02	13.93	1	1	2.93	3.66	1	?	1	?	1	?	3.74	1.84	1.11	?	?	?	?	?	?
Zygospira resupinata multicostata 14	**NA**	Non-type	7.39	7.66	5.52	0.965	3	25	24	0	1	0	?	?	2	33.22	16.59	1	1	2.51	3.21	1	?	1	?	1	?	3.13	3.01	2.31	?	?	?	?	?	?
Zygospira resupinata multicostata 15	**NA**	Non-type	6.89	6.96	4.53	0.99	3	27	26	0	1	0	71.05	2.69	2	35.52	18.76	1	1	2.31	2.82	1	?	1	?	1	?	3.73	2.22	1.71	?	?	?	?	?	?
Zygospira resupinata multicostata 16	**NA**	Non-type	7.58	6.78	5.33	1.118	3	29	28	0	1	0	?	?	2	39.27	17.35	1	1	3.13	3.37	1	?	1	?	1	?	4.13	2.2	1.96	?	?	?	?	?	?
Zygospira resupinata multicostata 17	**NA**	Non-type	7.3	7.5	5.1	0.973	3	33	32	0	1	0	?	?	2	31.56	16.99	1	1	2.88	3.48	1	?	1	?	1	?	4.26	2.22	1.62	?	?	?	?	?	?
Zygospira resupinata multicostata 18	**NA**	Non-type	7.18	7.38	4.69	0.973	3	27	26	0	1	0	?	?	2	34.08	16.03	1	1	3.04	2.77	1	?	1	?	1	?	3.52	1.65	1.92	?	?	?	?	?	?
Zygospira resupinata multicostata 19	**NA**	Non-type	7.23	7.23	5.33	1	3	29	28	0	1	0	63.1	2.4	2	36.58	16.05	1	1	3.12	3.62	1	?	1	?	1	?	3.87	2.21	1.71	?	?	?	?	?	?
Zygospira resupinata multicostata 20	**NA**	Non-type	7.99	8.16	5.13	0.979	3	29	28	0	1	0	?	?	2	40.17	16.14	1	1	2.27	3.19	1	?	1	?	1	?	3.43	2.86	1.94	?	?	?	?	?	?
Zygospira resupinata multicostata 21	**NA**	Non-type	7.6	7.68	5.15	0.99	3	31	30	0	1	0	58.62	2.79	2	36.92	16.09	1	1	2.53	3.07	1	?	1	?	1	?	3.90	2.62	2.08	?	?	?	?	?	?
Zygospira resupinata multicostata 22	**NA**	Non-type	6.82	6.85	4.51	0.996	3	27	26	0	1	0	?	?	2	40.54	15.8	1	1	3.07	3.05	1	?	1	?	1	?	3.79	1.44	1.46	?	?	?	?	?	?
Zygospira resupinata multicostata 23	**NA**	Non-type	7.87	7.3	5.63	1.078	3	27	26	0	1	0	?	?	2	35.04	17.52	1	1	3.27	3.41	1	?	1	?	1	?	3.56	2.36	2.22	?	?	?	?	?	?
Zygospira resupinata multicostata 24	**NA**	Non-type	8.33	9.06	5.44	0.919	3	35	34	0	1	0	72.92	2.56	2	36.26	16.17	1	1	3.13	3.32	1	?	1	?	1	?	3.75	2.31	2.12	?	?	?	?	?	?

Table A1 Continued

ID	1	2	3	4	5	6	7	8	9	10	11	12	13	14	15	16	17	18	19	20	21	22	23	24	25	26	27	28	29	30	31	32	33	34	35	36
***Zygospira resupinata multicostata* 25**	**NA**	Non-type	5.74	5.48	3.96	1.047	3	28	27	0	1	0	?	?	2	37.72	19.14	1	1	2.23	2.91	1	?	1	?	1	?	4.92	1.73	1.05	?	?	?	?	?	?
***Zygospira resupinata multicostata* 26**	**NA**	Non-type	5.73	5.15	3.65	1.113	3	27	26	0	1	0	61.25	1.75	2	51.22	15.14	1	1	2.17	2.33	1	?	1	?	1	?	5.04	1.48	1.32	?	?	?	?	?	?
***Zygospira resupinata multicostata* 27**	**NA**	Non-type	6.95	6.99	4.69	0.994	3	27	26	0	1	0	?	?	2	43.1	15.37	1	1	2.52	2.77	1	?	1	?	1	?	3.72	2.17	1.92	?	?	?	?	?	?
***Zygospira resupinata multicostata* 28**	**NA**	Non-type	6.74	6.36	5.23	1.06	3	25	24	0	1	0	?	?	2	37.76	16.7	1	1	2.91	3.03	1	?	1	?	1	?	3.77	2.32	2.2	?	?	?	?	?	?
***Zygospira resupinata multicostata* 29**	**NA**	Non-type	7.78	7.34	5.01	1.06	3	29	28	0	1	0	?	?	2	44.84	16.85	1	1	2.95	2.74	1	?	1	?	1	?	3.81	2.06	2.27	?	?	?	?	?	?
***Zygospira resupinata multicostata* 30**	**NA**	Non-type	6.46	6.49	4.33	0.995	3	31	30	0	1	0	61.37	2.24	2	40.66	15.02	1	1	2.41	2.7	1	?	1	?	1	?	4.62	1.92	1.63	?	?	?	?	?	?
***Zygospira resupinata multicostata* 31**	**NA**	Non-type	8.42	7.94	5.94	1.06	3	31	30	0	1	0	?	?	2	33.37	13.54	1	1	2.95	3.32	1	?	1	?	1	?	3.77	2.99	2.62	?	?	?	?	?	?
***Zygospira resupinata multicostata* 32**	**NA**	Non-type	6.5	5.72	4.3	1.136	3	27	26	0	1	0	?	?	2	42.38	14.14	1	3	2.45	2.63	1	?	1	?	1	?	4.54	1.85	1.67	?	?	?	?	?	?
***Zygospira resupinata multicostata* 33**	**NA**	Non-type	5.43	5.66	3.37	0.959	3	27	26	0	1	0	62.51	1.89	2	39.74	17.71	1	1	1.85	2.13	1	?	1	?	1	?	4.594	1.52	1.24	?	?	?	?	?	?
***Zygospira resupinata multicostata* 34**	**NA**	Non-type	5.69	5.31	3.83	1.072	3	25	24	0	1	0	59.97	2.17	2	40.7	17.62	1	1	2.08	2.57	1	?	1	?	1	?	4.52	1.75	1.26	?	?	?	?	?	?
***Zygospira resupinata multicostata* 35**	**NA**	Non-type	4.43	4.18	2.77	1.06	3	35	34	0	1	0	?	?	2	37.01	22.04	1	1	1.76	1.81	1	?	1	?	1	?	8.134	1.01	0.96	?	?	?	?	?	?
***Zygospira resupinata multicostata* 36**	**NA**	Non-type	6.39	6.18	3.98	1.034	3	27	26	0	1	0	?	?	2	35.21	15.97	1	1	2.08	2.68	1	?	1	?	1	?	4.207	1.9	1.3	?	?	?	?	?	?
***Zygospira resupinata multicostata* 37**	**NA**	Non-type	5.35	5.56	3.54	0.962	3	25	24	0	1	0	?	?	2	34.9	17.85	1	1	***2.06***	2.38	1	***?***	1	?	1	?	4.317	1.48	1.16	?	?	?	?	?	?
***Zygospira resupinata multicostata* 38**	**NA**	Non-type	8.03	7	5.56	1.147	3	31	30	0	1	0	62.95	2.38	2	39.65	14.79	1	1	***2.34***	3.43	1	***?***	1	?	1	?	4.286	3.22	2.13	?	?	?	?	?	?
***Zygospira resupinata multicostata* 39**	**NA**	Non-type	7.42	6.41	4.63	1.158	3	28	27	0	1	0	?	?	2	42.49	15.42	1	1	***2.7***	2.63	1	***?***	1	?	1	?	4.212	1.93	2	?	?	?	?	?	?
***Zygospira resupinata multicostata* 40**	**NA**	Non-type	7.47	6.5	4.82	1.149	3	35	34	0	1	0	?	?	2	34.48	14.88	1	1	***2.98***	2.91	1	***?***	1	?	1	?	5.231	1.84	1.91	?	?	?	?	?	?
***Zygospira resupinata multicostata* 41**	**NA**	Non-type	7.67	6.73	5.27	1.14	3	29	28	0	1	0	?	?	2	29.57	14.78	1	1	***3***	3.38	1	***?***	1	?	1	?	4.16	2.27	1.89	?	?	?	?	?	?
***Zygospira resupinata multicostata* 42**	**NA**	Non-type	6.23	5.49	4.31	1.135	3	27	26	0	1	0	?	?	2	36.05	16.68	1	3	***1.81***	2.65	1	***?***	1	?	1	?	4.736	2.5	1.66	?	?	?	?	?	?
***Zygospira resupinata multicostata* 43**	**NA**	Non-type	6.85	5.93	4.42	1.155	3	29	28	0	1	0	?	?	2	42.9	17.3	1	1	***3.16***	3.04	1	***?***	1	?	1	?	4.722	1.26	1.38	?	?	?	?	?	?
***Zygospira resupinata multicostata* 44**	**NA**	Non-type	6.8	5.69	4.18	1.195	3	29	28	0	1	0	70.17	2.23	2	38.34	18.22	1	1	***1.99***	2.58	1	***?***	1	?	1	?	4.921	2.19	1.6	?	?	?	?	?	?

Table A1 Continue

ID	1	2	3	4	5	6	7	8	9	10	11	12	13	14	15	16	17	18	19	20	21	22	23	24	25	26	27	28	29	30	31	32	33	34	35	36
Zygospira resupinata multicostata 45	**NA**	Non-type	7.19	6.3	4.26	1.141	3	29	28	0	1	0	?	?	2	42.84	11.92	1	1	2.58	2.7	1	?	1	?	1	?	4.444	1.68	1.56	?	?	?	?	?	?
Zygospira resupinata multicostata 46	**NA**	Non-type	7.23	6.37	4.49	1.135	3	27	26	0	1	0	62.35	2.24	2	44.68	17.06	1	1	2.8	2.79	1	?	1	?	1	?	4.082	1.69	1.7	?	?	?	?	?	?
Zygospira resupinata multicostata 47	**NA**	Non-type	6.43	5.4	4.51	1.191	3	25	24	0	1	0	68.72	2.69	2	43.1	17.15	1	1	2.24	2.79	1	?	1	?	1	?	4.444	2.27	1.72	?	?	?	?	?	?
Zygospira resupinata multicostata 48	NA	Non-type	6.1	5.4	3.95	1.13	3	27	26	0	1	0	?	?	2	41.05	15.23	1	1	2.53	2.41	1	?	1	?	1	?	4.82	1.42	1.54	?	?	?	?	?	?
Zygospira resupinata multicostata 49	NA	Non-type	7.21	6.41	4.83	1.125	3	27	26	0	1	0	?	?	2	34.54	18	1	1	3.44	2.98	1	?	1	?	1	?	4.056	1.39	1.85	?	?	?	?	?	?
Zygospira circularis 1	USNM133267	Plesiotype	3.52	3.63	2.12	0.97	1	23	22	0	1	1	?	?	2	49	49	0	1	0.88	1.35	0	1	0	1.05	0	1	6.061	1.24	0.77	?	?	?	?	?	?
Zygospira circularis 2	USNM133268	Plesiotype	3.61	3.73	1.77	0.968	1	22	22	0	1	1	?	?	2	49	35	0	1	0.87	1	0	1	0	?	0	1	5.898	0.9	0.77	?	?	?	?	?	?
Anazyga lebanonensis 1	USNM133270	Plesiotype	4.49	4.6	2.65	0.976	1	17	17	0	1	1	41	1.06	1	55	52	0	1	2	1.68	0	1	0	1.97	0	1	3.696	0.65	0.97	?	?	?	?	?	?
Anazyga lebanonensis 2	USNM133269	Plesiotype	3.87	4.02	2.12	0.963	1	17	18	0	1	1	35	0.5	1	48	53	0	1	1.46	1.75	0	1	0	1.52	0	1	4.478	0.66	0.37	?	?	?	?	?	?
Anazyga putilla 1	USNM133362	Plesiotype	3.6	3.31	1.98	1.088	3	13	12	0	1	0	?	?	2	71	65	0	2	1.26	1.04	0	1	1	1.36	1	1	3.625	0.72	0.94	?	?	?	?	?	?
Anazyga putilla 2	USNM133263	Plesiotype	3.95	3.31	1.91	1.193	3	15	12	0	1	0	55	0.7	2	55	62	0	2	0.96	0.93	0	1	1	1.4	1	1	3.625	0.95	0.98	?	?	?	?	?	?
Anazyga recurvirostra 1	USNM87057	Plesiotype	8.51	9.77	5.17	0.871	1	19	23	0	1	1	43	2.59	1	50	41	0	1	2.36	4.12	0	1	0	2.46	0	0	2.354	2.81	1.05	?	?	?	?	?	?
Anazyga recurvirostra 2	USNM97609	Plesiotype	8.29	9.23	5.58	0.898	1	18	18	0	1	1	39	2.65	1	50	35	0	1	3	3.33	0	1	0	3.23	0	0	1.95	2.58	2.25	?	?	?	?	?	?
Anazyga recurvirostra 3	USNM78460	Holotype	9.03	8.96	5.84	1.008	1	21	19	0	1	1	50	2.09	1	40	35	0	1	3	3.18	0	1	0	3.58	0	0	2.121	2.84	2.66	?	?	?	?	?	?
Anazyga recurvirostra 4	USNM248869	Non-type	4.56	4.6	3.08	0.991	0	16	20	0	1	0	45	1.38	2	40	35	0	1	1.6	1.93	0	1	0	1.22	0	0	4.348	1.48	1.15	?	?	?	?	?	?
Anazyga recurvirostra 5	USNM248771	Non-type	5.21	5	3.08	1.042	4	17	14	0	1	0	51	1.96	2	48	40	0	1	2.95	2.48	0	1	0	1.72	0	0	2.8	0.13	0.6	?	?	?	?	?	?
Anazyga recurvirostra 6	USNM124826	Plesiotype	5.05	5.24	2.97	0.964	1	19	17	0	1	0	45	0.7	2	50	41	0	0	0.99	0.6	0	0	0	1.6	0	1	3.244	1.98	2.37	?	?	?	?	?	?
Anazyga recurvirostra 7	USNM705.3	Holotype	?	?	?	?	4	?	?	?	0	0	?	?	?	?	?	?	?	?	?	?	?	?	?	?	?	?	?	?	3	3	0	2	2	?
Anazyga recurvirostra 8	P9509	Non-type	?	?	?	?	2	17	16	0	0	?	?	?	1	?	?	0	?	?	?	0	?	0	?	0	0	?	?	?	?	?	?	?	?	?
Anazyga variabilis 1	USNM111387	Plesiotype	5.98	6.06	5.18	0.987	1	19	16	0	1	0	48	2.21	2	50	40	0	1	2.29	2.77	0	1	0	2.04	0	1	2.64	2.89	2.41	?	?	?	?	?	?
Anazyga variabilis 2	USNM111387	Plesiotype	5.23	5.72	3.36	0.914	1	17	23	0	1	0	?	?	2	39	40	0	1	2.79	2.22	0	1	0	2.34	0	1	4.021	0.57	1.14	?	?	?	?	?	?

Table A1 Continued

ID	1	2	3	4	5	6	7	8	9	10	11	12	13	14	15	16	17	18	19	20	21	22	23	24	25	26	27	28	29	30	31	32	33	34	35	36
Anazyga variabilis 3	**USNM111388**	Non-type	5.21	*5.44*	2.93	0.96	1	12	14	0	1	0	*50*	1.3	2	40	25	0	1	1.48	1.99	*0*	1	0	1.92	0	1	2.57	1.45	0.94	?	?	?	?	?	?
Anazyga variabilis 4	**USNM111388**	Non-type	4.78	*5.2*	3.16	0.92	1	14	15	0	1	0	*45*	?	2	52	49	0	1	1.7	1.78	*0*	1	0	1.93	0	1	2.89	1.46	1.38	?	?	?	?	?	?
Anazyga calhounensis 1	**UC20757.1**	Non-type	5.08	*4.46*	4	1.14	3	20	17	0	2	2	*86*	1.3	1	42	46	0	3	1.72	1.77	*0*	1	0	-	0	0	3.81	2.28	2.23	?	?	?	?	?	?
Anazyga calhounensis 2	**UC20757.2**	Non-type	4.17	*4.06*	2.75	1.03	3	20	15	0	2	1	*50*	1.23	1	65	45	0	3	1.25	1.5	*0*	1	0	-	0	0	3.7	1.5	1.25	?	?	?	?	?	?
Anazyga calhounensis 3	**UC20757.3**	Non-type	5.24	*4.8*	3.76	1.09	3	14	18	0	2	0	*50*	2.06	1	46	40	0	0	0.9	1.3	*0*	1	0	-	0	0	3.8	2.9	2.5	?	?	?	?	?	?
Anazyga calhounensis 4	**UC20757.4**	Non-type	5.69	*4.99*	4.21	1.1	3	19	18	0	2	0	*57*	1.6	1	38	56	0	3	1.21	1.64	*0*	1	0	-	0	0	3.61	3	2.57	?	?	?	?	?	?
Catazyga headi 1	**USNM87052**	Plesiotype	17.05	*15.18*	11.12	1.12	3	?	48	0	2	0	*50*	5.98	2	65	40	0	3	3.3	4.2	*0*	1	0	?	0	0	3.16	7.82	6.92	?	?	?	?	?	?
Catazyga headi 2	**USNM87052**	Plesiotype	17.76	*16*	9.57	1.1	3	29	35	0	2	0	*45*	5.1	2	48	30	0	3	4.52	6.2	*0*	1	0	?	0	0	2.19	5.05	3.37	?	?	?	?	?	?
Catazyga headi 3	**GS45398**	Non-type	19	*14*	9	1.36	3	?	?	?	2	0	*?*	?	?	108	?	?	?	?	?	*?*	?	?	?	?	?	?	?	?	?	1	2	?	1
Catazyga headi 4	**PE89339**	Non-type	?	*?*	?	?	2	?	?	1	2	?	*?*	?	2	?	?	0	?	?	?	*0*	?	0	?	0	1	?	?	?	?	?	?	?	?	?
Catazyga headi 5	**CMNH95342**	Non-type	17.99	*16.5*	8.39	1.1	5	27	39	0	0	1	*49*	5.3	2	38	50	0	0	2.97	4.28	*1*	1	0	4.03	0	0	2.36	5.42	4.11	?	?	?	?	?	?
Catazyga headi 6	**CMNH89904**	Non-type	17.18	15.84	11.29	1.085	5	40	38	1	2	0	43	4.37	2	46	57	0	0	4.66	3.8	0	1	0	-	0	0	2.399	6.63	7.49	?	?	?	?	?	?
Catazyga headi 7	**CMNH89538**	Non-type	27.24	23.55	18.83	1.157	5	49	55	1	2	1	69	11.05	2	50	43	0	2	13.35	9.67	0	1	0	-	0	1	2.335	5.48	9.16	?	?	?	?	?	?
Catazyga headi 8	**CMNH6182**	Non-type	16.77	16	10.62	1.048	5	?	43	1	0	0	60	6.4	1	55	47	0	3	5.51	4.46	0	1	0	-	0	0	2.688	5.11	6.16	?	?	?	?	?	?
Catazyga headi 9	**PE89341a**	Non-type	15.86	13.48	9.61	1.177	5	35	39	1	2	0	55	4.7	1	55	48	0	0	3.71	4.77	0	1	0	-	0	0	2.893	5.9	4.84	?	?	?	?	?	?
Catazyga headi 10	**PE89341b**	Non-type	14.58	13.62	10.08	1.07	5	39	24	0	2	0	50	5.01	1	60	50	0	0	3.71	4.77	0	1	0	-	0	0	1.762	6.37	5.31	?	?	?	?	?	?
Catazyga cartieri 1	**USNM91786**	Holotype	16.29	15.28	9.46	1.066	3	31	31	0	2	0	58	3.82	2	47	39	0	0	3.17	5.98	0	1	0	5.27	0	0	2.029	6.29	3.48	?	?	?	?	?	?
Catazyga cartieri 2	**USNM91786a**	Paratype	16.92	16.47	11.33	1.027	3	30	33	0	2	0	60	6.3	2	50	45	0	0	4.9	7.3	0	1	0	6.22	0	0	2.004	6.43	4.03	?	?	?	?	?	?
Catazyga homeospiroides 1	**USNM145327**	Holotype	13.19	11.8	8.21	1.118	3	13	16	1	1	0	55	3.28	2	50	55	0	0	3.19	4.54	0	1	0	?	0	0	1.356	5.02	3.67	?	?	0	?	?	?
Catazyga homeospiroides 2	**USNM145331**	Paratype	10.6	10.2	?	1.039	3	?	23	0	1	?	?	?	2	?	?	?	?	?	?	0	1	0	?	0	0	2.255	?	?	?	?	0	?	?	?
Catazyga homeospiroides 3	**USNM145329**	Paratype	?	?	?	?	?	?	?	1	1	?	?	?	?	?	?	?	?	?	?	?	?	0	?	0	0	?	?	?	?	?	0	?	?	?

Table A1 Continued

ID	1	2	3	4	5	6	7	8	9	10	11	12	13	14	15	16	17	18	19	20	21	22	23	24	25	26	27	28	29	30	31	32	33	34	35	36
***Catazyga anticostiensis* 1**	**USNM94413a**	Non-type	13.25	10.69	8.36	1.239	3	34	27	1	1	0	60	5.14	2	57	53	0	0	4.26	5.88	0	0	0	-	0	0	2.526	4.1	2.48	?	?	?	?	?	?
***Catazyga anticostiensis* 2**	**USNM94413b**	Non-type	8.17	8.14	5.61	1.004	3	35	26	1	1	0	55	2.92	2	56	32	0	0	2.77	4.15	0	0	0	-	0	0	3.194	2.84	1.46	?	?	?	?	?	?
***Catazyga anticostiensis* 3**	**CMNH22638a**	Non-type	8.51	6.94	5.63	1.226	5	30	27	1	1	0	55	3.4	1	47	34	0	0	3.31	2.7	0	1	0	2.37	0	1	3.89	2.32	2.93	?	?	?	?	?	?
***Catazyga anticostiensis* 4**	**CMNH22638b**	Non-type	9.15	8.83	6.29	1.036	5	33	37	1	1	1	?	?	1	?	?	0	0	3.1	?	0	1	0	2.36	0	1	4.19	3.19	?	?	?	?	?	?	?	?
Catazyga arcana 1	**BB26733**	Holotype	14.5	14	4.07	1.036	4	40	39	1	2	1	?	?	1	?	?	0	3	?	?	0	?	0	?	0	1	2.786	?	?	?	?	?	?	?	?
Catazyga hicksi 1	**NA**	Lectotype	10	9.75	?	1.026	3	20	19	1	1	0	?	?	1	?	?	0	?	?	?	1	?	0	?	0	0	1.949	?	?	?	?	?	1	?	?
Catazyga uphami 1	**NA**	Non-type	7.72	6.56	4.99	1.177	5	29	30	0	1	1	55	2.08	2	40	32	0	0	2.19	2.81	0	0	0	2.63	0	0	4.573	2.8	2.18	?	?	?	?	?	?
Catazyga uphami 2	**NA**	Non-type	7.34	6.86	4.61	1.07	5	30	40	0	1	1	60	3.2	2	40	38	0	1	3.1	3.4	0	0	0	2.52	0	0	5.831	1.51	1.21	?	?	?	?	?	?
Catazyga uphami 3	**USNM24867**	Non-type	7.08	6.64	4.05	1.066	5	42	43	1	1	0	65	1.88	2	55	52	0	1	2.51	2.72	0	0	1	2.34	0	0	6.476	1.54	1.33	?	?	?	?	?	?
Catazyga uphami 4	**CMNHT6711**	Non-type	9.39	8.35	5.47	1.125	5	44	37	0	0	0	46	2.49	2	41	52	0	1	3.15	3.04	0	0	0	2.88	0	0	4.431	2.32	2.43	?	?	?	?	?	?
Protozyga exigua 1	**USNM117242**	Plesiotype	6.28	6.6	4.63	0.952	2	0	0	0	2	1	60	2.4	1	55	45	0	1	3.26	3.27	0	0	0	2.82	0	0	0	1.37	1.36	?	?	?	?	?	?
Protozyga exigua 2	**USNM112398**	Plesiotype	4.52	4.34	3.1	1.041	4	0	6	0	0	1	5	1.56	1	50	30	0	1	1.93	1.53	0	0	0	2.03	0	0	1.382	1.17	1.57	?	?	?	?	?	?
Protozyga exigua 3	**USNM714-1a**	Lectotype	?	3	?	?	2	?	?	?	2	2	?	?	?	?	?	?	1	?	?	?	?	?	?	?	?	?	?	?	2	3	?	1	2	?

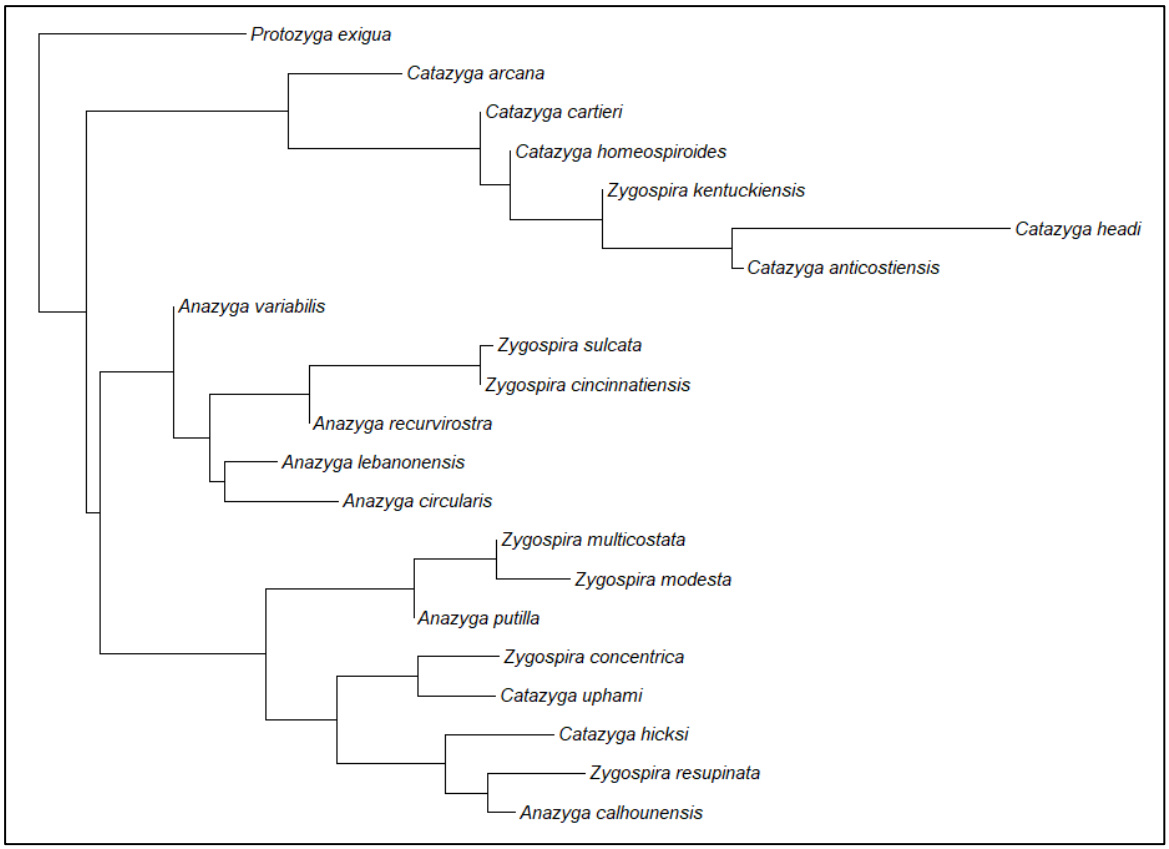

Figure A1. Bayesian phylogeny estimated using both external and internal morphological data and without constraints within the subfamily Anazygidae. The former taxonomic nomenclature is shown. Posterior probability: -327.56.

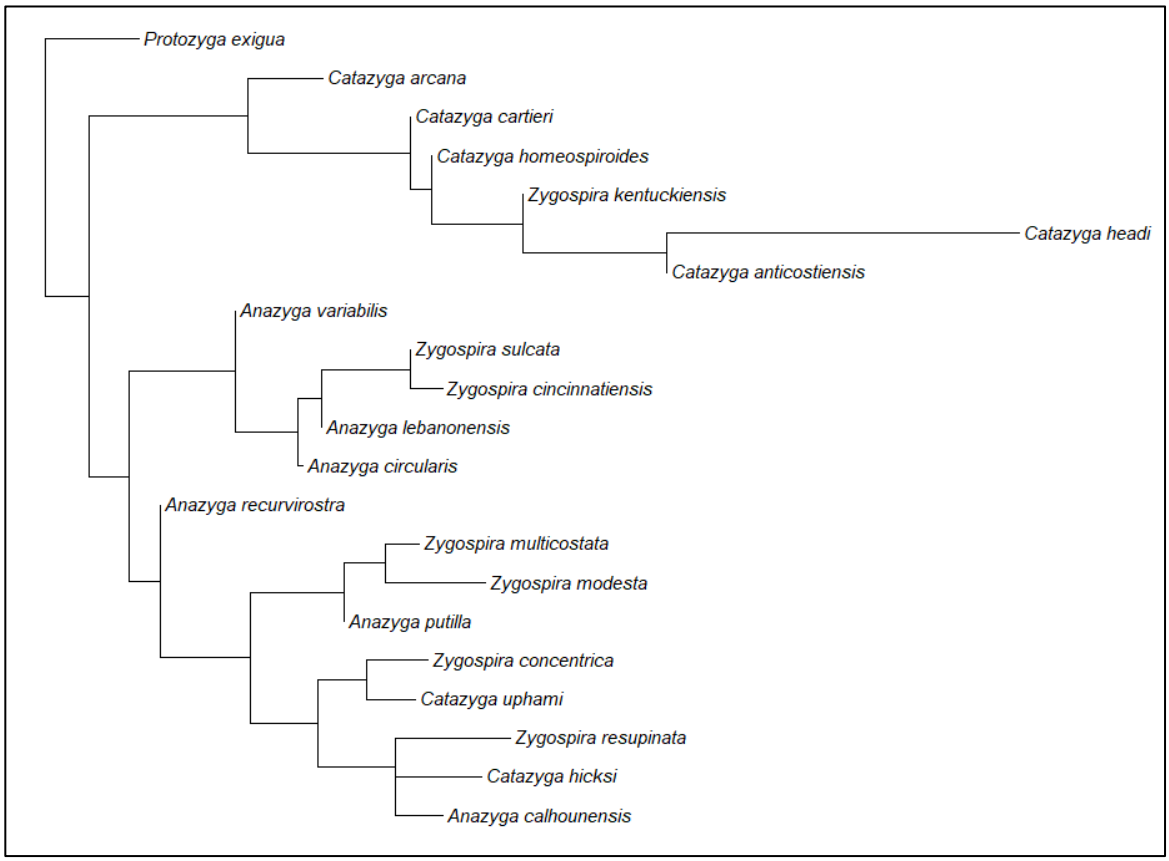

Figure A2. Bayesian phylogeny estimated using external morphological data only and without constraints within the subfamily Anazygidae. The former taxonomic nomenclature is shown. Posterior probability: -318.77.

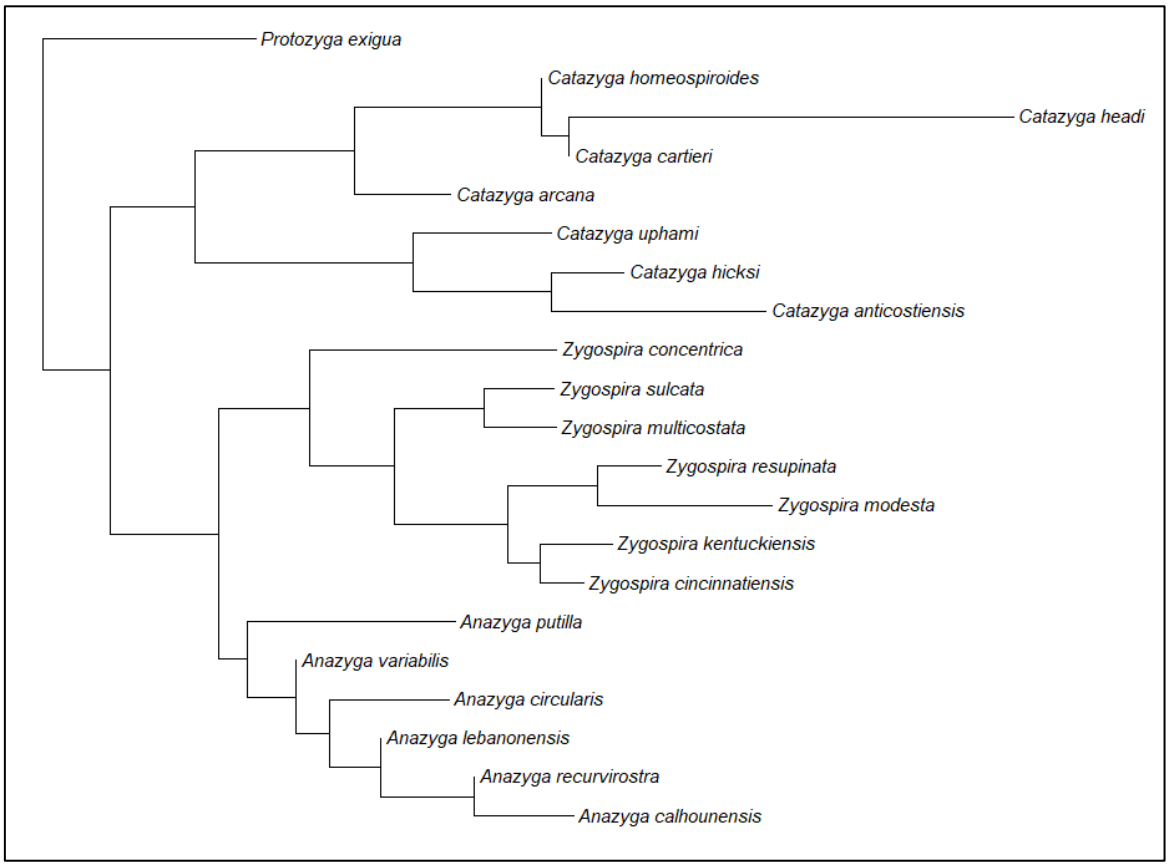

Figure A3. Bayesian phylogeny estimated using both internal and external characters with grouping constraints reflecting the previously published generic assignments. The former clade's taxonomic nomenclature is shown. Posterior probability: -342.19.

Table A2. Geographic distribution of taxa coded as presence (1) and absence (0) in the eight analyzed geographic areas. O, Scoto-Avalonia; W, Western Mid-Continent; U, Upper Mississippi Valley; E, Equatorial Laurentia; F, Foreland basin; N, Northern Appalachian basin; S, Southern Appalachian basin; A, Alaska.

Species	O	W	U	E	F	N	S	A
Zygospira modesta	0	0	0	0	0	1	1	0
Zygospira sulcata	0	1	0	0	0	0	0	0
Zygospira kentuckiensis	0	0	0	0	1	1	0	0
Zygospira resupinata	0	0	1	0	0	1	0	0
Zygospira cincinnatiensis	0	0	0	0	0	1	0	0
Zygospira multicostata	0	1	0	0	0	0	0	0
Zygospira concentrica	0	0	0	0	0	1	0	0
Zygospira circularis	0	1	0	0	0	0	0	0
Zygospira lebanonensis	0	1	0	0	0	0	0	0
Zygospira idahoensis	0	1	0	0	0	0	0	0
Zygospira recurvirostra	0	1	1	0	1	1	0	0
Zygospira variabilis	0	0	1	0	0	0	0	0
Zygospira calhounensis	0	0	1	0	0	0	0	0
Catazyga headi	0	0	0	1	0	1	0	0
Catazyga cartieri	0	0	0	1	0	0	0	0
Catazyga homeospiroides	0	0	0	0	0	0	0	1
Catazyga anticostiensis	0	0	0	1	0	0	0	0
Catazyga arcana	1	0	0	0	0	0	0	0
Catazyga hicksi	1	0	0	0	0	0	0	0
Catazyga uphami	0	0	1	0	0	0	0	0

VITA

Mariana Vilela de Andrade was born in Cuiabá, state of Mato Grosso, Brazil. After graduating from a public high school, she was selected through the National High School Exam (ENEM) to attend the Biological Sciences Undergraduate Program at the Federal University of Mato Grosso. Mariana was inspired by her mother, a Brazilian botanist specialized in the Amazon rainforest and biological conservation to pursue a degree in biology. During her undergraduate years, Mariana acquired field experiences in savannas, rainforests, and wetlands. However, her main strengths rely on theoretical and computational methods on ecological niche modelling, climate predictions for future and past environments, land-use cover analysis and impacts on natural areas, and dispersal modeling. In 2022, Mariana joined the Department of Earth, Environmental, and Planetary Sciences at the University of Tennessee, Knoxville as a master's student. She was advised by Dr. Alycia L. Stigall and dedicated the first years of her graduate studies to the understanding of past environments and evolutionary patterns. During her two years at UTK, Mariana attended one international conference, the 14th Symposium on the Ordovician System, in Tallinn, Estonia; and two national conferences, the 2023 Geological Society of America Annual Meeting in Pittsburgh, Pennsylvania, and the 12th North American Paleontological Convention in Ann Arbor, Michigan. In total, Mariana presented one poster and gave two presentations outside the University. Mariana also worked closely with undergraduate students at UTK, as a graduate teaching assistant (GTA), she taught for two years Earth, Life, and Time (GEOL 102) and Paleobiology (GEOL 320). Mariana will join the EEPS in Fall 2024 to pursue her PhD at the University of Tennessee, Knoxville.

ATTACHMENTS

File 1. b_MCC_catazyga_constraint.tre

((((((Anazyga_calhounensis:0.6134033294,(Catazyga_hicksi:0.3735932614,Zygospira_resupinata:0.643809179):0.6106337701):0.5965686076,Catazyga_uphami:1.091344001):0.3520637044,Zygospira_concentrica:1.47832898):0.372388792,(Anazyga_putilla:0.01,(Zygospira_modesta:1.187371153,Zygospira_multicostata:0.4017865602):0.3848817061):1.0277827):1.212675044,(((Anazyga_circularis:0.8203683636,Anazyga_lebanonensis:0.3299445074):0.1940667074,(Anazyga_variabilis:0.6585551316,((Zygospira_cincinnatiensis:0.8671209931,Zygospira_sulcata:0.6621436716):0.08121356392,Zygospira_kentuckiensis:1.044134806):0.131177249):0.9563538242):0.4454969467,Anazyga_recurvirostra:0.8184952942):0.7333408742):0.4966890046,((((Catazyga_anticostiensis:0.6815670194,Catazyga_headi:1.66780849):1.55005912,Catazyga_homeospiroides:0.01):0.2554364999,Catazyga_cartieri:0.01):1.752612097,Catazyga_arcana:1.002253498):1.659031958):0;

File 2. b_AICc_table.csv

"Model","LnL","numparams","d","e","j","AICc","AICc_wt"

"DEC","-62.68","2","0.055","0.019","0","130.1","0.0013"

"DEC+J","-54.82","3","0.030","1.0e-12","0.12","117.1","0.82"

"DIVALIKE","-61.56","2","0.072","1.0e-12","0","127.8","0.0039"

"DIVALIKE+J","-56.43","3","0.043","1.0e-12","0.072","120.4","0.16"

"BAYAREALIKE","-75.17","2","0.093","0.73","0","155","4.8e-09"

"BAYAREALIKE+J","-59.33","3","0.025","1.0e-07","0.16","126.2","0.0090"

File 3. b_BayArealike.png

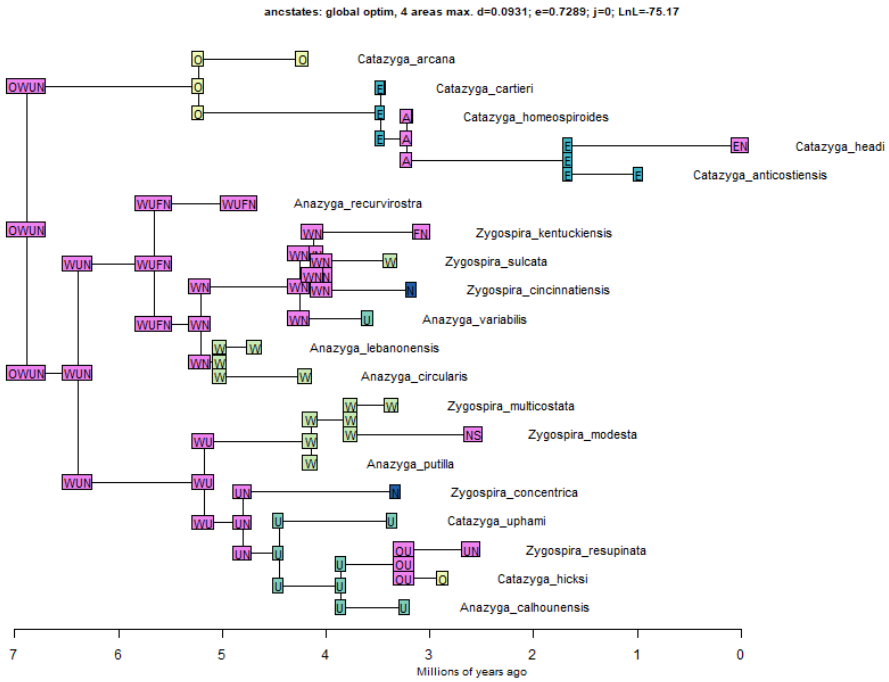

File 4. b_BayArealikeJ.png

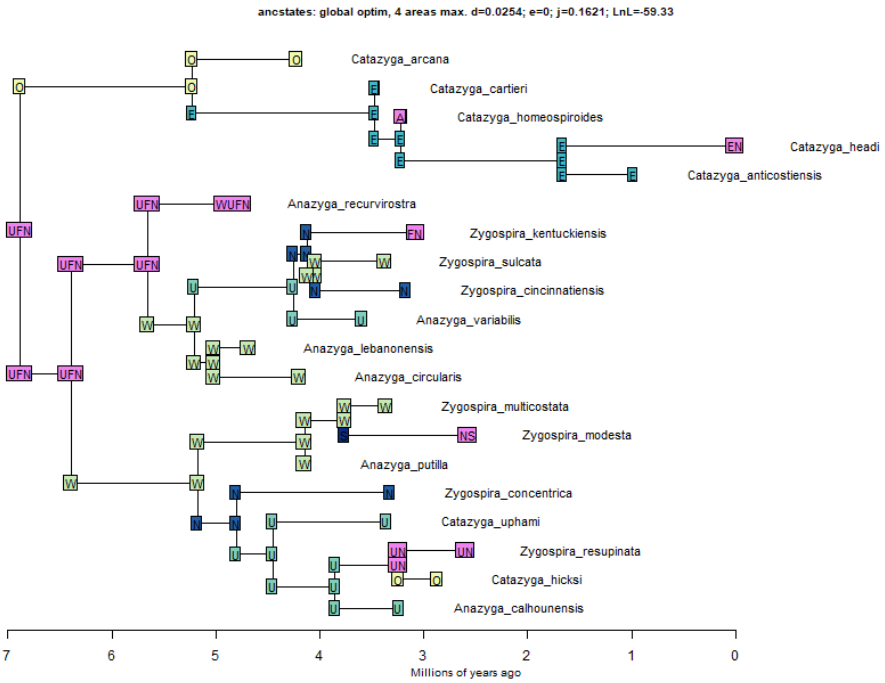

File 5. b_DEC.png

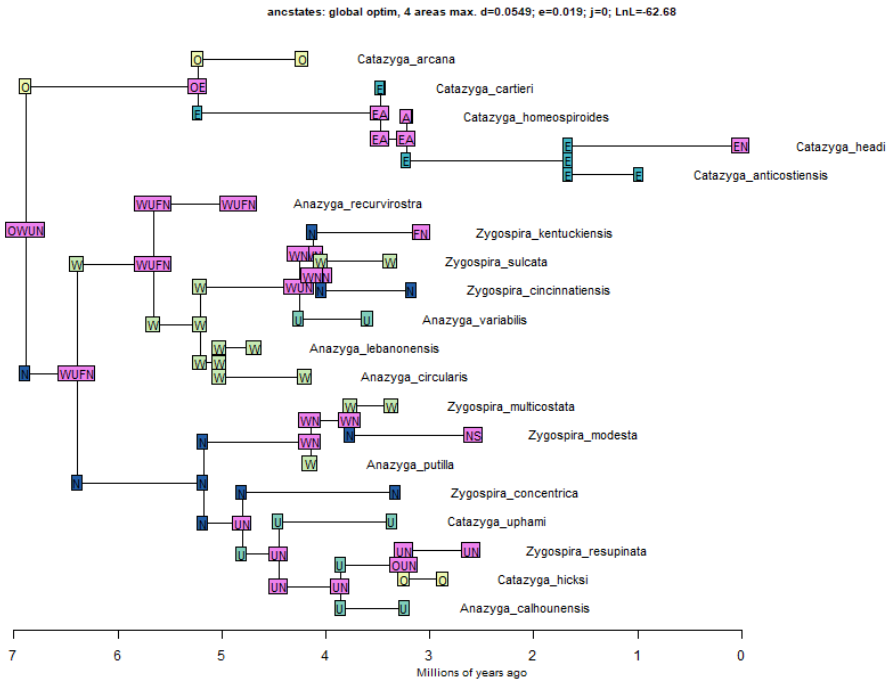

File 6. b_DECJ.png

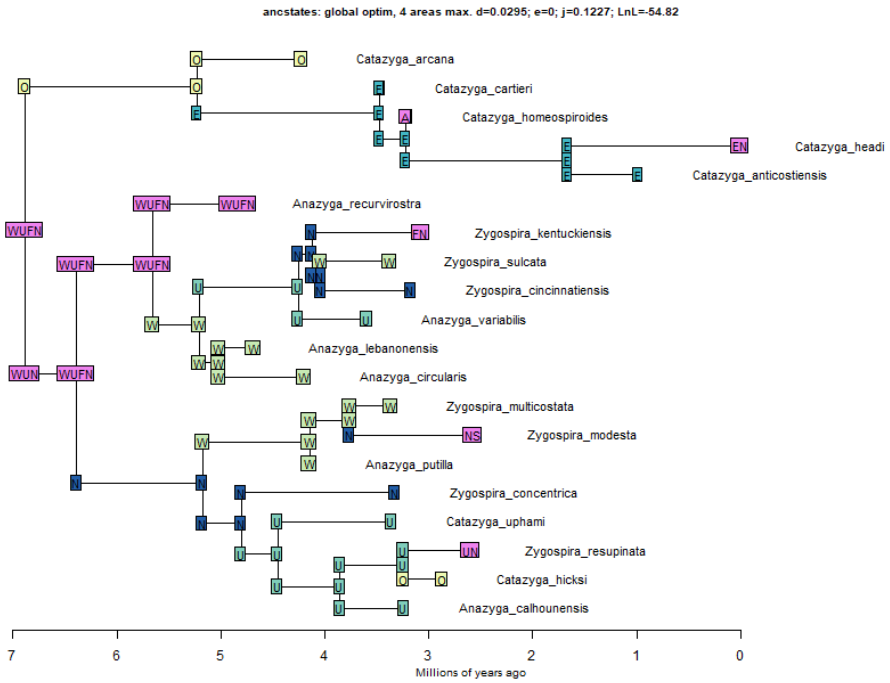

File 7. b_DIVALIKE.png

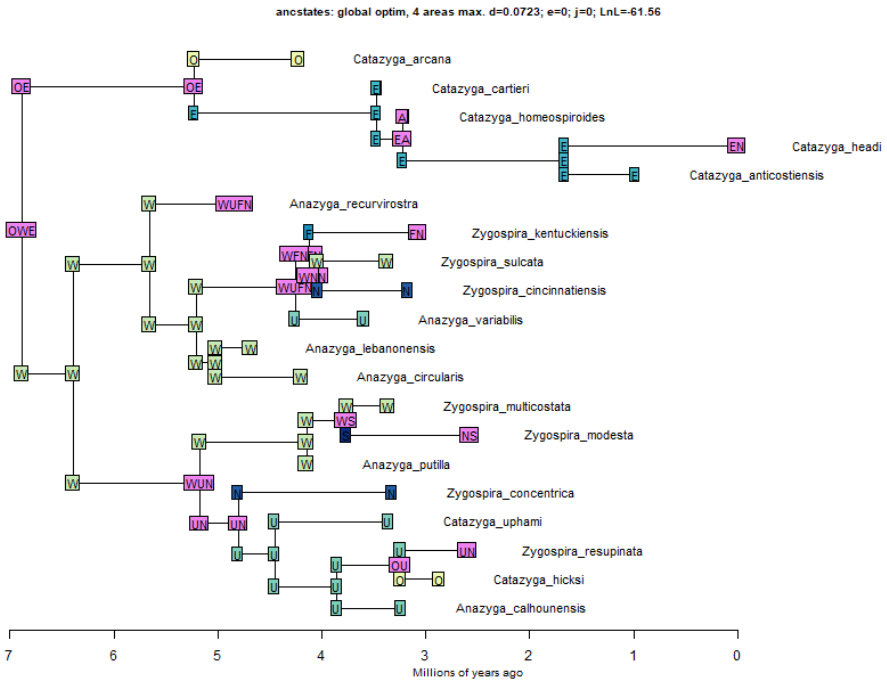

File 8. b_DIVALIKEJ.png

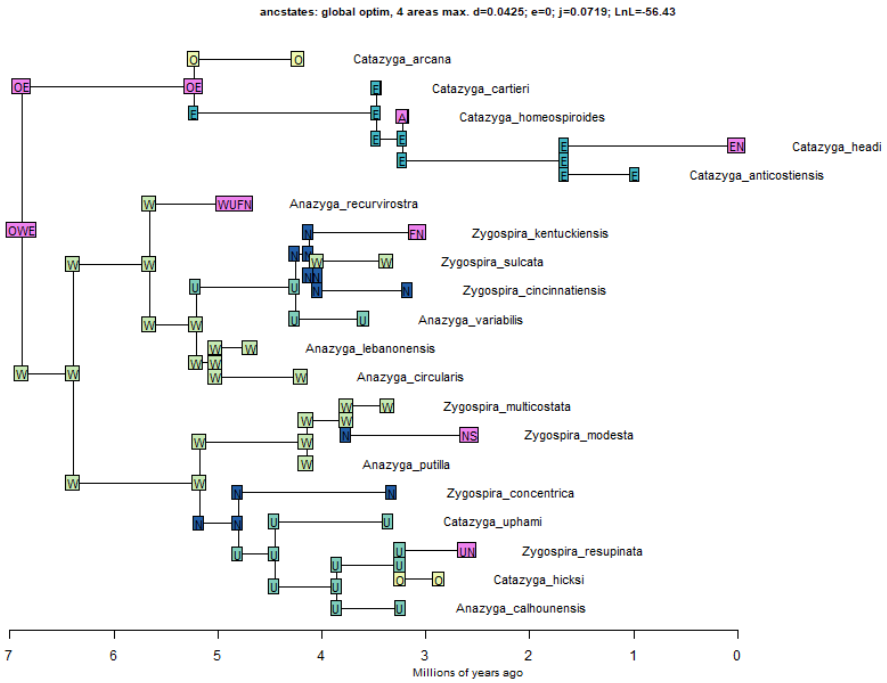

File 9. se_brach_attack

```
# set this to wherever your files are saved!

setwd("C:/Users/mrnvd/Desktop/R/Mariana")

# source useful R packages

library(paleotree)

library(strap)

#source additional R scripts for functions not in any R package (make sure it's in your working directory!)

source("functions.R")

#########################################################################################

# Plot results from analyses

#########################################################################################

# Select a taxon to analyze (choose one at a time)

genus <- paste("Anazygidae")

# get min taxon age for selected genus

#anchor <- getMinTaxonAge(genus)

anchor = 443.07

#paste0(genus,".t")

setwd("C:/Users/mrnvd/Desktop/R/Mariana")

# read in t and p files grab a sample of time-scaled trees

t.file <- read.nexus("anazygids_ne.nexus", tree.names = TRUE)

t.file

p.file <- read.table("anazygidae_pstat.txt", header = TRUE)

p.file

trees <- t.file[5000:20001]

for (i in 1:length(trees)){
```

```
  oldRootAge <- max(dateNodes(trees[[i]]))
  #print(oldRootAge)
  trees[[i]]$root.time <- oldRootAge + anchor #
  print(trees[[i]]$root.time)
}
# adjust branches from units of (# of changes * time) to units of (time) by dividing
# each tree by the mean clock rate
#clock.rate = p.file[5,2]
#clock.rate
#t.file[["edge.length"]] = t.file[["edge.length"]] / clock.rate
#for (i in 1:length(t.file)){
#  clock.rate <- p.file$ORCucldMean[i]
#  t.file[[i]]$edge.length <- t.file[[i]]$edge.length / clock.rate
#}
# grab post-burnin trees
#trees <- t.file[5000:20001]
# rescale the root age so node ages are in 'deep time'
#for (i in 1:length(trees)){
#  oldRootAge <- max(dateNodes(trees[[i]]))
#  print(oldRootAge)
  #trees[[i]]$root.time <- oldRootAge + anchor #
# }
#oldRootage = max(dateNodes(t.file))
#t.file$root.time = oldRootage + anchor
# Read in geologic time scale and store info for help with plotting later
geol_time<-read.table("Geologic_Timescale.txt",header=TRUE)
```

```
print(geol_time)

Stages<-cbind(geol_time[,3],geol_time[,4])

print(Stages)

row.names(Stages)<-geol_time[,2]

print(Stages)

midpoints<-(Stages[1:(length(Stages)-1)]+Stages[2:length(Stages)])/2

print(midpoints)

midpoints <- midpoints[4:7]# Sandbian, Katian, and Hirnatian

int.start <- c(467.30, 458.18,452.75,445.21, 443.07, 433.40)

# Diversity curves

# get diversity curves for multiple trees and plot the resulting median diversity with 95% quantiles

k <- multiDiv(trees, int.times = Stages[5:7,], drop.ZLB = TRUE, plot = TRUE) # Since it's only one tree

# store diversity data for each tree to plot later

div <- k$median.curve[,1]

lower.conf <- k$median.curve[,2]

upper.conf <- k$median.curve[,3]

# begin the plot

plot(midpoints, div, xlim = rev(c(440, 460)),ylim = c(-0.05, max(upper.conf)), type = "n", axes = F, xlab = "", ylab = "")

# make boxes for each stage

rect(440, 0, 460, 20, col = rep(c("grey95", "grey97")), border = NA)

# make polygons of upper and lower 95% quantiles

polygon(c(midpoints,rev(midpoints)),c(div,rev(upper.conf)), col = "seashell2", lty = 2)

polygon(c(midpoints,rev(midpoints)),c(div,rev(lower.conf)), col = "seashell2", lty = 2)

# plot lines & points

lines(midpoints, div, xlim = c(440,460), lwd = 2, col = "black")
```

```
points(midpoints, div, xlim = c(440,460), pch = 22, cex = 1.5, col = "black", bg =
"black")


# plot axes

axis(1, col = "black", line = 0, at=c(0, 440, 450,460), lwd=2, lwd.ticks = 2, cex.axis=1.5,
col.ticks = "black")

axis(2, col = "black", line = 0.5, at = seq(0, max(upper.conf), round(1.7)), lwd=2,
lwd.ticks = 2, cex.axis=1.5, col.ticks = "black")

mtext("Age (Ma)", side = 1, line = 2.5, cex=1.5)

mtext("Diversity (# of lineages)", side = 2, line = 2.8, cex=1.5)

pdf(file = "LineageDiversityGSAlog.pdf", height =5.5, width = 6, useDingbats = FALSE)

dev.off()

##########################################################################
######################

# Net diversification and sampling plots

##########################################################################
######################

# read in the p.stats file

print(p.file)

# sort 'param' into quantities to plote

netDiv <- p.file[1:4,2]

upper.div <- p.file[1:4,5]

lower.div <- p.file[1:4,4]

extinction <- p.file[5:8,2]

upper.e <- p.file[5:8,5]

lower.e <- p.file[5:8,4]

relSamp <- p.file[9:12,2]

upper.s <- p.file[9:12,5]
```

```
lower.s <- p.file[9:12,4]

# convert FBD parameters to speciation, extinction, and sampling rates

meanMu <- calcMu(netDiv, extinction)

meanLambda <- calcLambda(netDiv, meanMu)

meanPsi <- calcPsi(meanMu, relSamp)

# if you want medians instead

#meanMu <- calcMu(netDiv[,6], turnover[,6])

#meanLambda <- calcLambda(netDiv[,6], meanMu)

#meanPsi <- calcPsi(meanMu, relSamp[,6])

# set up plotting

midpoints = c(451,450,449.5,443.07)

# Net diversification

# plot

plot(midpoints, netDiv, xlim = c(460,440),ylim = c(-0.05, max(upper.div)), type = "n",
axes = F, xlab = "", ylab = "")

rect(int.start[-1], rep(0, 9), int.start[-10], rep(100, 9), col = rep(c("grey95", "grey97")),
border = NA)

segments(midpoints,netDiv,midpoints, lower.div, col = "darkblue", lty = 2, lwd = 2)

segments(midpoints,netDiv,midpoints, upper.div, col = "darkblue", lty = 2, lwd = 2)

lines(midpoints, netDiv, xlim = c(485.4,427.4), lwd = 2, col = "darkblue")

points(midpoints, netDiv, xlim = c(485.4,427.4), pch = 21, cex = 1.3, col = "black", bg =
"darkblue")

axis(1, at=seq(440, 460, 5), col = "black", line = -1.5)

axis(2, col = "black", line = 0.5, at = seq(0, max(upper.div), 0.05))

mtext("Age (Ma)", side = 1, line = 1.7, cex=1.5)

mtext("Net diversification (Lmy)", side = 2, line = 2.8, cex=1.5)

#pdf(file = "NetDiversificationGSA.pdf", height = 6, width = 5.5, useDingbats = FALSE)

#dev.off()
```

```
# Relative fossilization

# plot Sampling

plot(midpoints, relSamp, xlim = c(460,440),ylim = c(-0.00005, max(upper.s) ), type = "n", axes = F, xlab = "", ylab = "")

rect(int.start[-1], rep(0, 9), int.start[-10], rep(100, 9), col = rep(c("grey95", "grey97")), border = NA)

segments(midpoints,relSamp,midpoints, upper.s, col = "sienna1", lty = 2, lwd = 2)

segments(midpoints,relSamp,midpoints, lower.s, col = "sienna1", lty = 2, lwd = 2)

lines(midpoints, relSamp, xlim = c(440,460), lwd = 2, col = "sienna1")

points(midpoints, relSamp, xlim = c(440,460), pch = 21, cex = 1.3, col = "black", bg = "sienna1")

axis(1, col = "black", line = -1)

axis(2, col = "black", line = 0.5, at = seq(0, 2, 0.2))

mtext("Age (Ma)", side = 1, line = 1.7, cex=1.5)

mtext("Relative fossilization & sampling (r / (q + r)", side = 2, line = 2.8, cex=1.5)

#pdf(file = "RelativeSampling.pdf", height = 6, width = 5.5, useDingbats = FALSE)

#dev.off()

# Sampling probability per interval

int <- Stages[5:7,1] - Stages[5:7,2]

R <- 1 - exp(-meanPsi * int)

# plot Sampling

plot(midpoints, R, xlim = c(460,440),ylim = c(-0.0005, 1), type = "n", axes = F, xlab = "", ylab = "")

rect(int.start[-1], rep(0, 9), int.start[-10], rep(100, 9), col = rep(c("grey95", "grey97")), border = NA

lines(midpoints, R, xlim = c(485.4,427.4), lwd = 2, col = "sienna1")

points(midpoints, R, xlim = c(485.4,427.4), pch = 21, cex = 1.3, col = "black", bg = "sienna1")
```

```
axis(1, col = "grey75", line = 0)
axis(2, col = "grey75", line = 0.5, at = seq(0, 1, 0.2))

mtext("Age (Ma)", side = 1, line = 2)
mtext("Per-interval sampling probability (R)", side = 2, line = 2.7)

cor.test(R, div, method = "spearman") #

###
# PLOT SPECIATION & EXTINCTION WITH BOXPLOTS
###
#params <- read.table(paste0(genus,".p"), header = TRUE)
# Sort the file
param <- read.table("anazygidae_BDSKY_final.log", header = T)
param <- param[1250:5001,]

# get values
netDiv <- param[,6:9]
turnover <- param[,10:13]
relSamp <- param[,14:17]

# convert to lambda, mu, and psi
meanMu <- calcMu(netDiv, turnover)
meanLambda <- calcLambda(netDiv, meanMu)
meanPsi <- calcPsi(meanMu, relSamp)
```

```
# set up plotting

#STAGES <- c("Tremadoc", "Floian", "Dap/Darr", "Sandbian", "Katian/H", "Llan")

STAGES <- c("K1", "K2", "K3", "K4/Hirnantian")

# Speciation & extinction rates

# plot

plot(midpoints, midpoints, xlim = c(452,443),ylim = c(-10,10), type = "n", axes = F, xlab = "", ylab = "")

rect(int.start[-1], rep(-10, 50), int.start[-6], rep(100, 9), col = rep(c("grey95", "grey97")), border = NA)

rect(452, rep(-10, 50), 451, rep(100, 9), col = "burlywood1", border = NA)

rect(451, rep(-10, 50), 450, rep(100, 9), col = "peachpuff", border = NA)

rect(450, rep(-10, 50), 449.5, rep(100, 9), col = "burlywood1", border = NA)

rect(449.5, rep(-10, 50), 443.07, rep(100, 9), col = "peachpuff", border = NA)

# Redefining the midpoints list to fall within the skyline interval

# Reasoning: the boxes for time bin 2 and 3 were overlapping (too close to each other on the X-axis)

midpoints.lambda = c(451.7,450.8,449.8,447)

midpoints.mu = c(451.27,450.3,449.3,446.5)

boxplot(meanLambda, col = "lightblue", add = TRUE, at = midpoints.lambda, names = STAGES, border = TRUE, boxwex = .4, outline = FALSE, frame = FALSE, axes = FALSE)

boxplot(meanMu, col = "salmon", add = TRUE, at = midpoints.mu, names = STAGES, border = TRUE, boxwex = .4, outline = FALSE, frame = FALSE, axes = FALSE)

axis(1, col = "black", line = -1, at=455:443)

axis(2, col = "black", line = 0.5, at = seq(-10, 10, 2))

mtext("Geologic time (Ma)", side = 1, line = 1.3, cex=1.5)

mtext("Speciation & extinction rates (Lmy)", side = 2, line = 2.7, cex=1.5)
```

```
#pdf(file = "DiversificationRatesGSA.pdf", height = 6, width = 6.5, useDingbats = FALSE)

dev.off()

################

# plot a timescaled MCCT

################

# use the MCC from TreeAnnotator to find the MCCT in the posterior and get branch lengths in units of time

# new function--need to move to functions.R file to source. Requires dateNodes from paleotree.

get_MCCT <- function(genus){

  MCCT <- read.nexus("anazygids_ne.nexus")

  # use findTree to figure out which posterior tree == MCCT

  which_is_MCCT <- suppressWarnings(findTree(MCCT, t.file))

  MCCT <- t.file[[suppressWarnings(findTree(MCCT, t.file))]]

  # rescale the tree in units of time

  #MCCT$edge.length / p.file$clockrate[which_is_MCCT]

  # re-adjust the root to send the node ages back to 'deep time'

  MCCT$root.time <- max(dateNodes(MCCT)) + getMinTaxonAge(genus)


  return(MCCT)


}

MCCT <- get_MCCT(genus)

trees <- t.file[5000:20001]

MCCT <- read.tree("catazyga_cons_MCC_after_ape.tre")

MCCT$root.time = 453.48

#for (i in 1:length(trees)){
```

```
#  oldRootAge <- max(dateNodes(trees[[i]]))
  #print(oldRootAge)
#  trees[[i]]$root.time <- oldRootAge + anchor #
  #print(M[[i]]$MCCT)
#}
#basic plot
plot(ladderize(MCCT)); axisPhylo()
slices = read.table("global_ordovician_slices_plot.txt", header=T)
slices$Name = as.factor(slices$Name)
slices = as.data.frame(slices)
summary(slices)
FA = read.table("anazygidae_FA_new.txt", header=T)
# w/ geologic timescale, can play around w/ options to make a prettier plot
geoscalePhylo(ladderize(MCCT), units=c("Epoch","Age"),x.lim = c(458, 441),
            cex.age=2, cex.tip=1.5, boxes="Age",
            label.offset = 0.02, arotate=0, erotate=0, cex.ts=2, ages=FA, width=1.3,
            tick.scale="")
# #####
# plot the distribution of divergence times for genus origination
########
# call getCladeAge function from source
ages <- getCladeAge(trees)


z <- hist(ages,ylim = c(0,1), xlim = c(max(ages)+5,min(ages)-5), xlab = "Geologic time
(Ma)", ylab = "Probability density", freq = FALSE, main = "", col = "salmon")
#get mean age
mean(ages)
```

```
# get ~estimate of time interval with largest probability density

z$mids[which(z$density == max(z$density))]

############################

# Sampled ancestors

############################


# get probability of a taxon being a sampled ancestor

samp = samp.Anc(trees)


#plot a histogram

k <- hist(samp.Anc(trees), col = "darkgrey", xlab = "Pr(Ancestral taxon)", main = "")

#pdf(file = "SAs.pdf", height =5.5, width = 6, useDingbats = FALSE)

#dev.off()

####

# add time to zero-length branches (i.e., sampled ancestors). 'blens' parameter sets length for ZLB (recommended to be very small but non-zero!)

# Example for a single tree

MCCT$edge.length # the zero-length branches?

# add time

new.MCCT <- modify.edges(MCCT, blens = 0.01)

new.MCCT$edge.length # now they're gone & you can use PCMs without divide by zero / matrix inversion issues!

# also works for a distribution of trees

new.trees <- modify.edges(trees, blens = 0.01)
```

File 10. se_functions

```
# Library of (mostly crap) functions I wrote that might be useful for brach_attack project
# by David F. Wright

# some functions require the package 'paleotree' by D.W. Bapst


# Function to get posterior probabilities of a taxon being a sampled ancestor
# Note the the "trees" argument must be a post-burn-in sample of the posterior
distribution
samp.Anc <- function(trees){

  freq <- vector(mode = "numeric", length = Ntip(trees[[1]]))
  names(freq) <- trees[[1]]$tip.label

  for (i in 1:length(trees)){

    tip.br <-
setNames(trees[[i]]$edge.length[sapply(1:length(trees[[i]]$tip.label),function(x,y)
which(y == x),y = trees[[i]]$edge[,2])],trees[[i]]$tip.label)

    for (j in 1:length(tip.br)){

      if (tip.br[j] == 0){
        freq[j] <- freq[j] + 1

      }

    }

  }

  anc.prop <- (freq / length(trees))
  return(anc.prop)

}

# FUNCTION TO CHANGE BRANCH LENGTHS BELOW A THRESHOLD TO A
CONSTANT
# Can take either a list of trees or a single tree. Can also be used to scale branches to unit
length when NULL (e.g., a parsimony tree estimated in PHANGORN, etc.)

modify.edges <- function(trees, blens = 1, threshold = 1e-01){
  # Check whether object 'trees' is a single tree or list of trees
```

```
  # For multi-phylo objects

  if (class(trees) == "multiPhylo"){

    for(i in 1:length(trees)){  # loop over all trees a list of trees

      tree <- trees[[i]]

      # check to make sure there are branch lengths; otherwise add small value to get rid of
edge.length == NULL warnings()
      if (is.null(tree$edge.length)){
        N.edges <- (Ntip(tree) - 3) + Ntip(tree) # == number of internal branches + number
of tips

        for (j in 1:N.edges){

          tree$edge.length[j] <- 1e-02

        }

      }

      # Main loop to add edge.lengths below threshold for each jth tree
      for (j in 1:length(tree$edge.length)){

        edge <- tree$edge.length[j]

        if (edge <= threshold){
          tree$edge.length[j] <- blens

        }

      }

      trees[[i]] <- tree

    }

    return(trees) # returns a list of trees with modified edges

  }

  # For a single tree
  if (class(trees) == "phylo"){
    tree <- trees
```

```
   # check to make sure there are branch lengths; otherwise add small value to get rid of
edge.length == NULL warnings()
   if (is.null(tree$edge.length)){
     N.edges <- (Ntip(tree) - 3) + Ntip(tree) # == number of internal branches + number of
tips

     for (j in 1:N.edges){

       tree$edge.length[j] <- 1e-02

     }

   }

   # Main loop to add edge.lengths below threshold
   for (k in 1:length(tree$edge.length)){

     edge <- tree$edge.length[k]

     if (edge <= threshold){
       tree$edge.length[k] <- blens

     }

   }

   return(tree) # returns a single tree with modified edges

 }

}


# Convert MrBayes estimates of diversification dynamics & fossilization to speciation,
extinction, and sampling rates

calcMu <- function(netDiv, turnover){

 mu <- (netDiv * turnover) / (1 - turnover)
 return(mu)

}

calcLambda <- function(netDiv, mu){
```

```
  lambda <- netDiv + mu
  return(lambda)

}

calcPsi <- function(mu, relSamp){

  Psi <- (mu * relSamp) / (1 - relSamp)
  return(Psi)

}


# Function to add length to Zero Length Branches
removeZLB <- function(trees, blens = 1){

  for(i in 1:length(trees)){

    tree <- trees[[i]]

    for (j in 1:length(tree$edge.length)){

      edge <- tree$edge.length[j]

      if (edge <= 10e-6){
        tree$edge.length[j] <- blens

      }

    }

    trees[[i]] <- tree

  }

  return(trees)

}


# Sample MrBayes trees from the posterior and time scale them in units of relative time
(must use anchorTree function to scale to absolute time)
sample_timescaleMrBayes <- function(t.file, p.file, subsample = 100, burnin = 0.35){
```

```
  n <- length(t.file)
  clockrate <- p.file$clockrate
  samples <- sample(seq(from = round(n*burnin), to=n), size = subsample)
  scaled.trees <- list()

    for (i in 1:length(samples)) {

      tree <- samples[i]
      foo <- t.file[[tree]]
      foo$edge.length <-  foo$edge.length / clockrate[tree]
      scaled.trees[[i]] <- foo

    }

  return(scaled.trees)

}



# Scales all trees in the t.file to relative time. Use anchorTree to scale the tree to absolute
time after using this function.
timescaleMrBayes <- function(t.file, p.file){

  for (i in 1:length(t.file)){

    clock.rate <- p.file$clockrate[i]
    t.file[[i]]$edge.length <- t.file[[i]]$edge.length / clock.rate

  }

  return(t.file)

}

# Find a tree in the posterior distribution t.file. May be useful to get associated info from
p.file for a given tree (e.g., MCCT). May be slow if #trees is large.
findTree <- function(tree, t.file){

  clades <- vector(length = length(t.file))

   for (i in 1:length(t.file)){

     clades[i] <- dist.topo(t.file[[i]], tree)
```

```
  }

  return(which(clades == 0))

}



# Get min taxon age to anchor tree
getMinTaxonAge <- function(Taxon){
  if (Taxon == "Hesperorthis"){
    age <- 443.8
  }
  if (Taxon == "Mimella"){
    age <- 445.2
  }
  if (Taxon == "Oepikina"){
    age <- 450.3
  }
  return(age)
}

# get distribution for the age of the age of the clade

getCladeAge <- function(trees){

  age <- c()

  for (i in 1:length(trees)){

    age[i] <- max(dateNodes(trees[[i]]))

  }

  return(age)

}




  # Use anchor taxon to scale the tree to abosulte time. This only makes sense if trees are
already
  # scaled to relative time
```

```
 anchorTree <- function(trees, anchorTime){
  # for a list of trees
  if (class(trees) == "multiPhylo"){
   for (i in 1:length(trees)){
    oldRootAge <- max(dateNodes(trees[[i]]))
    trees[[i]]$root.time <- oldRootAge + anchorTime
   }
   return(trees)
  }
  #for a single tree
  if (class(trees) == "phylo"){
   oldRootAge <- max(dateNodes(trees))
   trees$root.time <- oldRootAge + anchorTime
  }
  return(trees)
}
```